



South Eastern Australian **Climate Initiative**

Program Annual Report 2009/10

November 2010



Citation

CSIRO (2010) Program Annual Report 2009/10. South Eastern Australian Climate Initiative (SEACI). CSIRO, Australia.

Contributors

Program Director Lu Zhang (July 2009 – March 2010), David Post (April 2010 onwards)

Program Coordinator Gemma Ansell (July 2009 – February 2010), Therese McGillion (March 2010 onwards)

Program Communicator Laura Wynne

Scientific Editor Becky Schmidt

Production Assistance Simon Gallant, Ben Wurcker

Design Siobhan Duffy

Theme Leaders Bertrand Timbal (Theme 1), Francis Chiew (Theme 2), Harry Hendon (Theme 3)

Project Leaders Peter Briggs, Wenju Cai, Francis Chiew, Harry Hendon, Michael Raupach, Bertrand Timbal, QJ Wang

Project Teams, by organisation

CSIRO: Stephen Charles, Tim Cowan, Randall Donohue, Guobin Fu, Vanessa Haverd, David Kent, Edward King, Dewi Kirono, Yun Li, Timothy McVicar, Matt Paget, Nicholas Potter, David Robertson, Ian Smith, Jin Teng, Kirien Whan
Bureau of Meteorology: Oscar Alves, Robert Fawcett, Elodie Fernandez, Eun-Pa Lim, Guo Liu, Chris Lucas, Guomin Wang

Science Panel Graeme Pearman (Independent Chairperson), Jason Alexandra (Murray–Darling Basin Authority), Tom Keenan (Bureau of Meteorology), Michael Manton (Independent), Michael Martin / Michael Zuckerman (Department of Climate Change and Energy Efficiency), Rae Moran (Victorian Department of Sustainability and Environment), Glen Walker (CSIRO)

Steering Committee John Higgins / Chris Johnston (Chairperson, Department of Climate Change and Energy Efficiency), Campbell Fitzpatrick (Victorian Department of Sustainability and Environment), Fraser McLeod / Jody Swirepik (Murray–Darling Basin Authority), Ian Prosser / Warwick McDonald (CSIRO), Neville Smith (Bureau of Meteorology)

© Copyright Commonwealth Scientific and Industrial Research Organisation (CSIRO Australia), 2010

Important notice:

All rights are reserved and no part of this publication covered by copyright may be reproduced or copied in any form or by any means except with the written permission of CSIRO.

The results and analyses contained in this Report are based on a number of technical, circumstantial or otherwise specified assumptions and parameters. The user must make its own assessment of the suitability for its use of the information or material contained in or generated from the Report. To the extent permitted by law, CSIRO excludes all liability to any party for expenses, losses, damages and costs arising directly or indirectly from using this Report.

Address and contact details:

CSIRO Water for a Healthy Country Flagship
Ph (+61 2) 62465617 Fax (+61 2) 62465800
Email: seaci@csiro.au

EXECUTIVE SUMMARY

The South Eastern Australian Climate Initiative (SEACI) was established in 2005 to investigate the causes, impacts and prediction of climate variability and change in south-eastern Australia. The first three years of SEACI made progress in characterising and explaining the nature and causes of the recent drought, produced climate and runoff projections out to 2030, and improved seasonal forecasts of rainfall and runoff across south-eastern Australia.

These research findings are summarised in the report *Climate variability and change in south-eastern Australia: A synthesis of findings from Phase 1 of the South Eastern Australian Climate Initiative (SEACI)* available for download from <http://www.seaci.org>.

Research in Phase 2 of SEACI is building on the findings of Phase 1. It is a three-year, \$9 million research partnership between the Murray–Darling Basin Authority, the Victorian Government Department of Sustainability and Environment, CSIRO Water for a Healthy Country Flagship, the Bureau of Meteorology and the Australian Government Department of Climate Change and Energy Efficiency. The SEACI study area incorporates the Murray–Darling Basin, the state of Victoria and southern South Australia, including the Eyre Peninsula.

Research in Phase 2 of SEACI is conducted through three related themes. This report summarises the progress made in the first year (2009/10) of Phase 2 of SEACI.

Theme 1: Understanding past hydroclimate variability and change in south-eastern Australia

Research in Theme 1 is contributing to a better understanding of the factors that influence climate and streamflow within south-eastern Australia, with a focus on the recent drought. The recent drought included 180 consecutive months (January 1995 to February 2010) without a ‘very wet’ month, that is, a month with rainfall greater than the 90th percentile of the long-term rainfall for that month. The recent drought is considered more severe than the two major historical droughts of the last 140 years (the Federation and World War II droughts) on any time scale between 3 and 20 years. Unlike historical droughts, much of the decline in rainfall has been in autumn, with decreases also occurring in winter and spring. In recent decades the wet season has become shorter due to a later commencement in autumn and an earlier ending in spring.

Ocean-atmosphere interactions in the Indian, Pacific and Southern Oceans, including the El Niño – Southern Oscillation (ENSO), the Indian Ocean Dipole (IOD) and the Southern Annular Mode (SAM), affect rainfall in south-eastern Australia. Recent research has updated and expanded an earlier analysis of the individual and combined impacts of ENSO and the IOD on Australian rainfall. Findings include a distinct asymmetry in the impacts of opposite phases of both ENSO and the IOD on Australian hydrology, and significant differences between the dominant tropical drivers of drought on inter-annual (ENSO and IOD both important) and decadal (IOD more important) timescales. Research has also indicated a link between an observed trend towards more frequent positive IOD (dry) events since 1950 and climate change. An examination of relationships between various climate indices and water-balance components showed that the tripole index (which was developed in Phase 1 of SEACI and captures differences in tropical sea surface temperatures between the Indian Ocean, the seas to the north of Australia and the Pacific Ocean) has the largest association with rainfall and soil moisture.

Theme 2: Long-term hydroclimate projections in south-eastern Australia

Research in Theme 2 aims to improve projections of climate and streamflow out to the year 2100 for south-eastern Australia. Research in Theme 2 is assessing and selecting global climate models (GCMs) for hydrological application. This year, research focused on GCM simulation of the sub-tropical ridge (STR) – a region of high atmospheric pressure that resides over south-eastern Australia and is associated with clear skies and therefore dry conditions, which research in Phase 1 of SEACI identified as a major driver of rainfall in south-eastern Australia. The GCMs projections show that the STR over Australia is likely to shift further south and that pressures along the ridge are likely to increase, and this will lead to lower rainfall across south-eastern Australia. At present, however, very few GCMs accurately simulate the STR and the STR-rainfall relationship. Further research is necessary to evaluate model performance, with a view to determining whether improved climate change projections can be obtained by using a selected suite of models and appropriate regional downscaling techniques.

During the recent drought in south-eastern Australia, streamflow was lower than would be expected based on the historical relationship between streamflow and mean annual rainfall. Hydrological modelling experiments for the Campaspe River found that 58 percent of the decline in streamflow can be explained by the reduction in mean annual rainfall. A further 15 percent of the reduction is attributed to lack of very wet months and years, and 12 percent to changed rainfall seasonality. This indicates that the changing climate is bringing about a shift in the nature of the relationship between rainfall, temperature and runoff.

A degree of uncertainty is associated with predicting future water availability. Research in Theme 2 has shown that the largest source of uncertainty in predicting future water availability comes from the GCM projections of future rainfall. Downscaling of GCM rainfall projections to the catchment scale is another significant, but lesser, source of uncertainty, while outputs from rainfall-runoff models have even less uncertainty associated with them. For south-eastern Australia, rainfall-runoff models calibrated with more than 20 years of historical data can generally be used for climate impact studies when the projected change in mean annual rainfall is less than around 15 percent. For larger changes into the future, hydrological models need to account for potential changes in the rainfall-temperature-runoff relationship and dominant hydrological processes in a warmer, drier and higher CO₂ environment.

Theme 3: Seasonal hydroclimate prediction in south-eastern Australia

Research in Theme 3 is exploring the potential for improving seasonal forecasts of rainfall and streamflow. This work produced two new versions of the Predictive Ocean Atmosphere model for Australia, (POAMA; p24a and p24b), and compared rainfall forecasts using these new versions to those using the original version (p15b). New versions of POAMA showed skill that is similar to or higher than the original version in predicting above median rainfall in winter, spring and summer over south-eastern Australia. In addition, combining results from the three models into a multi-model mean resulted in a greater percentage of correct predictions for rainfall across the region compared to any of the individual models for all four seasons. In general, results of rainfall projections for one month ahead were quite good for autumn and spring, but were poorer for winter. Projections for the summer months produced results that were little better than chance. Results for shorter lead times were better than those for 3 months ahead.

In Phase 1 of SEACI, a modelling approach (referred to as the Bayesian joint probability) was developed to provide forecasts of seasonal streamflow at multiple sites. This approach has now been adopted by the Bureau of Meteorology (BoM) for forecasting streamflow up to 3 months ahead. An experimental seasonal streamflow forecasting service, available via the BoM website, was developed in collaboration between the BoM, CSIRO and water managers. The public release of the operational forecast service is scheduled for January 2011. Research over the past year has involved further development of this forecasting approach and improvement in the methods for forecast verification. Predictive skill has been shown to vary with catchment and season, with most of the forecast skill being derived from predictors representing initial catchment conditions. In contrast, predictors of future climate make only a small contribution to the predictive skill and only for the late-winter and spring seasons.

CONTENTS

Executive Summary.....	I
Contents.....	IV
Figures.....	V
Tables.....	IX
Acronyms.....	X
Chapter 1: Introduction	1
Chapter 2: Project 1.1a.....	5
Chapter 3: Project 1.1b.....	27
Chapter 4: Project 1.2.....	39
Chapter 5: Project 2.1	51
Chapter 6: Project 2.2.....	65
Chapter 7: Project 3.1	73
Chapter 8: Project 3.2.....	87
Chapter 9: Next Steps.....	93
References	95
List Of Publications Arising From SEACI Research In 2009/10.....	99

FIGURES

Figure 1. The study area of the South Eastern Australian Climate Initiative.....	1
Figure 2. Locations of the 14 stations included in the south-eastern Australian network. Composites made of several individual stations are indicated by red circles. See Table 1 for the corresponding Bureau of Meteorology station numbers	7
Figure 3. South-eastern Australian average monthly rainfall values (in millimetres) using the 14-station south-eastern Australian network versus the 5-kilometre Australian Water Availability Project rainfall analyses, for 1900–2009. The slope of the best fit line and the percentage of explained variance are shown in the bottom right corner	8
Figure 4. Annual rainfall totals (1872–2009, in millimetres) based on the 14-station south-eastern Australian network (blue bars) and 11-year moving average (black line). Also shown is the 11-year running mean from the high-resolution Australian Water Availability Project rainfall analyses averaged over south-eastern Australia (red line) 9	9
Figure 5. Drought depth duration based on the annual rainfall average in the 14-station network for 20-year periods for the recent drought (red line); the World War II drought (green line); the Federation drought (blue line); the mean of the Federation and World War II droughts (red dashed line); the average of 20-year periods after randomisation of 138 years of data (black short-dashed line); and the average of the worst 20-year periods after randomisation of 138 years of data (black long-dashed line).....	10
Figure 6. Drought depth duration based on the seasonal rainfall average in the 14-station network for 20-year periods for the recent drought (red line); the World War II drought (green line); the Federation drought (blue line); the mean of the Federation and World War II droughts (red dashed line); the average of 20-year periods after randomisation of 138 years of data (black dotted line); and the average of the worst 20-year periods after randomisation of 138 years of data (black dashed line).....	11
Figure 7. Number of months per year with rainfall above the 90th percentile (updated to May 2010). Percentiles are based on 20th-century (1900–1999) climatology and are computed month by month.....	15
Figure 8. Monthly standard deviations in south-eastern Australian rainfall during the 20th century (blue bars) normalised by the monthly means. The y-axis for the raw standard deviation is shown on the left (in millimetres/month) and on the right for the normalised values (in percent).....	15
Figure 9. Number of rain days (above 0.2 mm) for each calendar month recorded at four locations across south-eastern Australia, in (a) absolute terms (days), and (b) as a percentage of the annual mean total number of rain days. The length of the observation record varies between 137 and 155 years for the four locations	17
Figure 10. Largest observed daily rainfall for each calendar month recorded at four locations across south-eastern Australia, in (a) absolute terms (millimetres), and (b) as a percentage of the monthly mean values. Percentages above 400 percent (and up to 800 percent) in (b) were truncated. The length of the observation record varies between 137 and 155 years for the four locations.....	18
Figure 11. Standard three-cell model of the mean meridional circulation during December, January and February based on the vertical integration of the zonal-mean meridional wind. Flow is counter-clockwise around a positive centre.....	20
Figure 12. Schematic view of the mean meridional circulation	21
Figure 13. Annual cycle of rainfall over Victoria averaged over 1950–1979 (blue) and 1980–2007 (red). The rainfall climatology is based on daily rainfall outputs from station data averaged over Victoria (140 to 150 °E, 32 to 40 °S), smoothed using a 30-day running average	30

Figure 14. Maps of autumn (Mar-Apr-May) rainfall trends from 24 CMIP3 models for 1950–1999, compared to observations from 1950–2008 (bottom right-hand panel). Units are percent of long-term average rainfall (1950–1999). Red indicates decrease in autumn rainfall, while blue indicates increase.....	31
Figure 15. The density of autumn extra-tropical systems in southern Australia (94 to 174 °E, 30 to 50 °S) over 1950–2009, as defined by the Bureau of Meteorology. The top panel shows the density of low-pressure systems (extra-tropical cyclones) and the bottom panel shows the density of high-pressure systems (extra-tropical anti-cyclones)	32
Figure 16. One-standard-deviation anomalies in spring (Sep-Oct-Nov) of (left panels) sea-surface temperature (°C per degree global warming), and (right panels) outgoing longwave radiation (watts per square metre per degree global warming), associated with (first row) El Niño – Southern Oscillation, (second row) El Niño – Southern Oscillation with the Indian Ocean Dipole removed, (third row) Indian Ocean Dipole with El Niño – Southern Oscillation removed, and (fourth row) Indian Ocean Dipole. Bold green contours show the statistically significant correlations at the 95 percent confidence interval, which is ± 0.349 for 30 years (1979–2008).....	33
Figure 17. Schematic illustration of the typical processes associated with the (a) Indian Ocean Dipole and (b) El Niño – Southern Oscillation for spring (Sep-Oct-Nov). Shaded blue areas indicate regions of increased convection, and red areas indicate regions of decreased convection. Blue contours indicate anomalously low upper-level height, while red contours indicate anomalously high upper-level height. This description is for El Niño and positive Indian Ocean Dipole events, but the opposite description is true for La Niña and negative Indian Ocean Dipole events. The dashed lines trace the wave-trains: grey for the eastern Indian Ocean wave-train (EIO) and green for the western Indian Ocean wave-train (WIO)	34
Figure 18. Time series of the Indian Ocean Dipole Mode Index (DMI) averaged over an ensemble of 19 individual models (green) and a linear trend line (red). The grey shaded area indicates inter-model variations, shown as the mean \pm the one-standard-deviation value of the inter-model variations. The ensemble trend rate is 0.016 per year, and the correlation coefficient is 0.74 (Cai et al. (2009c)).....	35
Figure 19. The relationship between the winter-spring Murray–Darling Basin inflow (black) and predicted inflow based on a simple regression model based on climate drivers (red). The results for 1950–1989 correspond to the training period, while the results for 1990–2007 correspond to the verification period. The blue shaded area indicates the upper and lower bounds of the 95 percent confidence interval for the verified predictions.....	36
Figure 20. Monthly time series of differences in rainfall (mm/d) between two versions of the Bureau of Meteorology Australian Water Availability Project datasets (V3 minus V1) for three sub-divisions of the Murray–Darling Basin by rainfall.....	41
Figure 21. Annual Australian Water Availability Project total runoff (local discharge, in mm/d) for three sub-divisions of the Murray–Darling Basin by rainfall.....	42
Figure 22. Composite of Australian Water Availability Project lower-layer soil-moisture anomalies in the different El Niño – Southern Oscillation and Indian Ocean Dipole categories: El Niño; La Niña; and positive or negative Indian Ocean Dipole. The number of members (n) in each category are indicated. Anomalies are for the June to October months over the period 1900–2006. The only anomalies that are shown are those which are significant at the 80 percent confidence level as estimated by a two-tailed t-test. Figure adapted from Ummenhofer et al., (in press).....	44
Figure 23. Zero-lag correlations between monthly winter (Jun-Jul-Aug) upper-layer soil moisture and rainfall with El Niño – Southern Oscillation (ENSO), the Indian Ocean Dipole (IOD) and the tripole index.....	45
Figure 24. Simultaneous correlations between rainfall and indices for three modes of tropical sea-surface temperature variability: El Niño – Southern Oscillation (ENSO), the Indian Ocean Dipole (IOD) and the tripole index. Results are shown for winter (Jun-Jul-Aug) and spring (Sep-Oct-Nov), as these are the seasons when tropical variability is the most active. Due to the use of northern Australian sea-surface temperature in its definition, the tripole index has the largest association with rainfall	46
Figure 25. Modelling climate change impact on runoff	52

Figure 26. The annual cycle of sub-tropical ridge intensity (STR-intensity) and sub-tropical ridge position (STR-position). Observations from NCEP reanalysis are shown in green; observations from the Bureau of Meteorology are shown in blue; and modelled results using 23 global climate models (and a multi-model mean) are shown in red	55
Figure 27. (a) Projected annual cycle of sub-tropical ridge intensity (STR-intensity) and sub-tropical ridge position (STR-position) for five time periods, based on a multi-model mean (using 23 models). (b) Observed and modelled STR-intensity (smoothed) for 1900–2100.....	56
Figure 28. Projected percentage changes in rainfall per degree global warming for selected regions from south-eastern Australia: (a) Murray–Darling Basin; (b) northern Murray–Darling Basin; (c) south-west eastern Australia; and (d) the eastern seaboard. Different numbers of global climate models are used, based on their ability to reproduce the observed sub-tropical ridge.....	57
Figure 29. Percentage change in future mean annual runoff (for a 1 °C global warming) modelled by five rainfall-runoff models informed by rainfall projections from 15 global climate models.....	59
Figure 30. Range of percentage change in future mean annual, summer and winter runoff (for a 1 °C global warming) from five rainfall-runoff models and 15 global climate models averaged across south-eastern Australia.....	60
Figure 31. Percentage change in runoff characteristics for the future period (2046–2065) relative to the historical period (1981–2000) modelled by the SIMHYD rainfall-runoff model with daily rainfall downscaled using five downscaling models informed by three global climate models. The data points show the weighted values for the eight catchments, weighted by the values of the variables on the x-axis.....	62
Figure 32. Modelling climate change impact on runoff	66
Figure 33. Attribution of reduction in mean annual runoff over 1997–2008 compared to the long term in the Campaspe River basin	68
Figure 34. Reduction in daily modelled runoffs (measured by the Nash-Sutcliffe efficiency (NSE)) in the four rainfall-runoff models when parameter values from calibration against another period are used compared to the calibration results. Reduction in NSE is plotted against the percentage difference in the mean annual rainfall in the two modelling periods	69
Figure 35. Climatic water limitation across south-eastern Australia. (a) The annual wetness index (precipitation (P) divided by Penman potential evaporation (Ep)), with energy-limited areas in blue. (b) The average number of months within the year for which the evaporative demand exceeds precipitation.....	70
Figure 36. Differences between observed and predicted catchment streamflow trends (dQ/dt). Green indicates energy-limited catchments and blue indicates water-limited catchments (based on the annual average climatology from 1981–2006).....	71
Figure 37. Regression of monthly sea-surface temperature anomaly on the NINO3 Index (NINO3), El Niño Modoki Index (EMI), and Indian Ocean Dipole Mode Index (DMI)	74
Figure 38. Correlation of seasonally averaged south-eastern Australian mean rainfall (left) and maximum temperature (Tmax) (right) with the NINO3 Index (NINO3), El Niño Modoki Index (EMI), and Indian Ocean Dipole Mode Index (DMI) as a function of calendar month.....	75
Figure 39. Correlation of predicted NINO3 Index (NINO3), El Niño Modoki Index (EMI), and Indian Ocean Dipole Mode Index (DMI) from POAMA1.5b (p15b), non-flux-corrected POAMA2 (p24a), and flux-corrected POAMA2 (p24b) verified against respective observed indices using the HadISST dataset.....	76
Figure 40. Normalised root-mean-square error (NRMSE) of predicted NINO3 Index (NINO3), El Niño Modoki Index (EMI), and Indian Ocean Dipole Mode Index (DMI) from POAMA1.5b (p15b), non-flux-corrected POAMA2 (p24a), and flux-corrected POAMA2 (p24b) verified against respective observed indices using the HadISST dataset.....	77

Figure 41. Normalised standard deviation (NSTDDEV) of predicted NINO3 Index (NINO3), El Niño Modoki Index (EMI), and Indian Ocean Dipole Mode Index (DMI) from POAMA1.5b (p15b), non-flux-corrected POAMA2 (p24a), and flux-corrected POAMA2 (p24b) verified against respective observed indices using the HadISST dataset	78
Figure 42. Percentage of forecasts which correctly predict rainfall being above the median at a lead time of zero months using (a) POAMA1.5b (p15b); (b) non-flux-corrected POAMA2 (p24a); (c) flux-corrected POAMA2 (p24b); and (d) the multi-model ensemble (MME). Each row shows results for 3-month moving windows.....	79
Figure 43. Mean percentage of forecasts (averaged over south-eastern Australia) which correctly predict rainfall being above the median using POAMA1.5b (p15b); non-flux-corrected POAMA2 (p24a); flux-corrected POAMA2 (p24b); and the multi-model ensemble (MME) at lead times of zero to 3 months.....	80
Figure 44. Percentage of forecasts which correctly predict rainfall being above the median at a lead time of 3 months using (a) POAMA1.5b (p15b); (b) non-flux-corrected POAMA2 (p24a); (c) flux-corrected POAMA2 (p24b); and (d) the multi-model ensemble (MME). Each row shows results for 3-month moving windows.....	81
Figure 45. Percentage of forecasts which correctly predict maximum temperature (Tmax) being above the median at a lead time of zero months using (a) POAMA1.5b (p15b); (b) non-flux-corrected POAMA2 (p24a); (c) flux-corrected POAMA2 (p24b); and (d) the multi-model ensemble (MME). Each row shows results for 3-month moving windows	82
Figure 46. Percentage of forecasts which correctly predict maximum temperature (Tmax) being above the median at a lead time of 3 months using (a) POAMA1.5b (p15b); (b) non-flux-corrected POAMA2 (p24a); (c) flux-corrected POAMA2 (p24b); and (d) the multi-model ensemble (MME). Each row shows results for 3-month moving windows	83
Figure 47. Seasonal streamflow forecast issued by the Bureau of Meteorology for total flows of the Ovens River to the Murray River for July to September 2009. The probabilistic forecast was produced by using the Bayesian joint probability modelling approach.....	91

TABLES

Table 1. Names and Bureau of Meteorology station numbers for the 14 stations used to reconstruct pre-Federation rainfall across south-eastern Australia. Multiple station numbers denote composites of neighbouring stations 7

Table 2. South-eastern Australian rainfall anomalies in percentage terms calculated relative to the 1872–2009 long-term mean using the 14-station network. Both annual and seasonal means are shown. Anomalies are calculated for the three long-term droughts using the annual mean for the lowest 11-year and 13-year period within a 20-year period encompassing each drought..... 9

Table 3. Percentages by which the rainfall during the last 20 years needs to be increased for the recent period to be in line with randomly generated average and worst 20-year periods.....13

Table 4. Pearson correlation coefficients between monthly 1997–2009 rainfall deficit and monthly 20th-century rainfall variability for the eight individual months from March to October (numbers in brackets are for the 12 calendar months). Bold and italic figures are significant at the 99 percent and 95 percent level, respectively16

Table 5. Correlation between winter-spring (Jun-Jul-Aug-Sep-Oct-Nov) Murray–Darling Basin inflow and climate drivers averaged over May to October (MJJASO) and June to November (JJASON) during 1950–2007. Values significant at the 0.05 level (95 percent confidence level) are in bold. Climate drivers include the blocking index, El Niño – Southern Oscillation (NINO3.4), Indian Ocean Dipole (DMI), sub-tropical ridge intensity (STRI), and the Southern Annular Mode (SAM).36

ACRONYMS

AWAP	Australian Water Availability Project
BJP	Bayesian joint probability
BoM	Bureau of Meteorology
CAWCR	Centre for Australian Weather and Climate Research
CCAM	cubic conformal atmospheric model
DDD	drought depth duration
DMI	Indian Ocean Dipole Mode Index
EMI	El Niño Modoki Index
ENSO	El Niño – Southern Oscillation
Ep	potential evaporation
ESCCI	Eastern Seaboard Climate Change Initiative
GCM	global climate model
IOD	Indian Ocean Dipole
IPCC AR4	Intergovernmental Panel on Climate Change Fourth Assessment Report
MDB	Murray–Darling Basin
MMC	mean meridional circulation
MME	multi-model ensemble
MSLP	mean sea-level pressure
NCC	National Climate Centre
NCEP	National Center for Environmental Prediction
NHMM	non-homogenous hidden Markov Model
NSE	Nash-Sutcliffe efficiency
PEODAS	POAMA Ensemble Ocean Data Assimilation System
POAMA	Predictive Ocean Atmosphere Model for Australia
P _s BF	pseudo Bayes factor
SAM	Southern Annular Mode
SEA	south-eastern Australia
SEACI	South Eastern Australian Climate Initiative
SST	sea-surface temperature
STR	sub-tropical ridge
T _{max}	maximum temperature
WIRADA	Water Information Research and Development Alliance

CHAPTER 1: INTRODUCTION

The South Eastern Australian Climate Initiative

Phase 2 of the South Eastern Australian Climate Initiative (SEACI) is a three-year, \$9 million research program investigating the causes and impacts of climate change and climate variability across south-eastern Australia. The SEACI geographical study area incorporates the Murray–Darling Basin, the state of Victoria and southern South Australia, including the Eyre Peninsula, as shown in Figure 1.

Planning for future management of Australia’s water resources requires an understanding of the future state of Australia’s climate. This program aims to deliver a holistic and better integrated understanding of climate change and climate variability across south-eastern Australia to support water managers and policy makers.

The research program includes studies of the nature and causes of climate variability on time scales from weeks to decades. This range of scales is relevant to the stakeholders. Issues on short-term time scales (weeks and months) arise in the operational management of water, while horizons for water resources planning and policy are of a long-term nature (years and decades).

SEACI is a partnership between CSIRO Water for a Healthy Country Flagship, the Australian Government Department of Climate Change and Energy Efficiency, the Murray–Darling Basin Authority, the Australian Government Bureau of Meteorology and the Victorian Department of Sustainability and Environment. CSIRO is the managing agency.

A Steering Committee, comprising representatives of each partner agency, sets and monitors the strategic direction of SEACI. In 2009/10 a representative from the Department of Climate Change and Energy Efficiency chaired the Steering Committee (initially John Higgins, followed by Chris Johnston). The Steering Committee is supported by a Science Panel, which provides advice on implementation of the initiative. The Science Panel is chaired by an independent expert, Dr Graeme Pearman.

In 2009/10 a new Program Director, Dr David Post, was appointed to SEACI. Dr Post is a hydrologist with CSIRO, and was previously the Project Leader of the Tasmania Sustainable Yields Project.

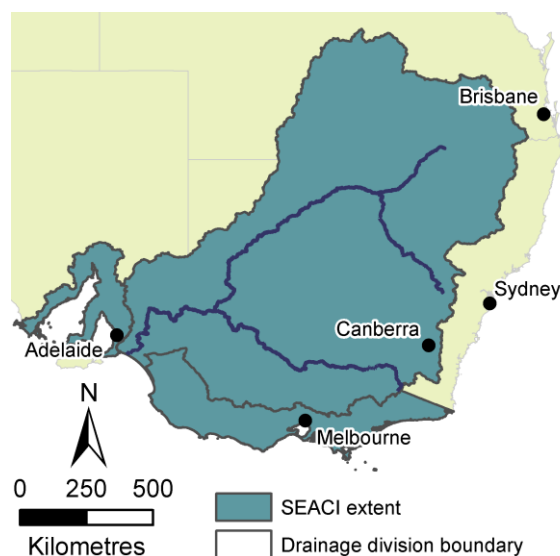


Figure 1. The study area of the South Eastern Australian Climate Initiative

Research context

The variability of Australia's climate has always been a challenge for water management and agricultural industries. Global climate change is now recognised as a threat to water resources, agriculture and natural ecosystems in many parts of the world. In south-eastern Australia, temperatures have been rising steadily and rainfall has been low since the 1990s. Similar rainfall declines started in the mid-1970s in south-west Western Australia, prompting the establishment of the Indian Ocean Climate Initiative (IOCI) in 1997. IOCI research focused on understanding variability and change in the region's climate, and showed that climate change is likely to be a significant factor in the observed changes in the region. The clear benefits of IOCI motivated the establishment of SEACI.

Findings from Phase 1 of the South Eastern Australian Climate Initiative

Research in Phase 1 of SEACI included an investigation into the nature and causes of the recent drought which has occurred since 1997 in south-eastern Australia. Research concluded that the recent drought is unprecedented with regards to its extent, the low degree of inter-annual rainfall variability, and the seasons in which the rainfall has declined. In particular, SEACI research found that throughout the recent drought the rainfall decline was greatest in the autumn months, unlike in previous droughts where the rainfall decline was greatest in winter and spring.

The sub-tropical ridge (STR) is a band of high pressure which affects rainfall across southern Australia. SEACI research found a strong relationship between increased pressures along the STR and the recent rainfall decline. Further, modelling studies conducted within SEACI showed that this observed intensification of the STR could only be reproduced when anthropogenic forcing was included. This suggests a link between global warming and the recent rainfall decline in south-eastern Australia.

Research throughout Phase 1 of SEACI also showed that the 13 percent decline in rainfall in the southern Murray–Darling Basin led to a 44 percent reduction in streamflow. The magnitude of this reduction in streamflow was greater than expected. This is thought to be likely due to the absence of wet years over the decade, and to the seasons in which the rainfall has declined. The decline in autumn rainfall has meant that winter rains must moisten the soil before any useful streamflow can begin. It is expected that in the future this effect will be amplified as average temperatures across the region continue to rise due to climate change.

Phase 1 of SEACI also achieved improvements to the coupled atmosphere–ocean–land climate model (POAMA) to increase the accuracy of seasonal forecasting, especially for south-eastern Australia. Ongoing research efforts will further refine POAMA and aim to increase the accuracy of prediction at longer lead times.

Research in Phase 2 of SEACI is building upon the findings and progress made in Phase 1. Phase 2 is addressing key research questions through three linked research themes, described below.

Details of the findings of Phase 1 of SEACI can be found in:

CSIRO (2010) Climate variability and change in south-eastern Australia: a synthesis of findings from Phase 1 of the South Eastern Australian Climate Initiative (SEACI). SEACI report, 36 pp.

<http://www.seaci.org/publications/documents/SEACI-1%20Reports/Phase1_SynthesisReport.pdf>

Research themes

Theme 1: Understanding past hydroclimate variability and change in south-eastern Australia

Research in Theme 1 will lead to a better understanding of the factors that drive changes in both climate and streamflow within the region. The projects aim to understand and attribute causes of observed climate change in south-eastern Australia, as well as diagnose the relationships between climate variability and the water balance.

The projects in Theme 1 are:

- Project 1.1a: Understanding and attributing climate change in south-eastern Australia
- Project 1.1b: Dynamics of south-eastern Australian rainfall variability and change
- Project 1.2: Impact of climate variability and change on the water balance.

Theme 2: Long-term hydroclimate projections in south-eastern Australia

Research in Theme 2 will lead to improved hydroclimate projections for south-eastern Australia. The research aims to identify the most suitable global climate models (GCMs), assess methods to downscale projections from GCMs to obtain catchment-scale climate series, and adapt hydrological models to represent changed rainfall–temperature–streamflow relationships and dominant hydrological processes in a warmer, drier environment with increased levels of CO₂.

The projects in Theme 2 are:

- Project 2.1: Climate change projections
- Project 2.2: Hydroclimate impacts for south-eastern Australia.

Theme 3: Seasonal hydroclimate prediction in south-eastern Australia

Theme 3 is aiming to improve predictions of rainfall and streamflow in south-eastern Australia, extending to the development of operational products. It assesses the skill of models in producing useful predictions of streamflow. Additionally, it is further developing modelling approaches and assessing the utility of seasonal forecasts to improve the skill of hydrological modelling for south-eastern Australia.

The projects in Theme 3 are:

- Project 3.1: Advancing seasonal predictions for south-eastern Australia
- Project 3.2: Hydrological application of seasonal predictions.

About this report

This report provides detailed information about the progress made in each of the seven SEACI research projects in the 2009/10 financial year. Publications arising from this year's research are listed at the end of the document.

CHAPTER 2: PROJECT 1.1a

Understanding and attributing climate change in south-eastern Australia

Bertrand Timbal, Chris Lucas, Harry Hendon and Robert Fawcett

Abstract

Progress has been made towards better understanding and attribution of the recent rainfall deficiency across south-eastern Australia (SEA) by:

- improving the characterisation of the abnormality of the recent period by extending our ability to use the instrumental record back to 1872, thus providing a better comparison between the recent deficiency and that of the Federation drought
- characterising the annual cycle of the natural variability of rainfall in SEA and its relationship with the annual cycle of the recent rainfall deficiency; discussing the relative importance of weather noise within the natural variability; and characterising daily rainfall across SEA
- reviewing the existing literature regarding the meridional component of the general circulation of the atmosphere, its observed changes and its likely response to global warming, with a focus on the known relevant features which influence SEA climate (significant sub-tropical ridge (STR) intensification and its observed relationship with global warming).

Background

Phase 1 of SEACI made substantial progress in documenting recent climate changes in south-eastern Australia (SEA) and in identifying the large-scale circulations that control the regional climate of the region. The role of large-scale phenomena that significantly influence the natural variability of the climate of SEA was clarified. These influential phenomena include the El Niño – Southern Oscillation (ENSO), the Indian Ocean Dipole (IOD), and the Southern Annular Mode (SAM).

A key finding was that the recent decline in rainfall observed in SEA has occurred predominantly in the autumn and early winter, and that much of this decline is accounted for primarily by an increased intensity of the sub-tropical ridge (STR-intensity). During Phase 1 of SEACI it became clearer that SEA is influenced by ongoing global warming. In particular, it was established that the rise in STR-intensity followed the rise of global temperature, but while the STR-intensity and STR-position are convenient diagnostics closely linked to rainfall in SEA, the causality of the relationship between temperature and STR remains to be established and requires further investigation.

Objectives

The project objectives for the 2009/10 financial year were to:

- describe the key features of the observed rainfall decline including its seasonality, spatial characteristics (e.g. north–south and east–west features), and changes in rainfall amounts at daily time scales; and compare these features with those of past dry periods, including the World War II and Federation droughts
- contribute to a better understanding of interactions between the meridional circulations (in particular the Hadley circulation) and other variables, including: surface indicators (primarily the intensity and position of the STR); tropical zonal circulations (the Walker circulation and ENSO); and other drivers such as high-latitude circulation (including the SAM).

Methods

The work continued to advance the description (undertaken in Phase 1 of SEACI) of key features of the observed rainfall decline, including both its seasonal and spatial characteristics. It compared these features with those of past dry periods, including the World War II and Federation droughts. The novelty lies in relating these to observed changes in the STR and the global meridional circulation (Hadley and Ferrel cells) and the tropical zonal circulation (Walker circulation).

Another important development was a comprehensive review of the rapidly growing literature relevant to the scientific questions posed in this project (e.g. the impact of global warming on meridional circulations, and interactions between zonal and meridional circulations).

Results

Long-term perspective on south-eastern Australian rainfall

As part of Phase 1 of SEACI, the recent drought was compared to the World War II drought and an attempt was made to compare both to the Federation drought. Unfortunately, the Bureau of Meteorology (BoM) gridded rainfall analyses, such as the latest Australian Water Availability Project (AWAP) monthly gridded rainfall dataset (Jones et al., 2009), do not extend prior to 1900 due to lack of sufficient observations at the national scale. Other products – such as the SILO data drill – do, but the lack of sufficient observations makes their use in studying the Federation drought dubious.

Instead, we chose to construct a network based on a limited number of stations with long continuous records to depict the monthly variability across SEA (continental Australia south of 33.5 °S and east of 135.5 °E) following the methodology described by Trewin and Fawcett (2010) for the Murray–Darling Basin. Fourteen stations were selected (some are composites of several neighbouring sites with enough overlap to ensure these composites are meaningful (Table 1 and Figure 2)). This provides a monthly rainfall reconstruction for SEA as far back as 1872.

Table 1. Names and Bureau of Meteorology station numbers for the 14 stations used to reconstruct pre-Federation rainfall across south-eastern Australia. Multiple station numbers denote composites of neighbouring stations

Bureau station number	Location (state)
090015	Cape Otway (Vic)
087046	Mount Buninyong (Vic)
070009	Bukalong (NSW)
047053	Wentworth (NSW)
074128	Deniliquin (NSW)
084016	Gabo Island (SA)
066062	Sydney (NSW)
075048 / 077025	Swan Hill (Vic)
081003 / 081086	Bendigo (Vic)
026020 / 026021	Mount Gambier (SA)
085133 / 085020	Sale (Vic)
023000 / 023011	Adelaide (SA)
026023 / 026075	Naracoorte (SA)
072151 / 073127 / 072042	Wagga Wagga (NSW)

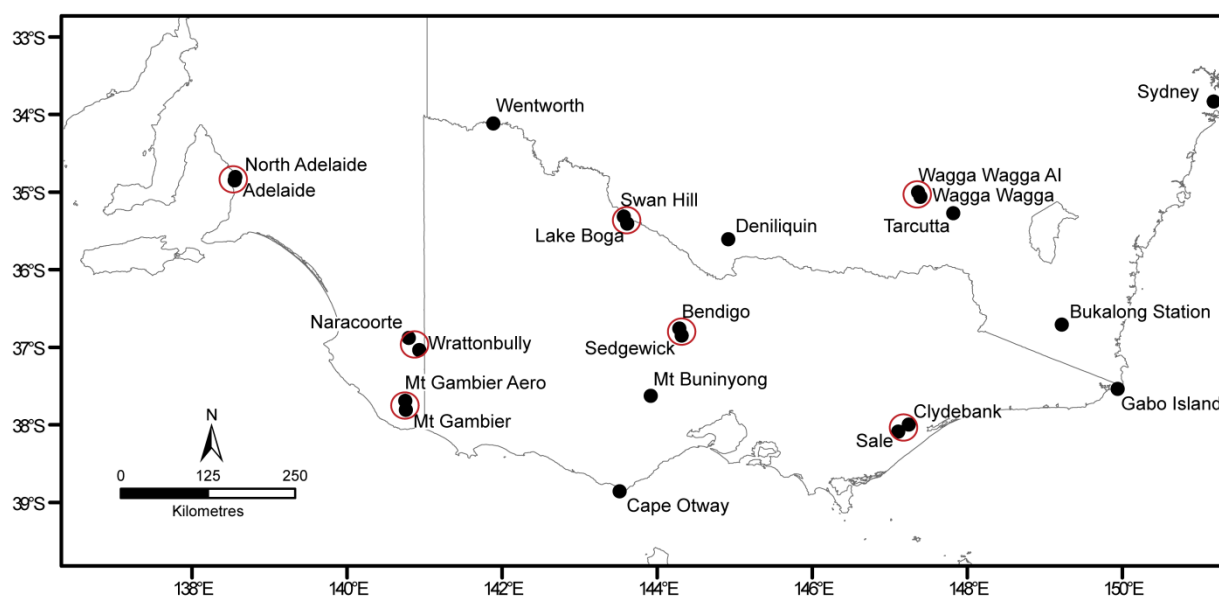


Figure 2. Locations of the 14 stations included in the south-eastern Australian network. Composites made of several individual stations are indicated by red circles. See Table 1 for the corresponding Bureau of Meteorology station numbers

This network captures 95 percent of the month-to-month variability of rainfall in SEA as obtained by a straight averaging of the 0.05° AWAP analyses across SEA (Figure 3) during the overlapping period, 1900–2009. Annual values for the SEA 14-station network and the AWAP average are very close and the 11-year running means for the two methods are nearly indistinguishable (Figure 4).

Figure 4 and Table 2 enable an appropriate comparison of the Federation drought with the World War II and recent droughts. Low rainfall was recorded in 1895–1914. Relative to the 1872–2009 mean climatology, the deficiency was –7.7 percent for the 13-year period 1897–1909, and –9.4 percent for the 11-year period 1895–1905. For both periods, the Federation drought was less severe than the recent drought and the World War II drought.

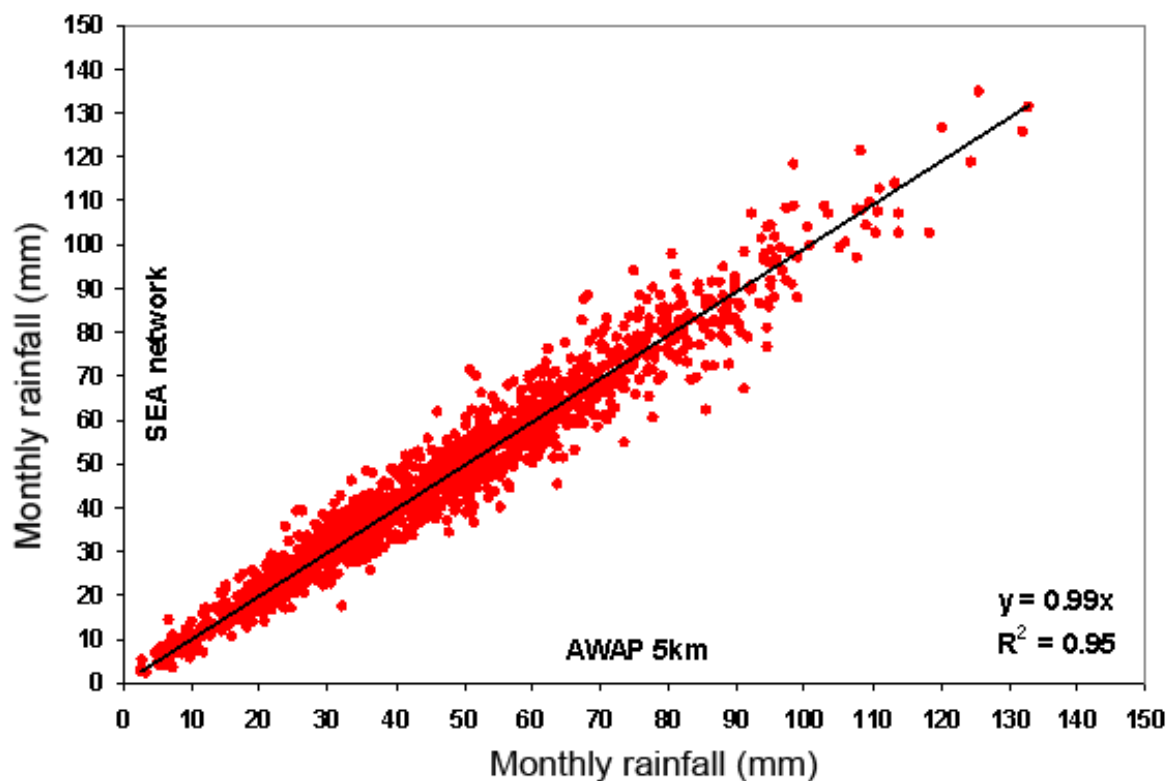


Figure 3. South-eastern Australian average monthly rainfall values (in millimetres) using the 14-station south-eastern Australian network versus the 5-kilometre Australian Water Availability Project rainfall analyses, for 1900–2009. The slope of the best fit line and the percentage of explained variance are shown in the bottom right corner

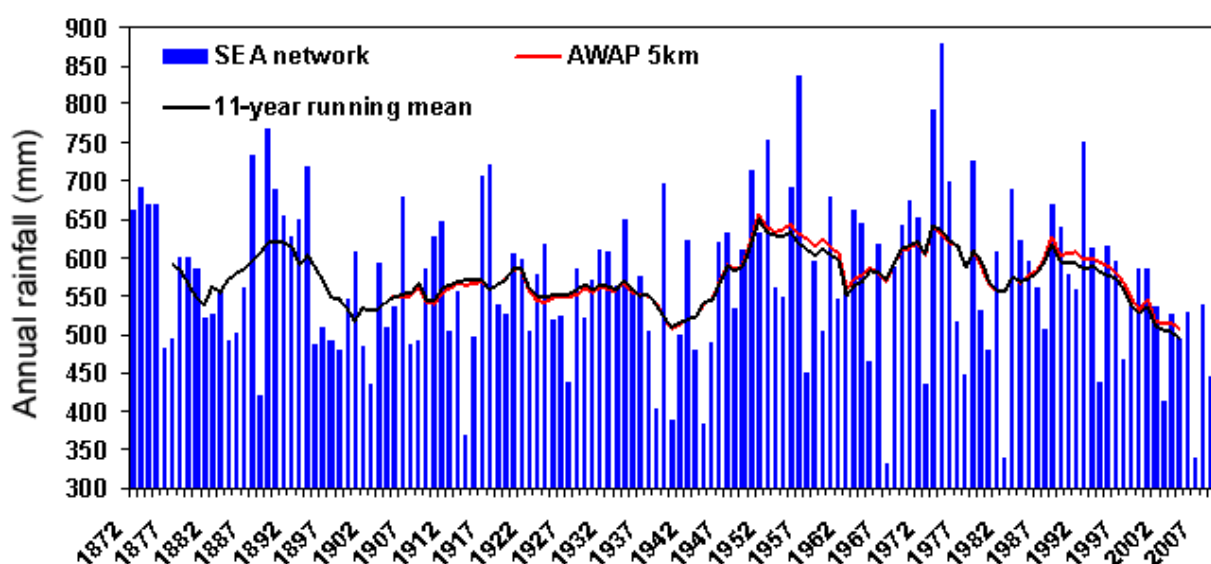


Figure 4. Annual rainfall totals (1872–2009, in millimetres) based on the 14-station south-eastern Australian network (blue bars) and 11-year moving average (black line). Also shown is the 11-year running mean from the high-resolution Australian Water Availability Project rainfall analyses averaged over south-eastern Australia (red line)

Table 2. South-eastern Australian rainfall anomalies in percentage terms calculated relative to the 1872–2009 long-term mean using the 14-station network. Both annual and seasonal means are shown. Anomalies are calculated for the three long-term droughts using the annual mean for the lowest 11-year and 13-year period within a 20-year period encompassing each drought

11- or 13-year period		Annual	Summer (DJF)	Autumn (MAM)	Winter (JJA)	Spring (SON)
Federation drought	1897–1909	–7.7%	–20.8%	–3.1%	5.8 %	–18.8 %
	1895–1905	–9.4%	–7.1%	–6.1 %	1.7 %	–22.8 %
World War II drought	1933–1945	–8.1%	–0.4%	–13.0%	–8.3%	–8.6%
	1935–1945	–10.7%	–4.9%	–11.1%	–9.2%	–16.1%
Recent drought	1997–2009	–13.0%	–9.0%	–25.5%	–11.3%	–6.5%
	1999–2009	–13.1%	–5.4%	–26.2%	–11.7%	–8.7%

The Federation drought has a complex seasonal signature (Table 2). It occurred predominantly in summer (with a rainfall anomaly of –20.8 percent for the later 1897–1909 period) and spring (–22.8 percent for the earlier and shorter 1895–1905 period). It then extended into a very short but severe winter drought from 1911–1914 (–20.7 percent); winter rainfall in 1913 and 1914 is the lowest two-winter consecutive combination in the 138-year record. This complex seasonal behaviour gives the impression that the Federation drought is a good illustration of drought

due to natural variability: low rainfall during summer (the most variable part of the annual cycle (see Figure 5 and Figure 6) with a decade of low rainfall in spring (the season with the most marked decadal variability, see Chapter 10 in Timbal et al., (2010)) and then a short winter deficit.

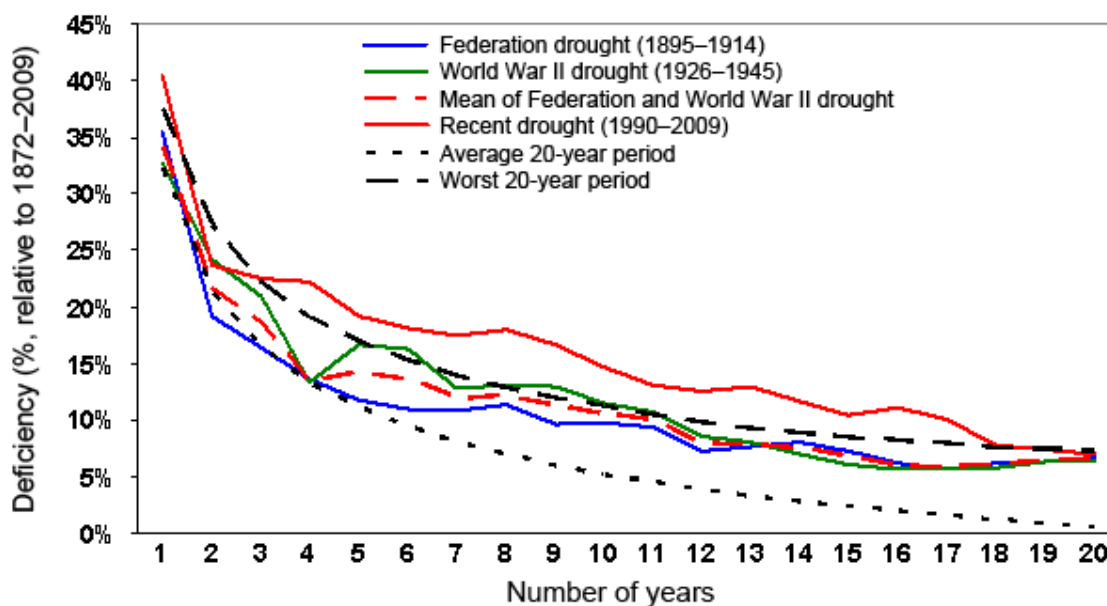
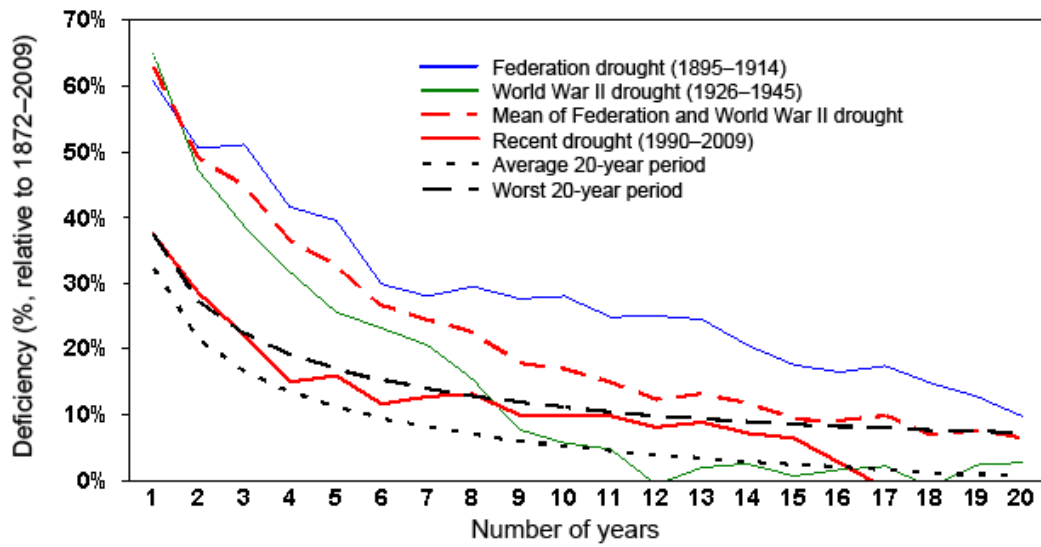


Figure 5. Drought depth duration based on the annual rainfall average in the 14-station network for 20-year periods for the recent drought (red line); the World War II drought (green line); the Federation drought (blue line); the mean of the Federation and World War II droughts (red dashed line); the average of 20-year periods after randomisation of 138 years of data (black short-dashed line); and the average of the worst 20-year periods after randomisation of 138 years of data (black long-dashed line)

A more in-depth comparison of the three historical low-rainfall periods (the Federation, World War II and recent drought) was conducted by analysing the drought depth duration (DDD) for periods ranging from 1 to 20 years. For each period, the 20 years with the lowest rainfall encompassing each drought were chosen: 1895–1914 (Federation drought), 1926–1945 (World War II drought) and 1990–2009 (recent drought). Within each period the lowest n-year total was computed (for n varying between 1 and 20) and plotted for the annual mean (Figure 5) and the four calendar seasons (Figure 6). On this basis, the recent drought is far worse than the previous two historical droughts (note the comparison is made easier by using an average of the numbers obtained for the Federation drought and the World War II drought). Eleven years is often used as a period to analyse protracted drought. In this case this period shows the smallest difference between the recent drought and the average of the two historical droughts: a deficiency of 13.1 percent compared to 10.1 percent, in other words 30.7 percent worse. But for all durations between 4 and 17 years, the recent drought is 30 to 87 percent worse. The smallest difference is for the 11-year duration, the largest (11.2 percent compared to 6 percent) is for the 16-year duration.

(a) summer (DJF)



(b) autumn (MAM)

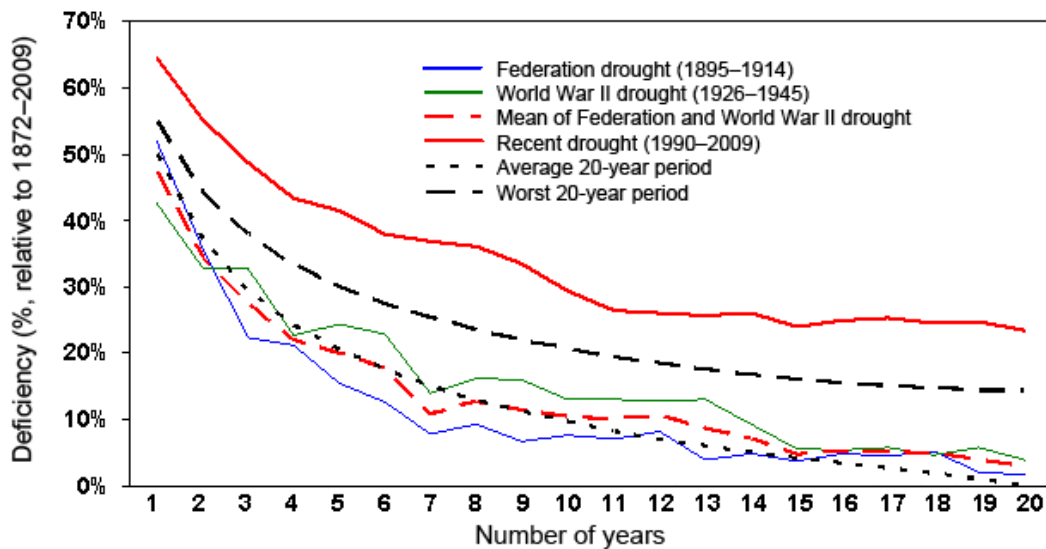
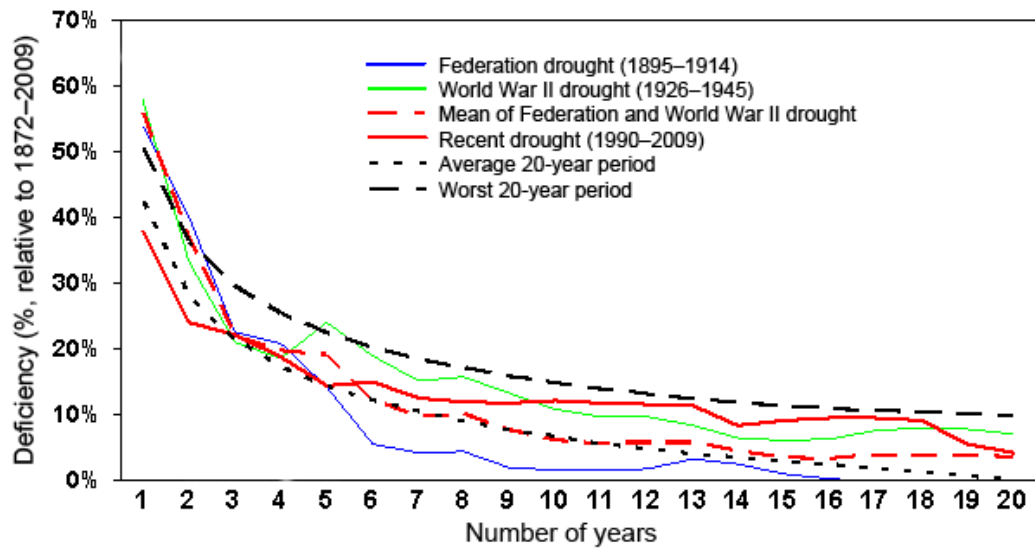


Figure 6. Drought depth duration based on the seasonal rainfall average in the 14-station network for 20-year periods for the recent drought (red line); the World War II drought (green line); the Federation drought (blue line); the mean of the Federation and World War II droughts (red dashed line); the average of 20-year periods after randomisation of 138 years of data (black dotted line); and the average of the worst 20-year periods after randomisation of 138 years of data (black dashed line).

(c) winter (JJA)



(d) spring (SON)

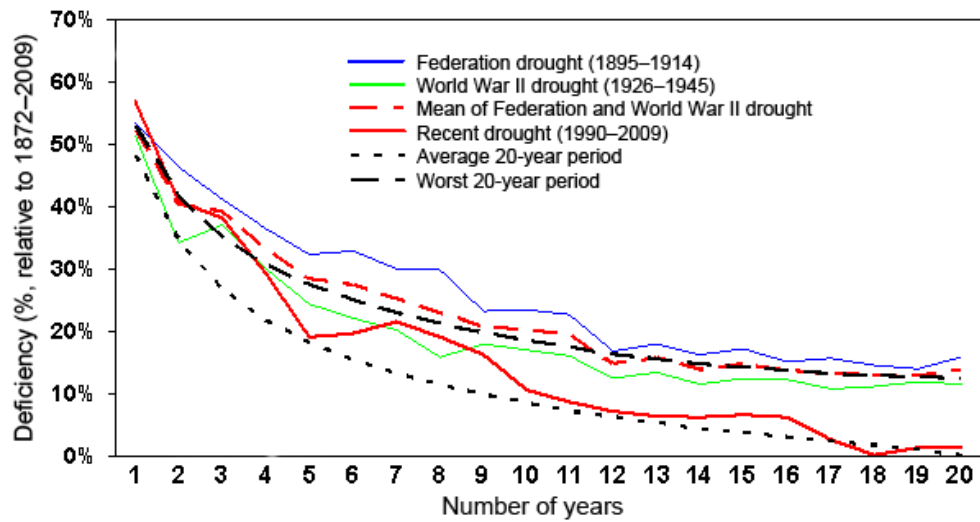


Figure 6. (continued)

In all cases, an average of the Federation drought and World War II drought is provided as a benchmark to compare the recent decline with prior droughts of the instrumental era. However, it is worth remembering that during Phase 1 of SEACI, it was shown that the severity of the World War II drought was partly attributed (about 30 percent) to the global warming of the first half of the 20th century and the intensification of the STR (Chapter 8 in Timbal et al. (2010)).

In addition, the entire record was randomised to create a synthetic record of 138 years. This process was repeated 10,000 times. Each time, the DDD curve was computed for the average 20-year period and for the worst 20-year period of the synthetic record; these are labelled 'average 20-year periods' and 'worst 20-year periods', respectively, in Figure 5 and Figure 6. The randomisation was done separately for the annual mean and for each calendar season.

From that perspective, it is clear that the recent rainfall deficiency is not normal; it is larger than what one can expect by chance for any duration between 3 and 18 years. Not so for the previous two historical droughts for which the DDD curves are close to (World War II drought) or below (Federation drought) the worst random case for most durations. In autumn, the period for which the rainfall decline has been the most pronounced (see Murphy and Timbal (2008) and Table 2 for similar numbers which were calculated from the SEA network), the DDD for the recent drought is worse than all the other curves.

For each curve, the entire 138 years was used in the randomisation process. It is possible, based on SEACI findings (Timbal et al., 2010), to take the view that the current period is abnormal and thus not use it. By including all years until 2009, the impact of the last 20 years is apparent when the worst curve for autumn is compared to the same curve for the other seasons; it gives higher rainfall deficiencies for the entire 20 years. This clearly shows the impact of the very low autumn rainfall during the last 20 years. However, it was decided to include the recent 20-year period in order to ensure that the methodology did not assume that this recent period was abnormal. This provides a statistical framework suitable to accept or reject the hypothesis of the normality of the recent period. For autumn rainfall, this normality hypothesis is rejected at a very high significance level.

It is then possible to evaluate by what percentage the recent rainfall decline is below the 'average' or 'worst' curve. To do so, the rainfall during the last 20 years was increased (in increments of 1 percent) until the adjusted last 20 year curve became similar to the 'average' or 'worst' curves. The percentage increase necessary for the recent period to be considered as average or the worst on record is shown in Table 3 for the annual mean and the three seasons with meaningful recent decline (autumn, winter and spring). Negative values mean that the recent period was not as severe as the worst possible by chance. This provides a perspective on the relative position of the recent period compared with the average and worst cases that might be expected given natural variability. In turn, the percentages in Table 3 can be used as an estimate of the approximate magnitude of the shift in the climate baseline, with the decision as to whether the shift should be characterised relative to the average or worst case being based on the understanding thus far of the role of natural variability in the recent rainfall decline (see subsequent sections and Conclusions).

Table 3. Percentages by which the rainfall during the last 20 years needs to be increased for the recent period to be in line with randomly generated average and worst 20-year periods

	Annual	Autumn (MAM)	Winter (JJA)	Spring (SON)
Worst	3%	18%	-5%	-6%
Average	12%	37%	5%	6%

The reconstruction of rainfall in SEA back to 1872 also provides an interesting insight into the later part of the 19th century. It was argued during Phase 1 of SEACI that the period of very high rainfall during the 1950s to the 1970s coincided with a period when the global temperature of the planet was stable due to a relaxation of 20th-century global warming and that very high rainfalls observed at the time were due to that relaxation (see Chapter 10 in Timbal et al. (2010) for details). The argument is based on the relationship between rainfall, STR and global warming. Therefore it is interesting to observe that during the later part of the 19th century (a period similar to the 1950s to 1970s with no ongoing warming), rainfall was slightly above the long-term average (the 1872–1900 average is 2.8 percent above the 1872–2009 average).

There is marked decadal variability in rainfall (Figure 4). Between 1886 and 1896 the largest 11-year mean rainfall was 620 mm. This is the third highest peak after 1946–1956 (649 mm) and 1968–1978 (641 mm).

Confirming the relationship between very wet decades and the time evolution of the global temperature of the planet would be very interesting but after complete analysis of the BoM archive, further analysis will require analysing prior historical information and palaeo-climatic data.

‘Random’ natural variability of south-eastern Australian rainfall

As part of Phase 1 of SEACI, the natural variability of rainfall in SEA was carefully examined, but primarily from the perspective of that part of the natural variability which is driven by large-scale modes which are known to influence rainfall in SEA. Very little of the recent rainfall deficiency could be related to any form of tropical modes of variability (Chapters 2 and 8 in Timbal et al. (2010)). However, it was also noted that it does not altogether eliminate the role of natural variability in the recent rainfall decline, since a large part of the natural variability is related to daily synoptic timescale (‘weather noise’). This ‘weather noise’ is not necessarily affected by large-scale modes which at most only explain 30 percent of the observed rainfall variance.

There was a wet start to the year 2010: rainfall from January to March 2010 in SEA was 176.8 mm, the largest amount since 1984, and more than 50 percent above the long-term average for January to March. This is a timely reminder of the importance of random natural variability. The recent drought has been characterised by low rainfall and low inter-annual variability (Murphy and Timbal, 2008). The combination of low rainfall and low variability led to a remarkable period of 180 months in a row without a very wet month (defined as a monthly total above the 90th percentile of that month) since January 1995. This finally ended in February 2010 (Figure 7).

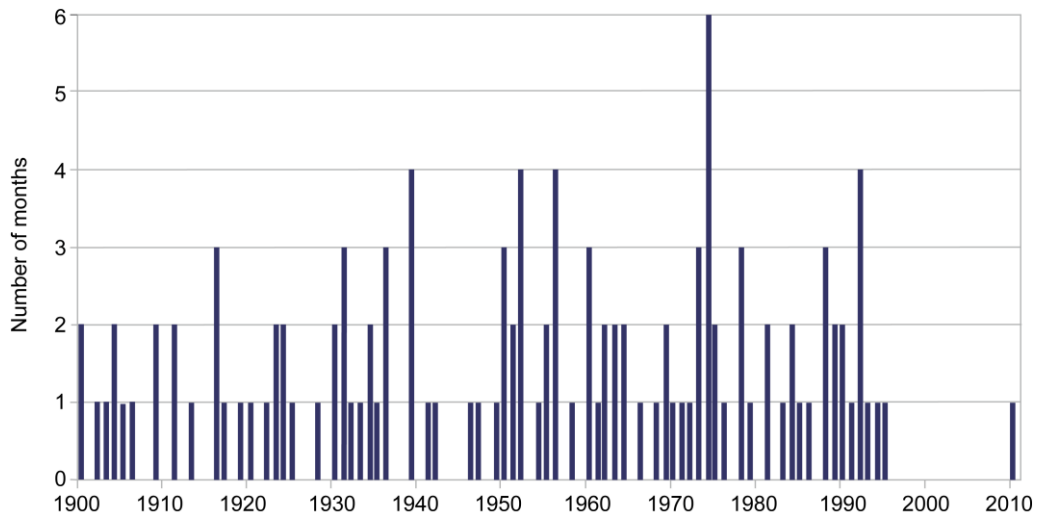


Figure 7. Number of months per year with rainfall above the 90th percentile (updated to May 2010). Percentiles are based on 20th-century (1900–1999) climatology and are computed month by month

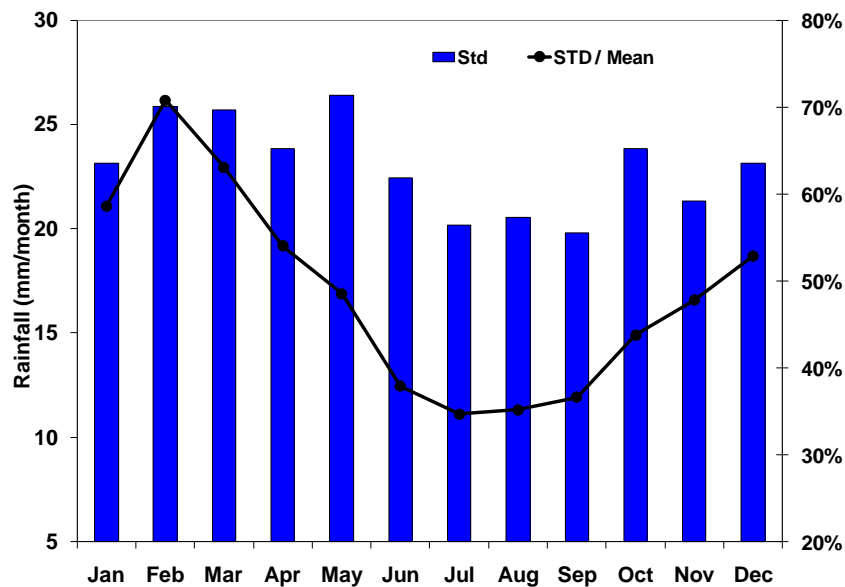


Figure 8. Monthly standard deviations in south-eastern Australian rainfall during the 20th century (blue bars) normalised by the monthly means. The y-axis for the raw standard deviation is shown on the left (in millimetres/month) and on the right for the normalised values (in percent)

The annual cycle of the natural variability of rainfall in SEA (measured by the monthly standard deviation divided by the mean monthly rainfall) has marked seasonal variations (Figure 8) which peak in late summer (February). Interestingly, the magnitude of the monthly rainfall deficiency during the March to October period appears related to the magnitude of the inter-annual variability of that monthly rainfall (Table 4). This relationship is strong and

significant, despite the very small sample size, but decreases dramatically as soon as the other calendar months are considered. The sudden jump is not necessarily evidence that this relationship is coincidental, since it was anticipated based on the relationship between STR-intensity and rainfall across SEA. This relationship is insignificant during the warmer months and is understood to be a key mechanism that explains the recent rainfall deficit (Chapters 3 and 8 in Timbal et al. (2010)).

Table 4. Pearson correlation coefficients between monthly 1997–2009 rainfall deficit and monthly 20th-century rainfall variability for the eight individual months from March to October (numbers in brackets are for the 12 calendar months). Bold and italic figures are significant at the 99 percent and 95 percent level, respectively

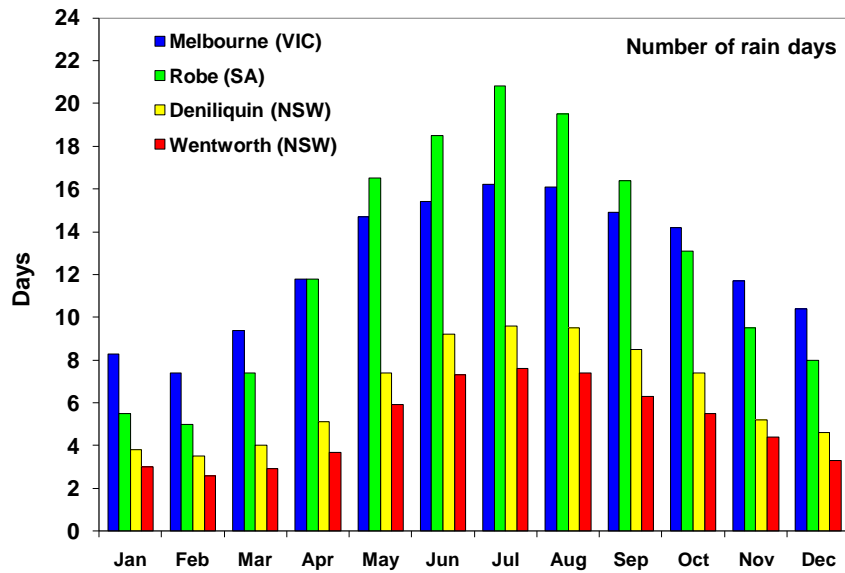
		1997–2009 rainfall deficit	
		Absolute (mm)	Percent
20th century rainfall variability	Standard deviation (mm)	<i>0.81</i> (0.33)	0.85 (0.36)
	Standard deviation normalised by monthly means (%)	<i>0.67</i> (0.11)	0.85 (0.01)

In this regard, the wet month of March 2010 has contributed to reducing the magnitude of the autumn-rainfall decline since 1997, thus reducing the discrepancy between the annual cycle of the expected rainfall decline due to the STR intensification compared to the observed decline which is largest in March (Chapter 8 in Timbal et al. (2010)). It is also consistent with the attribution study conducted during Phase 1 of SEACI (Chapter 6 in Timbal et al. (2010)), which found that autumn is when the rainfall decline due to natural variability is most likely to be largest compared to the component that is a response to global warming. Finally, the wet month of March 2010 has contributed to a reduction of the disagreement between the observed rainfall decline (predominantly in autumn) and the projected decline in response to anthropogenic forcings (predominantly in winter and spring).

The random component of the natural variability (or ‘weather noise’) was investigated further by looking at simple statistics of daily rainfall in various locations across SEA. The picture emerging from these daily rainfall statistics is that monthly winter rainfall consists of many rainfall days with few extreme rain events (Figure 9 and Figure 10). This nature of winter rainfall is consistent across SEA for both wet and dry locations. Therefore, a variation in the weather noise (i.e. the number of rain-bearing systems affecting SEA) will have a relatively small effect on monthly totals and hence the total inter-annual variability will be small despite the remotely controlled part of the variability being significant.

In contrast, monthly summer rainfall is far more erratic and consists of fewer rain occurrences. Therefore, the total monthly rainfall can vary considerably from year to year simply due to a small change in the number of rainfall events, leading to a decreased statistical significance for a similar magnitude of decline. This behaviour is accentuated inland in the drier locations (Figure 10). The period exhibiting rainfall deficiency currently is predominantly in the winter-like category although the early part of autumn (March) is more summer-like from this perspective and hence the magnitude of the recent decline for this month is more likely to be influenced by weather noise variability. This finding is consistent with the fact that for March, little rainfall decline was anticipated based on the observed changes in STR (Chapter 8 in Timbal et al. (2010)).

(a)



(b)

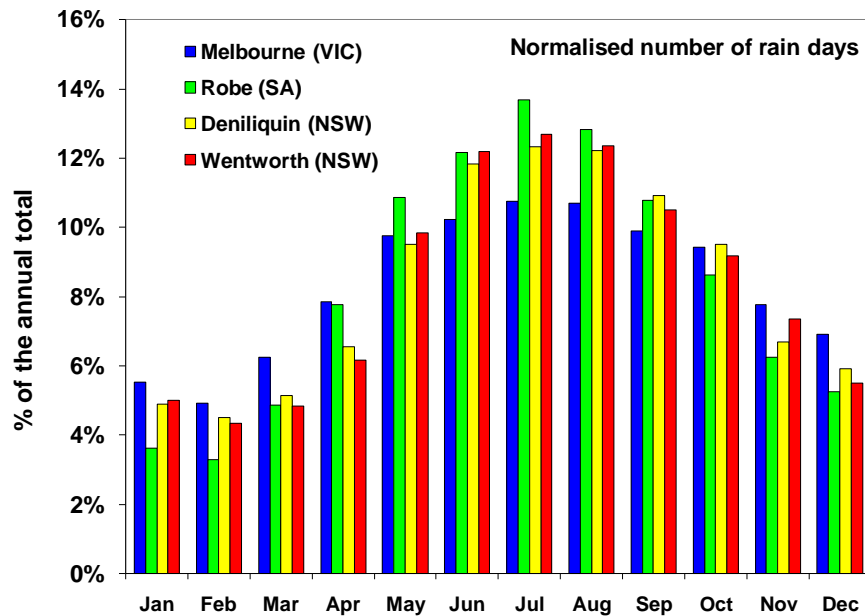
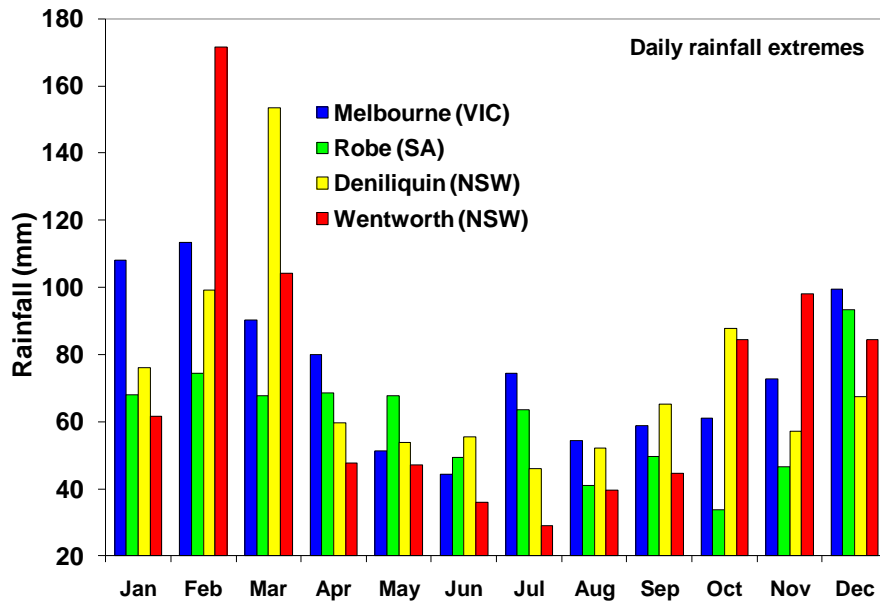


Figure 9. Number of rain days (above 0.2 mm) for each calendar month recorded at four locations across south-eastern Australia, in (a) absolute terms (days), and (b) as a percentage of the annual mean total number of rain days. The length of the observation record varies between 137 and 155 years for the four locations

(a)



(b)

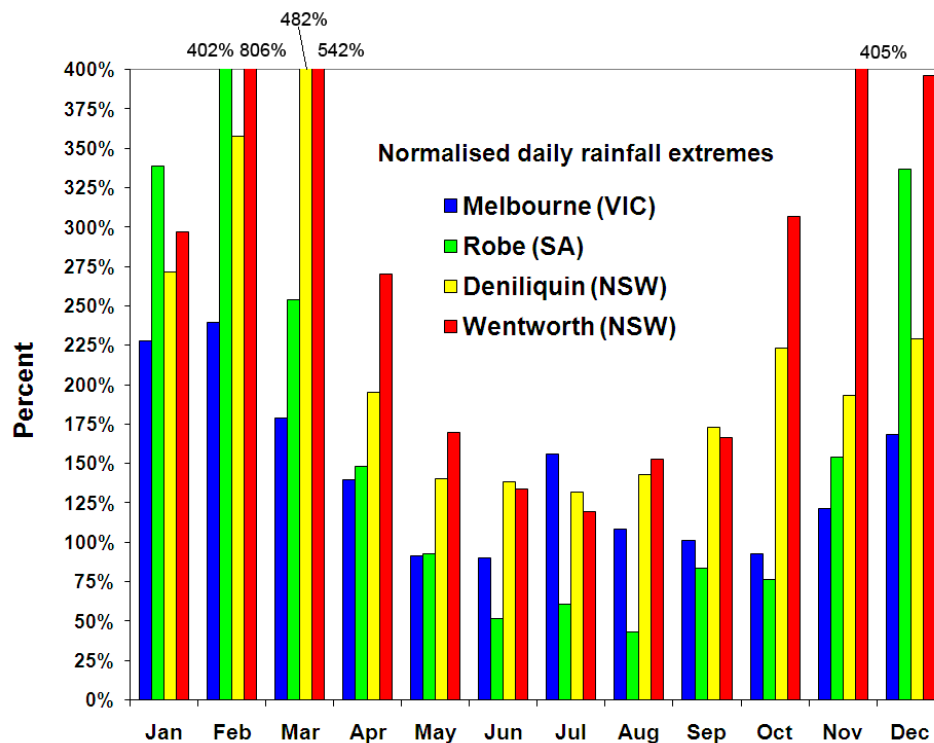


Figure 10. Largest observed daily rainfall for each calendar month recorded at four locations across south-eastern Australia, in (a) absolute terms (millimetres), and (b) as a percentage of the monthly mean values. Percentages above 400 percent (and up to 800 percent) in (b) were truncated. The length of the observation record varies between 137 and 155 years for the four locations

This analysis also sheds some light on the intriguing case of June identified by Murphy and Timbal (2008) as the only cold month with no rainfall decline. This is due to a combination of two factors. Firstly, the 1961–1990 World Meteorological Organization reference period was used. Secondly, rainfall in June is composed of a large number of low-rainfall days leading to a resilient month with limited inter-annual variability – and in particular when it comes to low-rainfall years (in the lowest 20th percentile), which have been numerous in the recent dry period. The fact that 1961–1990 is markedly above the long-term average is a reminder that using this period as a baseline is unwise as it compounds the estimation of the magnitude of the recent rainfall decline by comparing with an anomalously wet period.

Some of the observations made during this study regarding the inter-annual variability of total annual rainfall in SEA are simple checks to help evaluate the ability of climate models to provide meaningful future rainfall projections. In particular, it may be possible to evaluate the ability of climate models to reproduce the various processes governing rainfall variability in SEA – i.e., known modes of variability, and weather noise. This understanding may help answer why the recent deficiency (partly linked to global warming) is predominantly an autumn decline while future projections are predominantly pointing toward a winter-spring decline. This will be pursued further as part of the climate model analysis planned as part of the study of the meridional circulation. Further interactions with Theme 2 in SEACI are envisaged, in particular with Project 2.1.

Review of the scientific literature on the mean meridional circulation

The world is beginning to see changes to the climate resulting from anthropogenic emissions of carbon dioxide and other greenhouse gases (Solomon et al., 2007). In SEA, these changes have been felt as a widespread decline in precipitation and an increase in the strength of the STR, a component of the mean meridional circulation (MMC) (Chapters 2 and 3 in Timbal et al. (2010)). The MMC represents the largest scale of circulation on the Earth. It relieves planetary-scale temperature gradients (i.e. from equator to pole) wrought by differential heating of the surface and moves the planet towards a state of equilibrium. The MMC is important for modulating both the day-to-day weather and longer-term climate of the planet, but simultaneously it is also modulated by these same smaller-scale processes.

The ‘standard’ picture of the MMC is the so-called three-cell model (Figure 11). This figure illustrates the mean meridional stream function, computed in this case by vertically integrating the zonal-mean meridional wind (v). In the figure, three independent circulation cells are apparent in each hemisphere. Two very strong cells straddle the equator; these are the Hadley cells. Between 40° and 60° latitude lie the Ferrel cells, which rotate in an opposite direction to the Hadley cells. These cells are considerably weaker than the Hadley cells. Polewards of 60° lie the polar cells. These cells rotate in the same direction as the Hadley cells, but are very weak in this picture of the MMC.

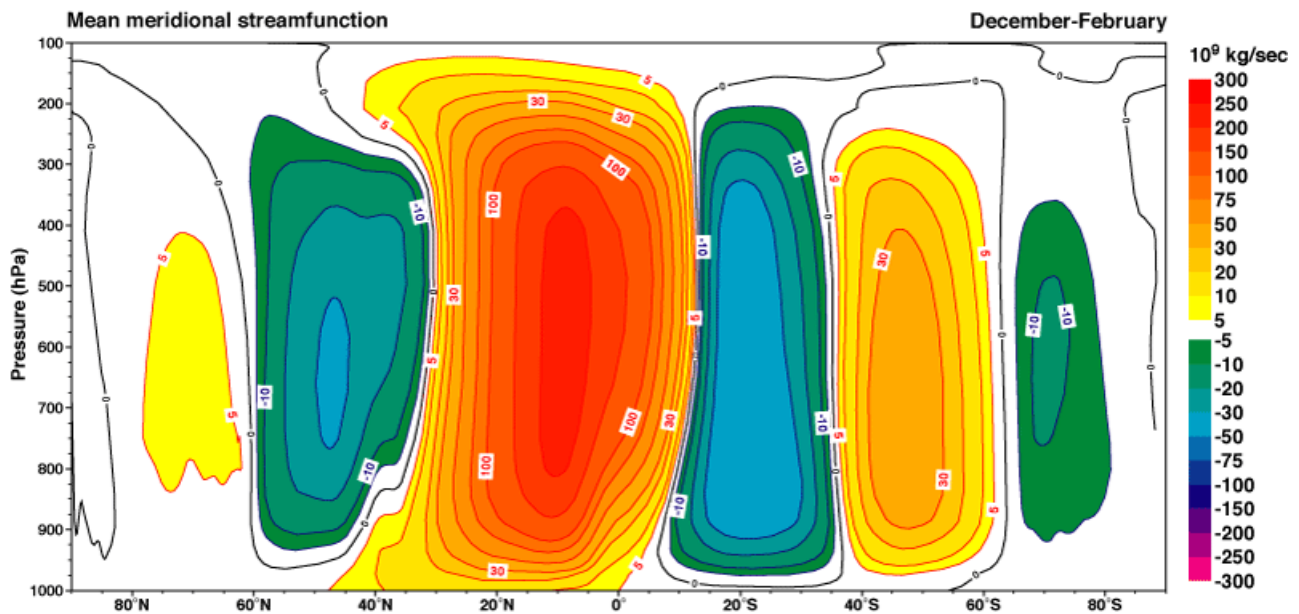


Figure 11. Standard three-cell model of the mean meridional circulation during December, January and February based on the vertical integration of the zonal-mean meridional wind. Flow is counter-clockwise around a positive centre

An alternate picture of the MMC is seen by considering the isentropic (i.e. constant potential temperature or entropy) mass flux stream function, computed by vertically integrating the flow along isentropic surfaces. The streamlines computed in this manner approximate the mean Lagrangian trajectories of air masses (Schneider, 2006). In this second picture, one continuous circulation cell is seen in each hemisphere, although two centres of action are noted in each of these cells. The Hadley cell, similarly in both pictures, shows strong cross-isentropic flow in both the rising and descending branches and the mass flux in this cell is comparable to the standard model. This alternate picture is considerably different in the extra-tropics. Instead of two separate cells, the isentropic mass flux shows one main (but broad) circulation centred between 40° and 50° latitude; the mass flux in this cell is considerably more than that observed in either the polar or Ferrel cells of the three-cell model, which likely underestimates the flow in the mid-latitudes. In fact, the thermally indirect Ferrel cell is completely absent from the isentropic mass flux picture, suggesting that to some degree it is an artefact of the analysis procedure.

A third picture of the MMC has been created, partially based on the isentropic view of the flow (Figure 12). In this picture, there exists one main, thermally direct circulation cell in each hemisphere, although each circulation has two components. The Hadley cell in the tropics is one component. In the other, the extra-tropical circulations of the three-cell model (Ferrel, Polar) are replaced with the Annular Mode, which is further interpreted in terms of 'classical' meteorological concepts like the polar front theory. Signs of anthropogenic climate change are beginning to become apparent in the components themselves.

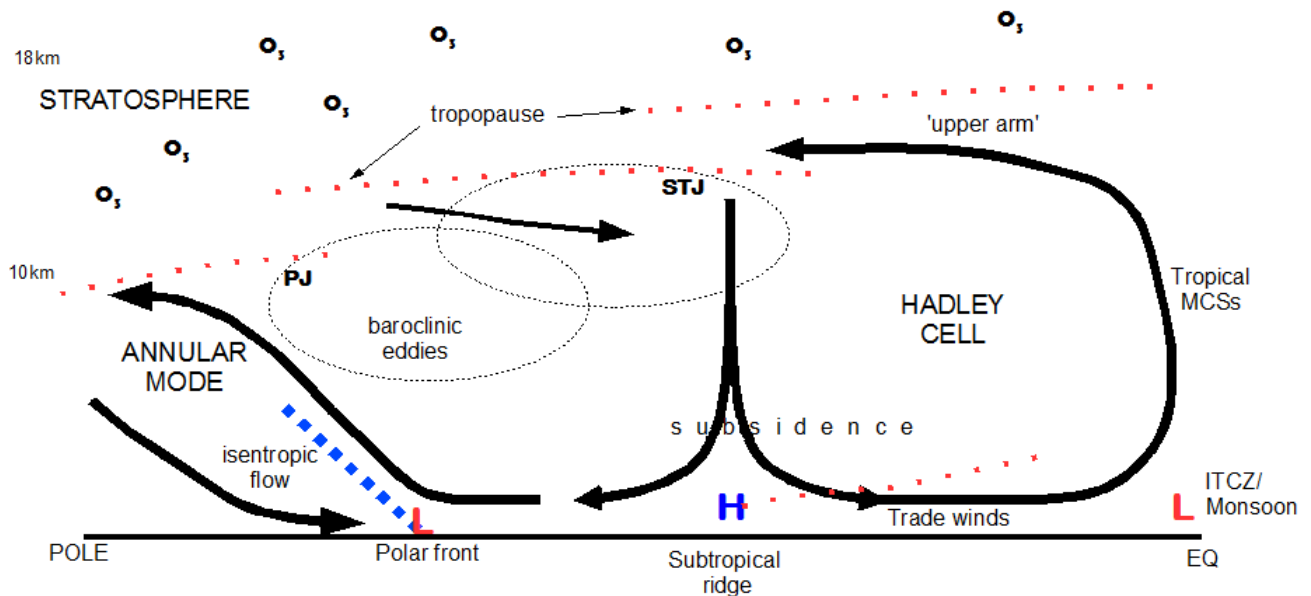


Figure 12. Schematic view of the mean meridional circulation

The Hadley cell represents the tropical portion of the MMC. It is thermally direct and has four 'branches' within the circulation:

- Heat, moisture and momentum are transported upward by mesoscale convective systems within the rising branch near the equator.
- In the upper arm, air is transported poleward from the rising branch into the sub-tropics. It gains westerly momentum as it moves towards the pole. The upper arm culminates in the sub-tropical jet stream.
- The air from the upper arm subsides in the descending branch. The STR is the surface signature of the descending branch of the Hadley cell.
- The trade winds flow out of the STR, easterly and towards the equator, to close the circulation of the Hadley cell. Over the ocean, heat and moisture are extracted from the surface to provide sufficient energy to the air which ultimately ascends in the rising column.

Recent studies indicate that, as a whole, the Hadley cell is undergoing significant changes, hypothesised as a result of the changing climate. In particular, the width of the circulation is expanding (see review of Seidel et al. (2007)). There are numerous lines of evidence to support this result, but the different methods to estimate the amount of expansion give widely varying results. These estimates range from 2° to 8° latitude of expansion for both cells, considerably more than projected from global climate models (e.g. Johanson and Fu, 2009). The intensity may also be changing, but the results from different studies are wildly inconsistent and cover the entire range of possibilities (e.g. Mitas and Clement, 2005, 2006).

In the extra-tropics, the dominant circulation features are the annular modes (e.g. Thompson and Wallace, 2000). In the picture here, the annular modes represent a proxy for the relative position of a set of interacting meteorological features. These include (i) the polar (or eddy-driven) jet stream, a wind-speed maximum in the upper troposphere which is maintained by eddy momentum flux convergence brought by travelling baroclinic waves; and (ii) the polar front, a region where the temperature gradient is highly concentrated. The polar front serves as a locus where baroclinic eddies preferentially form, deepen, occlude and decay. The polar front and the polar jet stream are mutually interacting phenomena, each necessary for the other's existence. When this symbiosis is equatorward of its climatological mean position, the annular mode index is negative, meaning that average sea-level pressure is

lower in the mid-latitudes and lower-frequency baroclinic waves are dominant. When these features are poleward of their normal position, the annular mode index is positive with higher mean pressures in the mid-latitudes and short, higher frequency waves being dominant.

The tropical and extra-tropical circulations mutually interact, but this interaction is episodic. Weather systems formed in the tropics (e.g. tropical cyclones) can propagate into the mid-latitudes and have a significant meteorological impact. Similarly, cold air transported equatorward from the polar region by baroclinic eddies can affect the tropics. For example, 'bursts' in the summer hemisphere monsoon are often linked to cold-air surges from the winter hemisphere (e.g. Love, 1985).

The extra-tropics are also undergoing changes. Both the Northern and Southern Annular Modes are trending positive in recent decades (e.g. Feldstein, 2002; Marshall, 2003). This implies a poleward shift in the location of the polar front/eddy-driven jet symbiosis, along with less storm activity and generally higher surface pressures in the mid-latitudes. This increasing trend and associated poleward shift is generally consistent with climate change projections which show such a shift, particularly in the Southern Hemisphere (e.g. Kushner et al., 2001 and Project 2.1).

This review provides a foundation for exploring the changes to the MMC and their impact on the weather and climate of SEA. Some of the immediate questions to answer include:

- What is the status of Hadley cell expansion over Australia? Can we reconcile the various estimates and reduce their uncertainty, in both an Australian and a global context?
- What is the seasonality of the changes to the MMC? Do these changes reflect the seasonal nature of the observed changes in Australia?
- Are changes to the MMC responsible for the observed changes to date over SEA? How?
- What impact are changes to the MMC likely to have on Australia in the future?

To answer these questions, future studies will use observations, reanalyses and global circulation models.

Conclusions

The reconstruction of the rainfall in SEA as far back as 1872 has reinforced the historical perspective on the abnormality of the recent rainfall decline, the severity of which far exceeds both the Federation drought and World War II drought for an extended range of periods (from short droughts of 3 to 4 years, to a prolonged decline of up to 20 years). A randomisation process showed that the recent situation is beyond what can be expected by chance. That longer historical perspective has also led to a possible quantification of the shift in climate baseline for the recent period. A range was provided for the annual mean and the three calendar seasons with sizeable declines (autumn, winter and spring). This range was characterised in terms of the percentage difference between recent rainfall and an average and worst case that might be expected by chance. Which end of the range is best used to characterise the shift in the climate baseline depends on available evidence regarding the role of natural variability in the recent decline.

For autumn, it can be argued that it is more likely that the shift in climate baseline is closer to the worst case than the average case and hence is in the vicinity of a 20 percent shift. The reasons for this are:

- Autumn is when natural variability is at its highest (Timbal, 2010): the random component of rainfall – and not large-scale modes – influences rainfall in SEA at this time of the year.

- An attribution study conducted during Phase 1 of SEACI (Chapter 6 in Timbal et al. (2010)) showed that the observed reduction in rainfall was at the extreme of the range of model projections, even when the models were forced with the full forcings (including anthropogenic forcings).
- The observed signal is not consistent with the climate model projections in response to anthropogenic forcings which only suggest a very small autumn rainfall decline, leading to a 'seasonal paradox' as discussed in Timbal (2010).

For winter, it can be argued that it is more likely that the shift in climate baseline is at least the magnitude of the shift from the average case (5 percent or slightly more). The reasons for this are:

- In winter, natural variability is low and rainfall is largely controlled by tropical modes of variability, which start to significantly influence rainfall in SEA and in particular relate well with decadal variability.
- Overall, tropical modes of variability in winter have had a small but positive influence on rainfall in SEA, hence suggesting that natural variability has acted to limit the shift in winter rainfall due to the strengthening of the STR (Chapter 8 in Timbal et al. (2010)).
- The attribution study (Chapter 6 in Timbal et al. (2010)) showed that the model response to anthropogenic forcings was similar in magnitude to what has been observed across SEA.
- Model projections indicate a sizeable rainfall decline across SEA in winter (CSIRO, 2010).

For spring, it can be argued that it is more likely that the shift in climate baseline is slightly less than the magnitude of the shift from the average case (less than 6 percent). The reasons for this are:

- In spring, natural variability starts to be sizeable again, mostly due to the strong influence of the tropical modes of variability.
- Overall, tropical modes of variability in spring have had a small negative influence on rainfall in SEA, slightly worsening the shift in spring rainfall due to the strengthening of the STR (Chapter 8 in Timbal et al. (2010)).
- The attribution study (Chapter 6 in Timbal et al. (2010)) showed that the model response to anthropogenic forcings was similar in magnitude to what has been observed across SEA.
- Model projections indicate a sizeable rainfall decline across SEA in spring (CSIRO, 2010).

The annual cycle of the natural variability of rainfall appears to modulate the magnitude of the annual cycle of the rainfall decline since 1997. The magnitude of the decline for every calendar month between March and October (the continuous part of the annual cycle where rainfall has been observed to decline) relates strongly to the natural variability observed in each of these calendar months: that is, smallest in winter and spring and largest in autumn.

The annual cycle of natural variability is in direct contradiction to the known influence of identified naturally-occurring modes of variability, which are influential mostly in winter and spring. It suggests that large-scale modes of variability in the tropics act as controllers of the random or weather noise-generated inter-annual variability, reducing the overall observed natural variability in spring and winter.

SEA is located under the influence of the descending branch of the Hadley circulation and the storm-track associated with the mid-latitude Ferrel circulation. The role of the overall MMC in controlling the weather noise affecting SEA and its response to global warming is an essential focus of this ongoing project. Impacts of variations of the MMC on SEA are critical in autumn (the season with the largest observed decline); in the absence of control due to large-scale modes of variability, it can be argued that the random part of the natural variability has responded more strongly to the global warming forcing imposed on the MMC and seen at the surface by the observed STR changes. But this is also important during the rest of the cool months (winter and spring). The scientific questions raised in this report will be the subject of further research.

Links to other projects

The findings on the relationship between STR and rainfall, which underpin our current understanding of the rainfall decline in SEA, have been used in other SEACI projects: to describe the impact of large-scale influence on the hydrological cycle in SEA (Project 1.2) and to evaluate climate model future projections reliability and similarity with observed features (Project 2.1).

Findings during Phase 1 of SEACI have helped define different sub-regions across SEA and, in particular, a clear separation along the Great Dividing Range between the south-west of eastern Australia and the eastern seaboard of Australia. The latter area has received renewed interest with the launch of the Eastern Seaboard Climate Change Initiative (ESCCI), for which SEACI findings are highly relevant.

CHAPTER 3: PROJECT 1.1b

Dynamics of south-eastern Australian rainfall variability and change

Wenju Cai, Yun Li, Tim Cowan, Peter van Rensch and Harry Hendon

Abstract

The recent rainfall reduction across south-eastern Australia (SEA) is seen as an extension of the dry season and an early cut-off of the wet season. The signature of this changing seasonality since 1980 has been a marked autumn rainfall decline and a (smaller) decline in late-winter and early-spring rainfall. Our results show that a significant contributor to the rainfall decline in winter and spring is skewness towards more positive Indian Ocean Dipole (IOD) events that weaken the rain-bearing westerly weather systems. Climate models suggest that this trend in Indian Ocean conditions is partly a result of anthropogenic climate change. El Niño – Southern Oscillation (ENSO) is shown to exert its influence on SEA through the Indian Ocean, but the contribution to the rainfall decline is small. The dynamics of the autumn rainfall decline across SEA remain elusive but have been shown to be associated with a significant reduction in the density of low-pressure systems in the region south of Australia, and an increase in the density of high-pressure systems. Since climate models fail to simulate the 1950 – 2008 autumn rainfall trends for much of Australia, a direct link between the post-1950 autumn rainfall decline and climate change cannot yet be established.

The flow-on effects of recent rainfall changes and higher local temperatures across SEA and the Murray–Darling Basin (MDB) have resulted in historically low streamflows across the basin. The relative importance of climate modes – including local drivers such as atmospheric blocking and the sub-tropical ridge (STR) position, and remote drivers such as the ENSO, the IOD and the Southern Annular Mode (SAM) (defined through various climate indices) – were assessed in terms of their influence on annual and winter-spring MDB inflow. The main findings show that drivers that are prevalent during May to November are highly coherent with inflow (e.g. the IOD). Also, ENSO does not display a strong direct relationship with inflow, as ENSO's influence on SEA is conveyed through the Indian Ocean in spring. In fact, systems associated with atmospheric blocking have a strong influence on inflow; however, the independence of such local modes from remote drivers is not clear, and awaits further investigation.

Note that some of the findings reported in the current Chapter contrast in some respects with those reported in Chapter 2. This is likely to be due in part to the different periods selected for analysis (post-1950 here, compared to post-1990 in Chapter 2). Ongoing research will serve to shed further light on these issues.

Background

Since around 1980, autumn rainfall across SEA has declined by about 40 percent, which is the largest decline experienced of all seasons. Our understanding of large-scale circulations that control climate variability and change over this region is not complete. Previous attribution studies have concluded that the rainfall decline is related to local influences, such as the sub-tropical ridge (STR) (e.g. Murphy and Timbal, 2008), and remote climate drivers, such as El Niño – Southern Oscillation (ENSO) (e.g. Cai and Cowan, 2008a) and the Southern Annular Mode (SAM) (e.g. Nicholls, 2010).

The other season in which rainfall has shown a recent decline is spring, and a weak declining trend has been observed in winter. There is virtually no long-term trend in early winter (June). A declining trend becomes pronounced in mid-late winter and extends through to mid-spring (July to October). Recent research suggests that this change in spring rainfall is associated with an increased frequency of positive Indian Ocean Dipole (IOD) events (Cai et al., 2009a), which are known causes of drier and warmer conditions over SEA. Establishing whether the seasonality of the rainfall decline is due to climate change or natural fluctuations in the climate system is important in our projections of future water resources. If the trend is induced by climate change it will have significant ramifications for future water availability.

Hydrological fields, such as inflow to water supply catchments, are directly sensitive to rainfall changes, and to the wider impacts of climate drivers. However, recent research analysing Victorian catchments, including the southern Murray–Darling Basin (MDB), suggests that no dominant climate driver can explain the temporal variability in streamflow (Kiem and Verdon-Kidd, 2009). A natural extension of this is to examine just how sensitive streamflow in the MDB (as an entire basin flow) is to various climate drivers. This sensitivity will provide insight in terms of future water availability, since it will provide an indication of water availability once indices of climate drivers are predicted. This was another focus of the work during 2009/10.

Objectives

Is the seasonality of rainfall change consistent with climate change?

This component addressed whether the observed rainfall change across SEA is manifested through a change in the annual cycle that is consistent with a maximum decline in autumn and a substantial change in spring, and examined whether climate models are able to simulate the associated characteristics.

Winter and spring are the main rainfall seasons for SEA; however, good autumn rain allows soil to become saturated, which coincides with useful runoff in the following seasons. The emerging picture is that the wet season (May to November) appears to be getting shorter, although rainfall in the middle of winter has not changed a great degree. We investigated whether the seasonality of rainfall change is manifested through a change in annual cycle induced by climate change. We aim to establish whether or not the recent autumn rainfall decline is a consequence of processes associated with the warm, dry summer season shifting or extending through to autumn. Further, we investigated the processes responsible for spring rainfall ending early in recent years. As the annual rainfall cycle over SEA is an average of highly varying fluctuations of weather systems influenced by climate drivers, it is important to determine whether climate drivers are displaying consistent responses. By advancing our understanding in this area, this work contributes to the question of whether climate change is a potential driver of the recent rainfall decline.

Is there a direct linkage between inflow within the Murray–Darling Basin and climate drivers?

Inflow within a catchment or a wider basin is usually predicted by a comprehensive hydrological model. Rainfall is the major component that allows the generation of streamflow within a catchment, and is more broadly linked to climate variability (e.g. El Niño, La Niña, positive and negative IOD events). Therefore, it is desirable to gauge how sensitive annual inflow is to a particular climate driver, such as ENSO, IOD or SAM. This leads to a better understanding of the relative importance of climate drivers, and their offsetting and/or superimposing effects in driving the MDB inflow. This also provides an indication of future water availability, once seasonal and long-term projections of the state of climate drivers are made.

Methods

Is the seasonality of rainfall change consistent with climate change?

We used daily rainfall data from the Bureau of Meteorology (BoM) with a $0.05^\circ \times 0.05^\circ$ resolution (Jones et al., 2009), and compiled a daily rainfall climatology for the periods 1950–1979 and 1980–2007. We compared the changes in the amplitude and seasonality of the rainfall cycle before and after 1980 for the state of Victoria and the wider region of SEA. We examined whether the changes in rainfall (e.g. the recent extended drought over southern Australia) can be explained in terms of seasonal circulation changes using reanalysis from the National Center for Environmental Prediction (NCEP), global sea-surface temperature (SST) from the Hadley Centre, and climate model outputs. We also utilised time series of the STR-intensity and STR-position based on data provided by the BoM and described in Drosowsky (2005), as well as extra-tropical cyclone (anti-cyclone) data generated by a tracking algorithm developed by the BoM and the University of Melbourne (Jones and Simmonds, 1993).

Is there a direct linkage between inflow within the Murray–Darling Basin and climate drivers?

To determine and compare the sensitivity of inflow to various climate drivers, we used a time series of monthly total-inflow to the Murray–Darling river system since 1900, provided by the Murray–Darling Basin Authority (MDBA) (see Cai and Cowan, 2008b). The inflows included those from the Murrumbidgee, Goulburn, Campaspe, Loddon and Darling rivers, which were adjusted through hydrological computer models of these systems for current levels of catchment development. Annual average and monthly mean data were used to build a relationship between inflow and climate drivers such as the IOD, SAM and ENSO. To avoid any relationship that may arise from trends in the inflow as well as in the climate drivers, all data were detrended, as in previous studies (e.g. Cai and Cowan (2008b)).

Results

Is the seasonality of rainfall change consistent with climate change?

A recent change in rainfall can be observed in Figure 13 for Victoria, which shows that late summer is drier in the post-1980 period than in the pre-1980 period. During 1950–1979 the rainfall season extended from May through to October (6 months), with a rather rapid transition into summer conditions. In the 1980–2007 period the ‘shoulder’ rainfall months in autumn and spring disappeared somewhat, with the transition period from summer (trough) to winter (peak) taking almost 2.5 months (compared to about 1.5 months for the 1950–1979 period). Interestingly, winter (Jun-Jul-Aug) rainfall shows very little difference, further highlighting the need to understand rainfall changes on a seasonal, and not annual, basis. Given that climatology is the average of climate variability, the impact of the drivers that govern variability will be a focus.

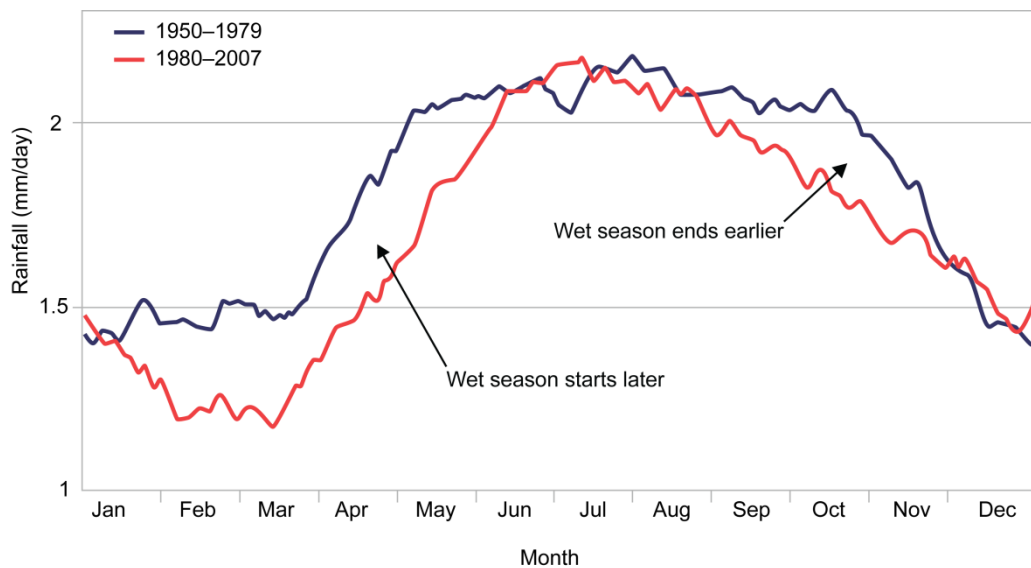


Figure 13. Annual cycle of rainfall over Victoria averaged over 1950–1979 (blue) and 1980–2007 (red). The rainfall climatology is based on daily rainfall outputs from station data averaged over Victoria (140 to 150 °E, 32 to 40 °S), smoothed using a 30-day running average

The autumn rainfall decline post-1950 across SEA is not generated by the majority of climate models with historical radiative forcings included (Figure 14). This suggests that it cannot therefore be directly attributed to climate change (assuming that climate models are able to simulate the relevant processes).

Previous studies have indicated that winter rainfall changes may be a result of storm tracks shifting south, related to increasing STR intensity and the SAM trending towards a more positive phase (e.g. Hendon et al., 2007; Meneghini et al., 2007). However, a linkage between SAM and autumn rainfall is weak over SEA (Murphy and Timbal, 2008). If storm systems are moving poleward, analysing the density of low- and high-pressure systems passing southern Australia should identify this. Since 1950 there has been a decrease of 1.7 low-pressure systems per degree of latitude squared (a grid area of 111 km × 111 km) (Figure 15). The density of high-pressure systems has increased by 3.2 over the same 58-year period, consistent with a shift in storm tracks. Both trends in high- and low-pressure systems are statistically significant at the 95 percent confidence level.

By comparison, changes in the density of low-pressure systems in spring are not as dramatic, with low-pressure systems decreasing by 0.8 per degree of latitude squared since 1950. However, high-pressure systems have increased by 2.6 per degree of latitude squared (not shown). Thus, the decline in rainfall in spring is manifested mostly through an increase in high-pressure systems. This is consistent with the change in IOD behaviour over the past decades.

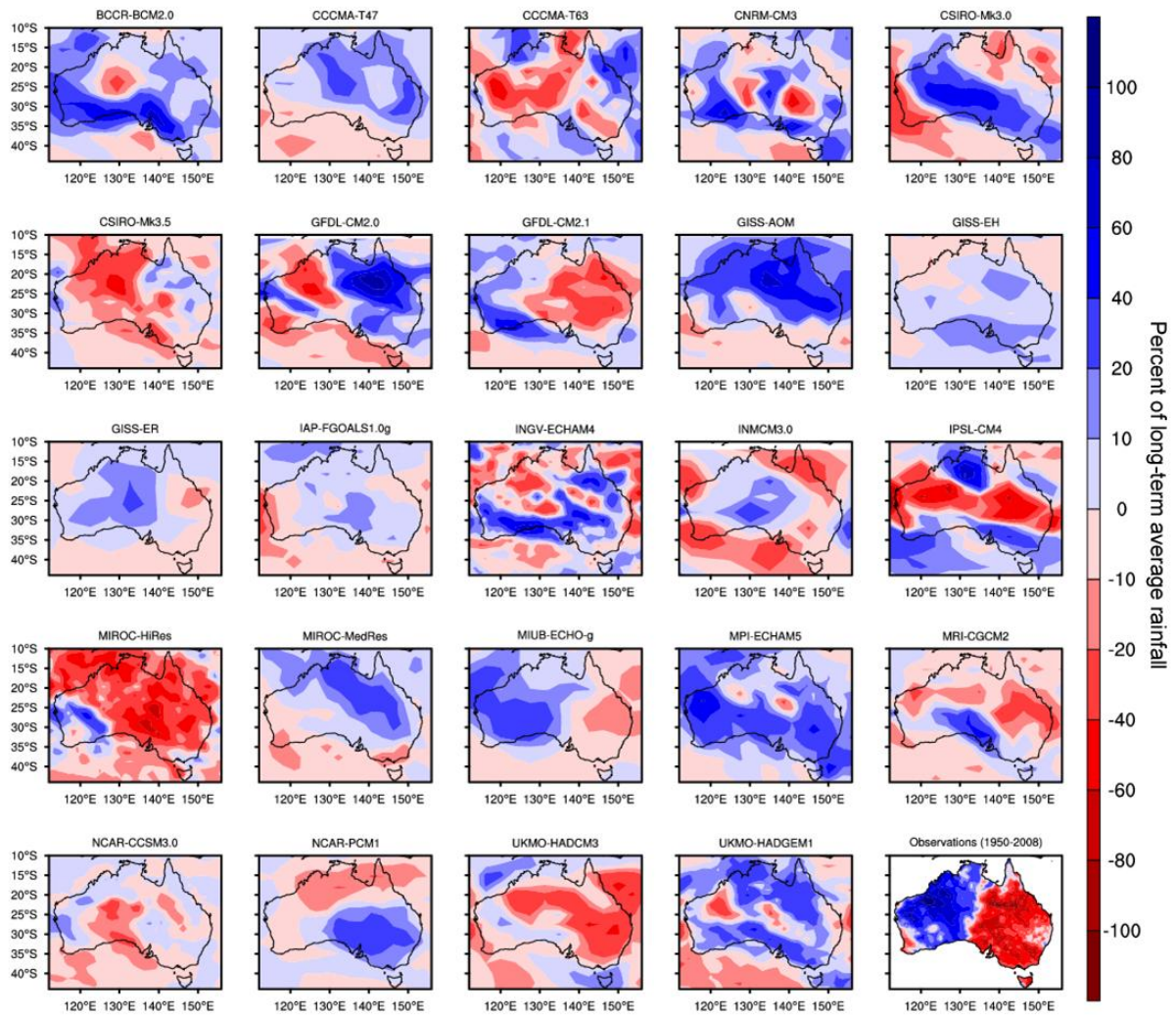


Figure 14. Maps of autumn (Mar-Apr-May) rainfall trends from 24 CMIP3 models for 1950–1999, compared to observations from 1950–2008 (bottom right-hand panel). Units are percent of long-term average rainfall (1950–1999). Red indicates decrease in autumn rainfall, while blue indicates increase

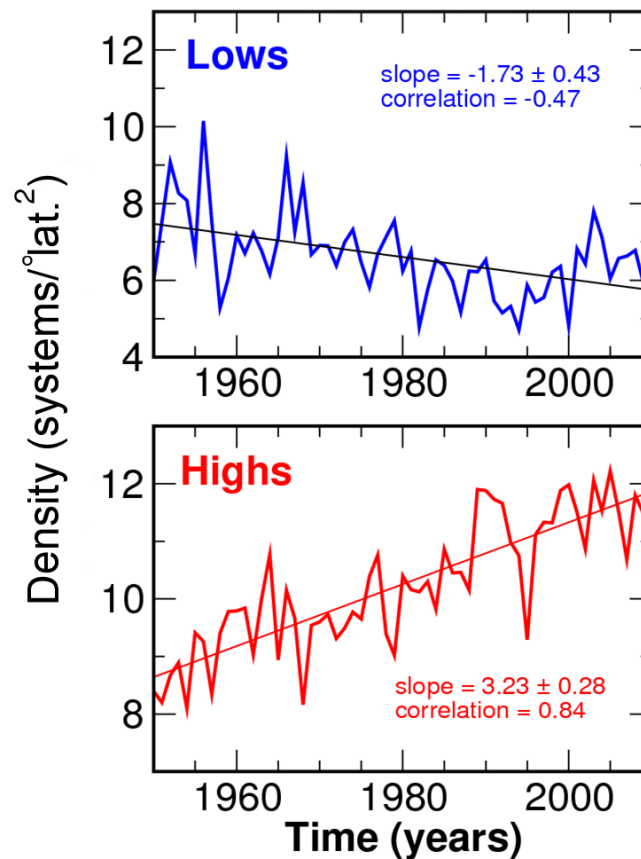


Figure 15. The density of autumn extra-tropical systems in southern Australia (94 to 174 °E, 30 to 50 °S) over 1950–2009, as defined by the Bureau of Meteorology. The top panel shows the density of low-pressure systems (extra-tropical cyclones) and the bottom panel shows the density of high-pressure systems (extra-tropical anti-cyclones)

During winter, the influence of the tropics on SEA rainfall becomes more apparent; in this season the IOD and ENSO are quite independent, with ENSO's impact mostly observed in northern and eastern Australia, while the IOD's imprint is across southern Australia. As an El Niño starts to develop in winter, much of the equatorial Indian Ocean (including eastern Africa) experiences high mean sea-level pressure (MSLP) as part of the western branch of the Southern Oscillation. This suppresses convection in the western Indian Ocean, offsetting the enhanced convection associated with the western pole of the IOD, as a concurrent positive IOD starts to develop. The IOD's impact on rainfall in SEA originates from the eastern pole (an area of ocean near Sumatra), through the emergence of an equivalent-barotropic wave-train (called the eastern Indian Ocean wave-train, or EIO), a downstream feature of which is a large positive MSLP anomaly over southern Victoria and Tasmania. Easterly anomalies, associated with this anomalous pressure centre, weaken the rain-bearing westerly weather systems leading to an austral winter rainfall decline over much of southern Australia during a positive IOD event.

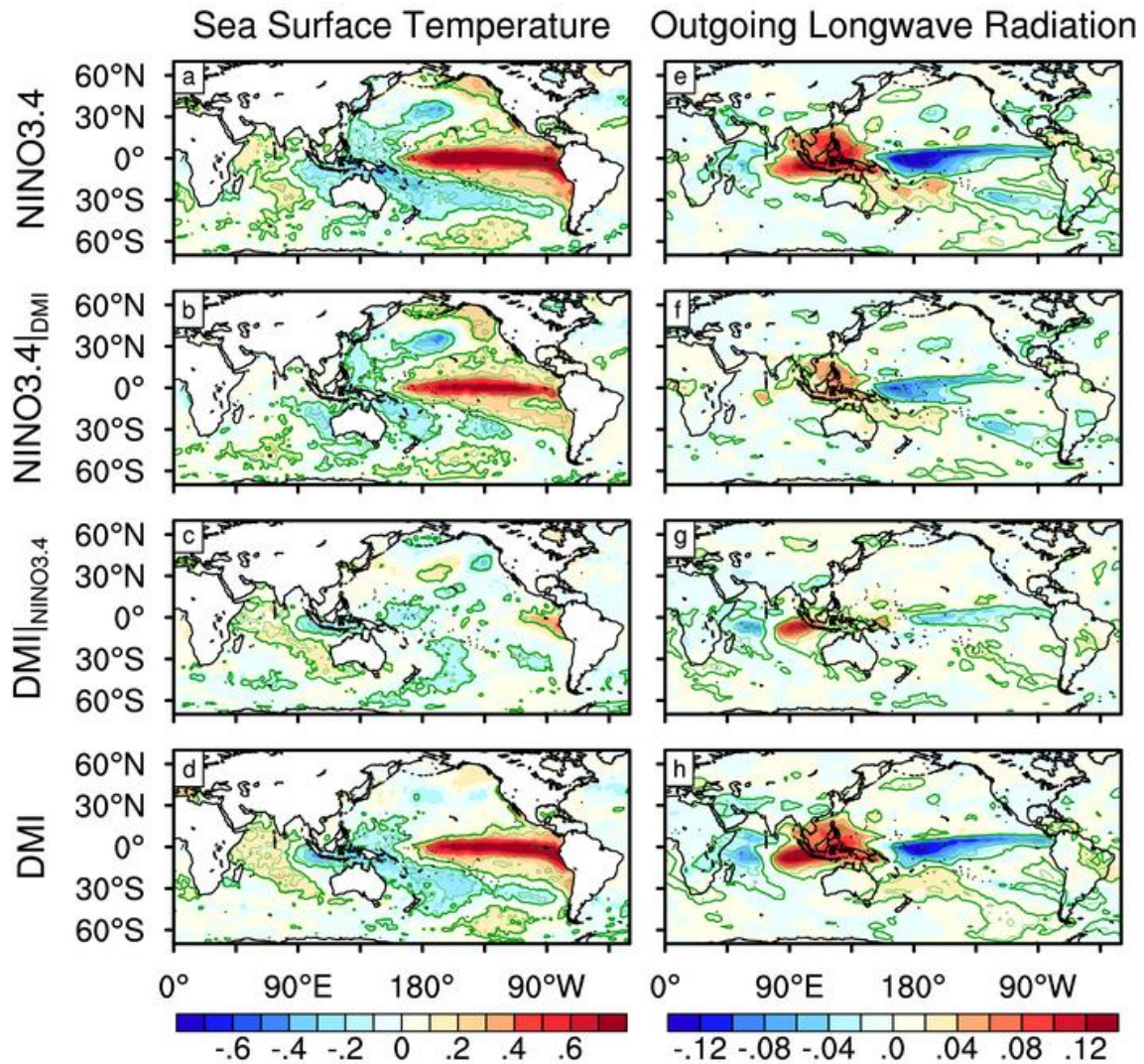


Figure 16. One-standard-deviation anomalies in spring (Sep-Oct-Nov) of (left panels) sea-surface temperature ($^{\circ}\text{C}$ per degree global warming), and (right panels) outgoing longwave radiation (watts per square metre per degree global warming), associated with (first row) El Niño – Southern Oscillation, (second row) El Niño – Southern Oscillation with the Indian Ocean Dipole removed, (third row) Indian Ocean Dipole with El Niño – Southern Oscillation removed, and (fourth row) Indian Ocean Dipole. Bold green contours show the statistically significant correlations at the 95 percent confidence interval, which is ± 0.349 for 30 years (1979–2008).

The impact of these tropical processes is also observed in spring when the IOD peaks. The persistence of the IOD overcomes the suppression of convection due to ENSO in the western Indian Ocean, inducing a wave-train from this region (called the western Indian Ocean wave-train, or WIO). The two wave-trains, associated with the east and west poles of the IOD, share the same high-pressure anomaly centre to the south of Australia, leading to a rainfall reduction over SEA (for a positive IOD event). However, in this season ENSO and the IOD exhibit strong coherence, meaning that separating out their imprint on circulation fields is more difficult. Figure 16 highlights this fact, showing that removing (through linear regression) the influence of the ENSO from that of the IOD greatly weakens the IOD-coherent signal (in SST and convection).

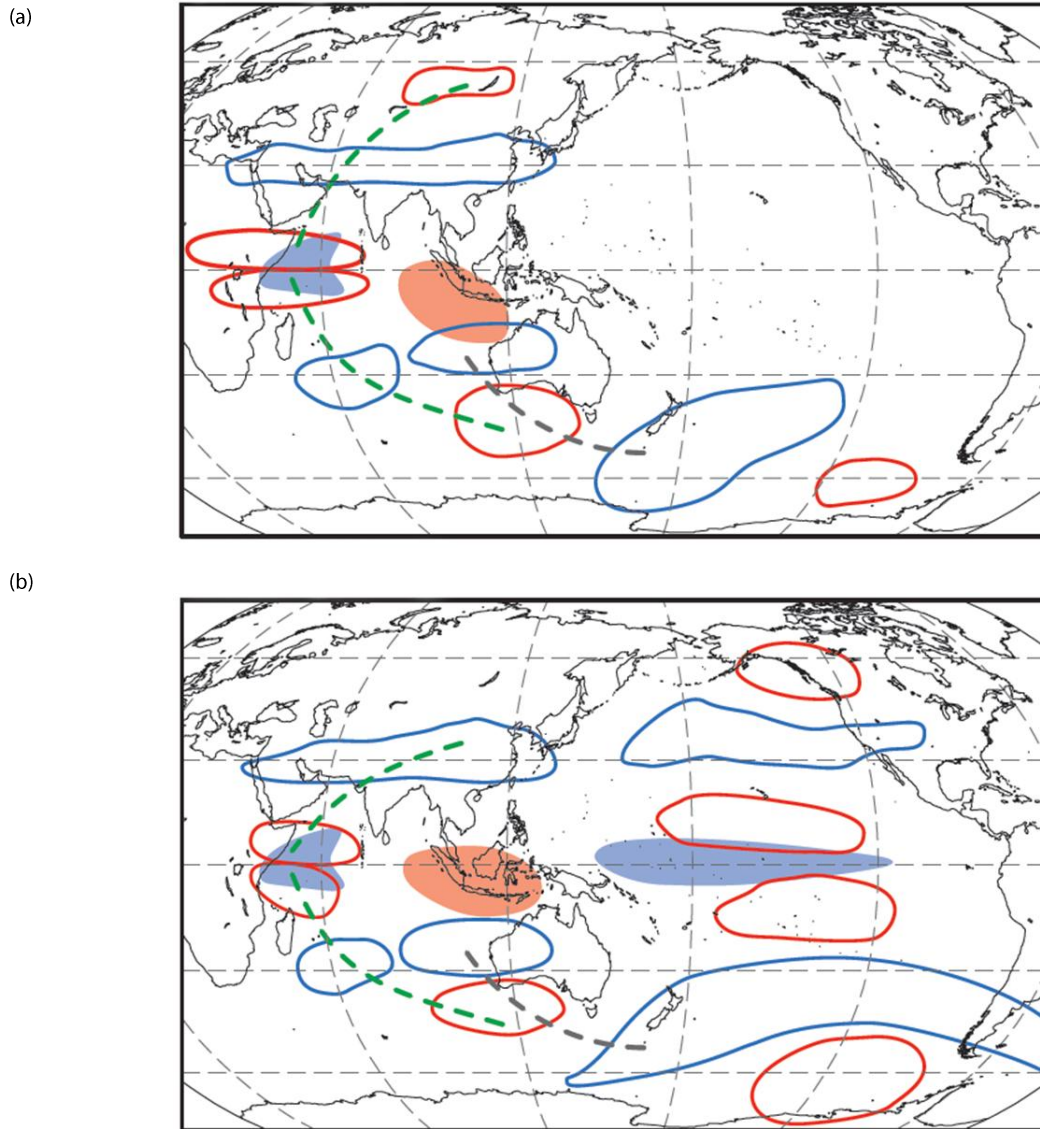


Figure 17. Schematic illustration of the typical processes associated with the (a) Indian Ocean Dipole and (b) El Niño – Southern Oscillation for spring (Sep–Oct–Nov). Shaded blue areas indicate regions of increased convection, and red areas indicate regions of decreased convection. Blue contours indicate anomalously low upper-level height, while red contours indicate anomalously high upper-level height. This description is for El Niño and positive Indian Ocean Dipole events, but the opposite description is true for La Niña and negative Indian Ocean Dipole events. The dashed lines trace the wave-trains: grey for the eastern Indian Ocean wave-train (EIO) and green for the western Indian Ocean wave-train (WIO)

The impact of ENSO on SEA is primarily through the tropical Indian Ocean, conducted through ENSO's influence on the convection in the eastern and western pole, where EIO and WIO are enacted (Figure 17). ENSO's tropical influence from the western Pacific is still observed in northern and eastern Australia. Further details can be found in Cai et al. (in prep.). A recent increase in the frequency of positive IOD events, with a concurrent reduction in rain-bearing negative IOD events, may be driving the recent rainfall decline in late winter and early spring (see Figure 1 in Cai et al. (2009a)). Significant impacts of such increases include a severe decline in soil moisture across SEA, and the strong linkages to recent major summer bushfires (Cai et al., 2009b).

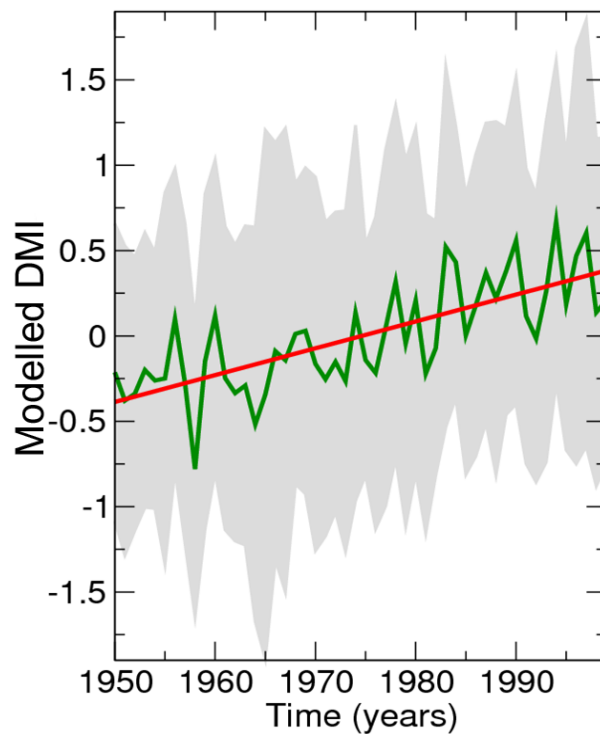


Figure 18. Time series of the Indian Ocean Dipole Mode Index (DMI) averaged over an ensemble of 19 individual models (green) and a linear trend line (red). The grey shaded area indicates inter-model variations, shown as the mean \pm the one-standard-deviation value of the inter-model variations. The ensemble trend rate is 0.016 per year, and the correlation coefficient is 0.74 (Cai et al. (2009c)).

Using 19 climate models, a recent study investigating whether the observed IOD trends can be linked to climate change showed that climate change can account for a 17 percent increase in positive IOD occurrences (Cai et al., 2009c). A model-averaged IOD index (the Indian Ocean Dipole Mode Index (DMI)) that removes individual model's inter-annual variability, leaving behind a climate-change signal, displays a statistically significant increasing trend (Figure 18), which reflects the Indian Ocean's response to climate change. For the definition of the Indian Ocean Dipole Mode Index refer to Saji et al. (1999). Much of the 17 percent increase in positive IOD events is through 2 and 3 consecutive years, as observed in 2006–2008, when spring rainfall across SEA was almost 35 percent below average.

Is there a direct linkage between inflow within the Murray–Darling Basin and climate drivers?

Climate modes, such as ENSO, IOD and SAM, are known drivers of rainfall on inter-annual to multi-decadal time scales. Assessing their impact on streamflow in the MDB is of particular interest to water managers and end-users, particularly in the context of the recent drought, where inflow has dramatically decreased, reaching the lowest level in 117 years of measurements (circa 2007). The annual inflow across the MDB is largely dominated by winter-spring (Jun-Jul-Aug-Sep-Oct-Nov) flow (and rainfall), accounting for 96 percent of the inter-annual variability. Therefore the focus of this research was to examine the climate drivers contributing to the modulation of winter-spring rainfall over the MDB and study the subsequent impacts on the inflow to the MDB.

Four climate drivers operating in the MDB wet season (May-Jun-Jul-Aug-Sep-Oct) can directly exert their impacts on winter-spring inflow (Table 5), with atmospheric blocking over southern Australia showing the largest impact. Further to this, the correlation is generally highest when climate indices lead by one month.

The large correlation with atmospheric blocking is somewhat surprising, and given that it is least understood, the associated dynamics require further examination. Other drivers, such as the IOD and STR-intensity, are well documented (e.g. Murphy and Timbal, 2008), but it is worth emphasising that the correlation with ENSO is not statistically significant at the 95 percent confidence level. The SAM has very little influence over the winter-spring inflow. However, many of the climate modes co-vary during these seasons (see previous section), and therefore cannot be considered as independent. See Li and Cai (2010) for further details of the climate indices which represent these climate drivers.

Table 5. Correlation between winter-spring (Jun-Jul-Aug-Sep-Oct-Nov) Murray–Darling Basin inflow and climate drivers averaged over May to October (MJJASO) and June to November (JJASON) during 1950–2007. Values significant at the 0.05 level (95 percent confidence level) are in bold. Climate drivers include the blocking index, El Niño – Southern Oscillation (NINO3.4), Indian Ocean Dipole (DMI), sub-tropical ridge intensity (STRI), and the Southern Annular Mode (SAM).

Season	Blocking index	NINO3.4	DMI	STRI	SAM
MJJASO	0.53	–0.41	–0.43	–0.59	0.07
JJASON	0.41	–0.41	–0.45	–0.55	–0.01

The model selection approach was based on the Akaike information criterion (Akaike, 1974), which objectively selects drivers to produce the highest inflow variance and to generate an optimal model that combines the influence of the most influential drivers over the 1950–1989 period. This approach results in 50 percent of the variance explained for MDB winter-spring inflow. The best fit equation is as below, where I_{ws} is the winter-spring inflow, BI is the atmospheric blocking index, and LSTR is the sub-tropical ridge intensity:

$$I_{ws}(t) = 9145 + 2952 \times BI(t) - 2238 \times IOD(t) - 1792 \times LSTR(t)$$

$$(R^2 = 50\%)$$

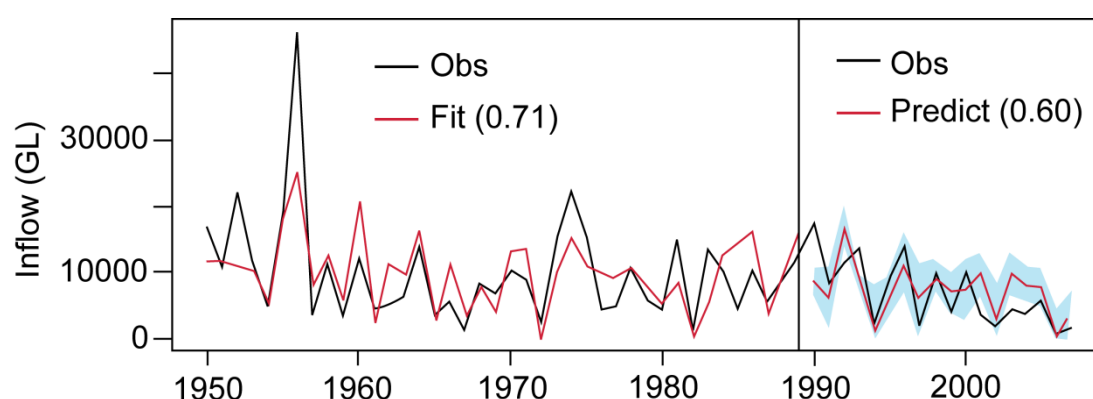


Figure 19. The relationship between the winter-spring Murray–Darling Basin inflow (black) and predicted inflow based on a simple regression model based on climate drivers (red). The results for 1950–1989 correspond to the training period, while the results for 1990–2007 correspond to the verification period. The blue shaded area indicates the upper and lower bounds of the 95 percent confidence interval for the verified predictions

In this process, ENSO is not selected as relevant, because adding ENSO as a driver does not result in an increase in the variance explained. This is consistent with the notion that much of the impact from ENSO is reflected in the IOD. The model in Figure 19 is useful for quantifying the influence of the combined climate drivers on the inflow; feeding the model with indices of climate drivers since 1989 produces a good gauge of the winter-spring inflow.

Conclusions

Our research in 2009/10 focused on two main areas:

- Is the seasonality of rainfall change over SEA consistent with climate change?
- Is there a direct linkage between climate drivers and the winter-spring inflow over the MDB?

For the first component of the project, we found that the wet season over SEA appears to have shortened in the last 30 years, with an extension of dry summer conditions into autumn, and a small decline in spring rainfall. Winter rainfall shows very little change. The autumn rainfall decline is associated with a significant increase in the density of high-pressure systems passing over southern Australia since 1950, with a decrease in the density of low-pressure systems. Reasons for such autumn circulation changes are yet to be explored; however, climate change cannot be ruled out. Preliminary analysis suggests that a breakdown in the relationship between the STR-intensity and STR-position in recent years could be a factor. Climate change does explain recent trends in spring in the pattern of the Indian Ocean (trending towards more positive IOD events), which is known to cause a decline in rainfall in SEA. The recent drought is therefore a superimposition of the reductions in spring rainfall associated with low-frequency variability, in addition to a longer term autumn rainfall decline. Investigating what drives this low-frequency variability is the next step in this research.

For the second component, we analysed the linkages between MDB inflow in the southern wet season (May to October) and climate drivers, including local patterns (such as atmospheric blocking and STR-position) and remote modes (such as ENSO, IOD and the SAM). We found statistically significant coherence between the inflow and atmospheric blocking, the IOD and the STR. SAM has little impact; further, ENSO has a weak direct influence on inflow, consistent with the notion that much of its impact is reflected through the IOD (in spring). Using a simple regression model we were able to account for 52 percent of the winter-spring inflow. An improved understanding of why the MDB inflow is sensitive to various climate drivers, particularly atmospheric blocking, will help provide improved inflows once indices of climate drivers are projected.

Links to other projects

This project has linkages to two projects external to SEACI: the Australian Climate Change Science Program project 1.8 'The response of Indo-Pacific ocean variability to climate change and its impact on Australian rainfall'; and the Urban Water Security Research Alliance project 'Climate Change Impact Assessments'.

CHAPTER 4: PROJECT 1.2

Impact of climate variability and change on the water balance

Michael Raupach, Peter Briggs, Vanessa Haverd, Kirien Whan and Caroline Ummenhofer

Abstract

- The Australian Water Availability Project (AWAP) hydrometeorological dataset has been recomputed with new (V3) meteorological data, revealing a significant (10 to 20 percent) decrease in Murray–Darling Basin (MDB) total runoff in the later part of the 20th century relative to the runoff from the earlier (V1) meteorological data.
- The AWAP dataset has been used to find a distinct asymmetry in the impacts of opposite phases of both El Niño – Southern Oscillation (ENSO) and the Indian Ocean Dipole (IOD) on Australian hydrology, and significant differences between the dominant drivers of drought at inter-annual and decadal timescales.
- Continental correlation maps between AWAP water-balance properties (rainfall and upper-layer soil moisture) and climate indices (the tripole index and the indices for ENSO and IOD) show that the tripole has the largest association with rainfall and soil moisture.

Background

The aim of the Australian Water Availability Project (AWAP) is to monitor the state and trend of the terrestrial water balance of the Australian continent, using model-data fusion methods to combine both measurements and modelling. The project determines the past history and present state of soil moisture and all water fluxes contributing to changes in soil moisture (rainfall, transpiration, soil evaporation, surface runoff and deep drainage), across the entire Australian continent at a spatial resolution of 5 km. Using the same basic framework, the project provides soil moistures and water fluxes over the Australian continent in three forms: (1) weekly near-real-time reporting, (2) historical monthly time series (1900 to present), and (3) monthly climatologies.

Past work in the Australian Water Availability Project (AWAP) has provided a 109-year (1900–present and ongoing) record of soil moisture and all terrestrial water fluxes over the Australian continent at 5-km spatial and daily temporal resolution (with monthly archive). This record has been validated by extensive testing against streamflow records from unimpaired gauged catchments – a sensitive test. This record provides an opportunity to better understand the relationships between climate and the terrestrial water balance, the current decreases in water availability, and the skill of prediction schemes when run in hindcast (i.e. retrospective) mode.

Objectives

The research in Project 1.2 falls into three main categories.

Australian Water Availability Project gridded hydrometeorological data

The objectives were to:

- produce time series of hydrological responses (soil moisture, runoff components, evaporation components) and proximate meteorological forcing variables (including rainfall, solar radiation and temperatures) over a limited set of test hydrological units (catchments, basins or grid cells) in south-eastern Australia (SEA), using the AWAP dataset
- ensure continuing flow of updated forcing data and model outputs to other projects in Phase 2 of SEACI, specifically Project 1.1 and Project 3.1, including Waterdyn code enhancements, data quality assessments, model reruns, and maintenance of webpages and ftp sites.

Statistical analysis of climate–water relationships

The objectives were to:

- assemble full data on indices for climate drivers (ENSO, IOD, the Southern Annular Mode (SAM), the sub-tropical ridge (STR), etc.), using websites, colleagues and other sources
- perform collaborative statistical analysis (with the University of New South Wales Climate Change Research Centre (UNSW CCRC)) of ENSO, IOD, rainfall, and AWAP soil moisture results to characterise inter-annual and inter-decadal signals in rainfall and soil moisture in SEA, and their implications for drought persistence and severity in SEA. We supplied AWAP data to UNSW CCRC colleagues, who were consulted and advised and who will be assisting in the production of a collaborative paper on the role of IOD and ENSO in droughts in SEA.

Multi-index statistical model for climate–water relationships

The objectives were to:

- create a general form for a statistical model (possibly non-linear) that relates water-balance responses over an arbitrary spatial domain (grid cell, catchment or basin) to a set of climate indices
- determine the parameters in the statistical model, using a trial set of water-balance properties over a limited set of small test catchments in SEA. This will include determination of confidence intervals, goodness of fit, explained variance and metrics of model skill. Parameter estimation methods will be selected according to the form of the statistical model from available linear and non-linear options.

Results

Australian Water Availability Project gridded hydrometeorological data

The major output from this part of the project in 2009/10 has been the successive incorporation of two improved versions (V2 and V3) of the Bureau of Meteorology (BoM) National Climate Centre (NCC) gridded meteorological data for rainfall, solar radiation and temperature. These update the V1 dataset (Jones et al.,

2007) used in earlier CSIRO AWAP work (Raupach et al., 2009; King et al., 2009) and also in associated projects in Phase 2 of SEACI up to this time. The V3 data (Jones et al., 2009) became available in February 2010, and are regarded by BoM-NCC as the first fully-supported product. There are significant differences between V1 and V3 datasets, including changes to rainfall and temperature surfaces associated with improved interpolation methods and station datasets in V3, and also differences in the treatment of no-data areas.

We have compared the V3 and V1 datasets carefully. The following examples use a sub-division of the Murray–Darling Basin (MDB) by rainfall: wet, moderate and semi-arid sub-divisions have a mean annual rainfall of >1,000 mm, 1,000 to 450 mm, and <450 mm respectively.

- Figure 20 shows an increase in the drying trend (V3 minus V1) in the MDB between the first and second half of the previous century. In wetter (higher altitude) areas (blue) the differences are positive pre-1945 and negative post-1955, indicating a greater drying trend in the new data compared to the old data. New data in agriculturally suitable areas (green) also show a decrease in the second half of the century compared with the original data.
- Figure 21 shows that this difference leads to a 10 to 20 percent decrease in AWAP estimates of annual local discharge or total runoff (defined as the sum of surface runoff and deep drainage) in the second half of the century, when V3 rainfall data are used.

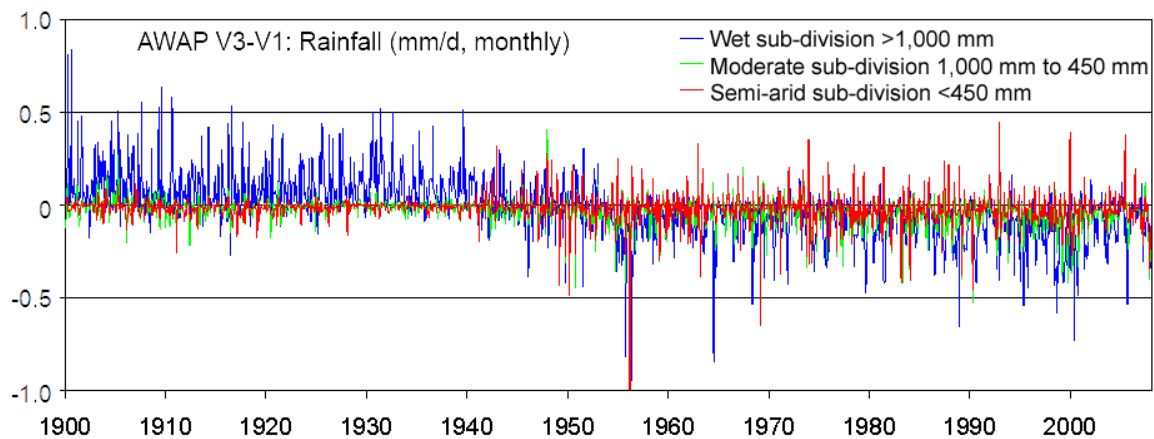


Figure 20. Monthly time series of differences in rainfall (mm/d) between two versions of the Bureau of Meteorology Australian Water Availability Project datasets (V3 minus V1) for three sub-divisions of the Murray–Darling Basin by rainfall

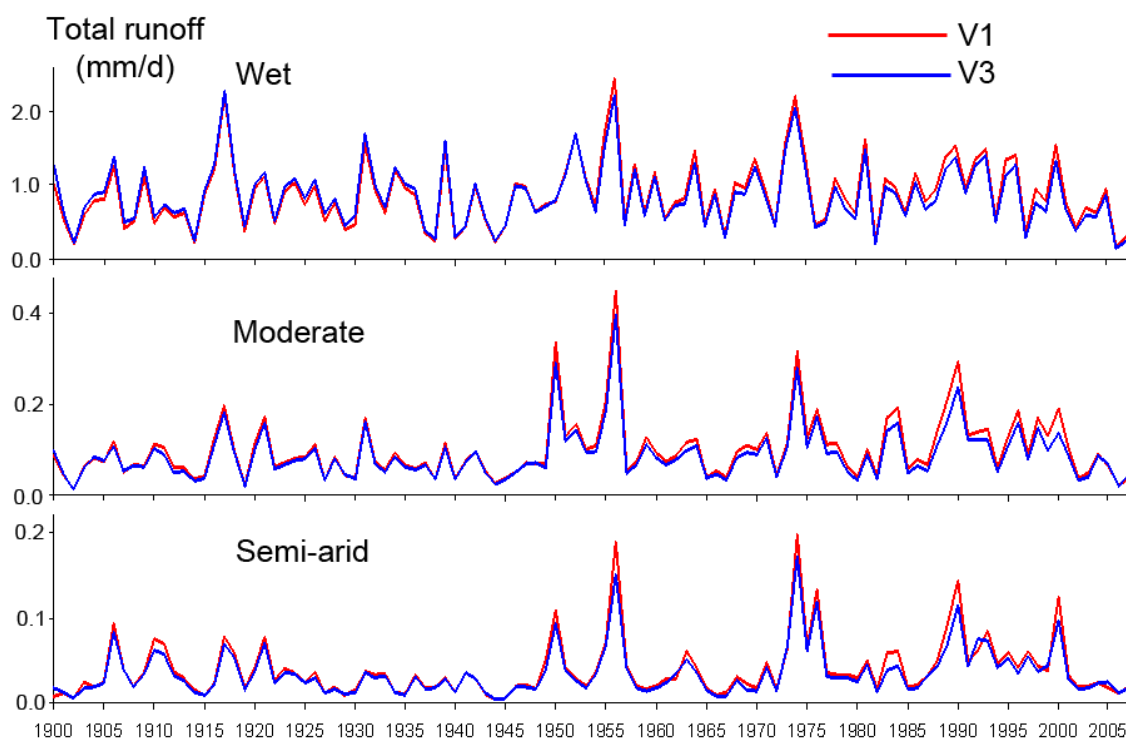


Figure 21. Annual Australian Water Availability Project total runoff (local discharge, in mm/d) for three sub-divisions of the Murray–Darling Basin by rainfall

The differences indicated above have meant that it has been necessary to repeat analyses for several products described later, including the basic AWAP hydrometeorological dataset; statistical analyses of climate–water relationships (Ummenhofer et al., in press; PhD work by Kirien Whan); and work with the CABLE model (Vanessa Haverd).

All other components of the tasks related to data collection have been completed, including:

- assembly of full data on climate indices
- preparation of V3 forcing meteorology
- new runs of AWAP WaterDyn for the continental spatial domain, including a 110-year spin-up for initialisation (Run 26b) and full 1900–2009 historical series with monthly outputs (Run 26c)
- time series of hydrological responses (soil moistures, runoff components, evaporation components) and proximate meteorological forcing variables (rainfall, solar radiation, temperatures, etc.) over a limited set of test hydrological units in SEA
- completion of regionally averaged monthly series (1900–2009) for unimpaired catchments
- assembly of river flow data for major Australian catchments towards attribution of reasons for the current major decreases in water availability and streamflow using AWAP data and the flow cascade approach.

Statistical analysis of climate–water relationships

Indian and Pacific ocean influences on south-eastern Australian drought and soil moisture (with Caroline Ummenhofer (UNSW) and others)

A collaboration with Caroline Ummenhofer and other colleagues from UNSW and CSIRO Marine and Atmospheric Sciences (Ummenhofer et al., in press) has applied AWAP data to increase understanding of the climate drivers of the water balance in SEA, particularly with respect to long periods of drought. This work is

an important precursor to the statistical modelling work that is being developed in this project (see subsequent section on the multi-index statistical model for climate–water relationships). In this work the relative influences of Indian and Pacific ocean modes of variability were investigated for seasonal, inter-annual and decadal timescales. For the period 1900–2006, observations, reanalysis products, and modelled AWAP soil moisture during the cool season were used to assess the impact of ENSO and the IOD on the MDB. Significant findings include:

- Opposite phases of both ENSO and IOD show a distinct asymmetry in their impact on Australian hydrology.
- The dominant drivers of drought differ significantly between inter-annual and decadal timescales. On inter-annual timescales, SEA soil moisture is modified by both ENSO and IOD: wettest conditions are observed during years with a La Niña co-occurring with a negative IOD event, while driest conditions occur in years when an El Niño event coincides with a positive IOD event (Figure 22). The atmospheric circulation associated with these responses is discussed in Ummenhofer et al. (in press). However, decadal variability over SEA including multi-year drought periods, was found to be more robustly related to Indian Ocean temperatures than Pacific conditions.
- During extended periods of drought, the frequencies of both negative and positive IOD events differ significantly from those during prolonged periods of ‘normal’ rainfall. More than 75 percent of all negative IOD events occur during prolonged wet periods. Conversely, no negative IOD years are recorded during droughts; instead, 60 percent of positive IOD events occur during these times. The frequency of ENSO events, in contrast, does not change.
- For the more extensive MDB, however, the impacts of La Niña become more prominent, with 63 percent of wet years occurring during a La Niña phase.
- Across the different categories of ENSO and IOD events, anomalies along the eastern seaboard (i.e., to the east of the Great Dividing Range) are not consistent with those of the wider eastern Australian region. Regional circulation patterns independent of ENSO and IOD seem to dominate rainfall along the eastern seaboard.
- The non-linearity between opposite phases of ENSO and IOD raises important issues for the techniques employed to investigate dominant drivers of climate variability on decadal to longer-term timescales.

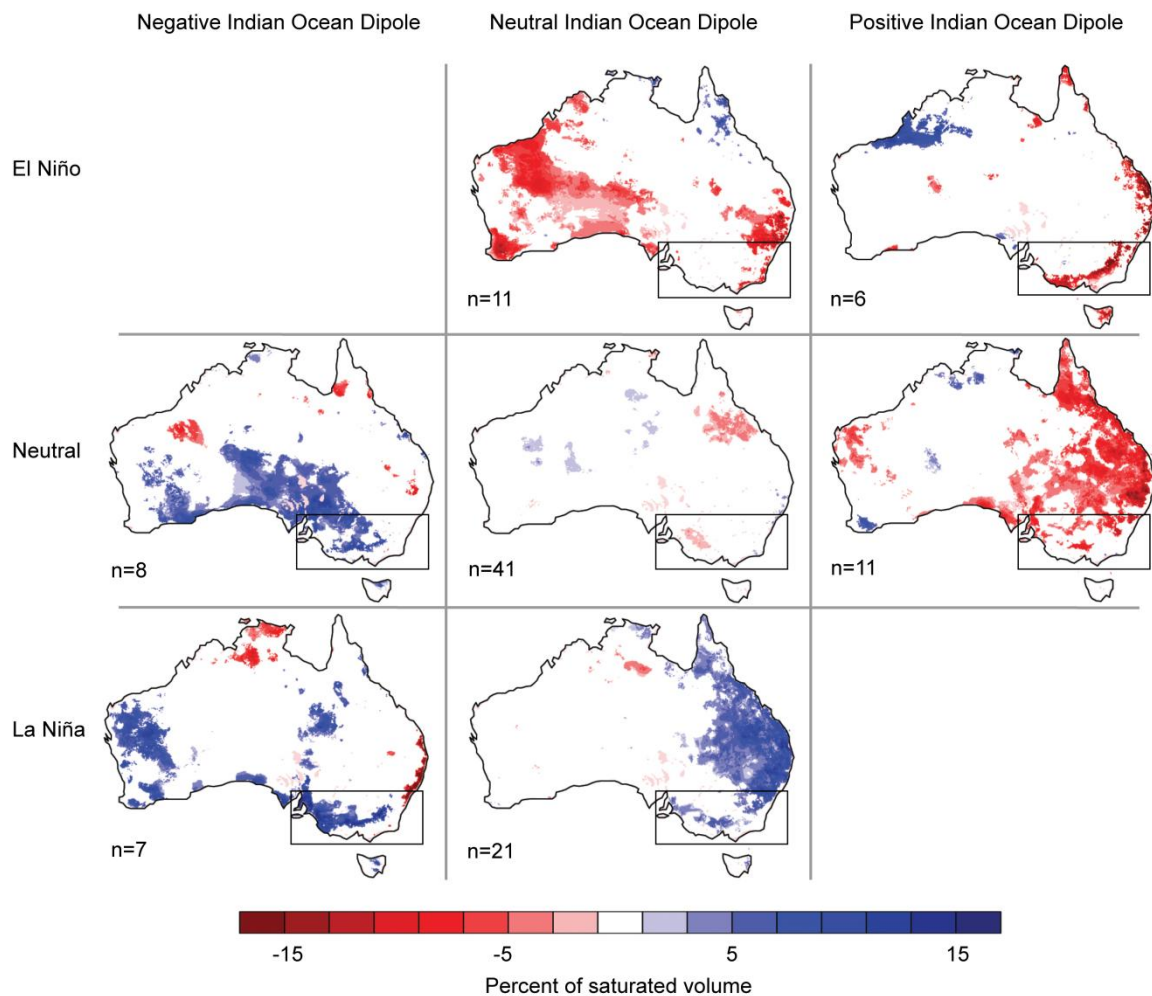


Figure 22. Composite of Australian Water Availability Project lower-layer soil-moisture anomalies in the different El Niño – Southern Oscillation and Indian Ocean Dipole categories: El Niño; La Niña; and positive or negative Indian Ocean Dipole. The number of members (n) in each category are indicated. Anomalies are for the June to October months over the period 1900–2006. The only anomalies that are shown are those which are significant at the 80 percent confidence level as estimated by a two-tailed t-test. Figure adapted from Ummenhofer et al., (in press)

Australian hydroclimatic response to tropical variability

This work focused on the seasonal correlations between climate modes (IOD, ENSO, the tropical sea-surface temperature (SST) tripole index of Timbal et al. 2010) and hydrological responses on the Australian continent as captured in the AWAP dataset. Originally completed using V1 products, this work is currently being reanalysed using V3 in preparation for publication as 'The Australian hydroclimatic response to tropical variability'.

Two sample results are provided. Figure 23 shows the zero-lag monthly correlation patterns between three climate modes (ENSO, IOD and the tripole index) and upper-layer soil moisture and rainfall in winter (Jun-Jul-Aug). For each climate mode, the correlation patterns with rainfall and upper-layer soil moisture are very similar. Precipitation recharges the upper layer of soil almost instantly, with any differences between precipitation and upper-layer soil moisture due to evaporation (driven by temperature) taking place before recharge. Due to the use of northern Australian SST in its definition, the tripole has the largest association with precipitation. Figure 24 shows correlations between rainfall and large-scale modes of variability in both winter and spring, as these are the seasons when tropical variability is the most active.

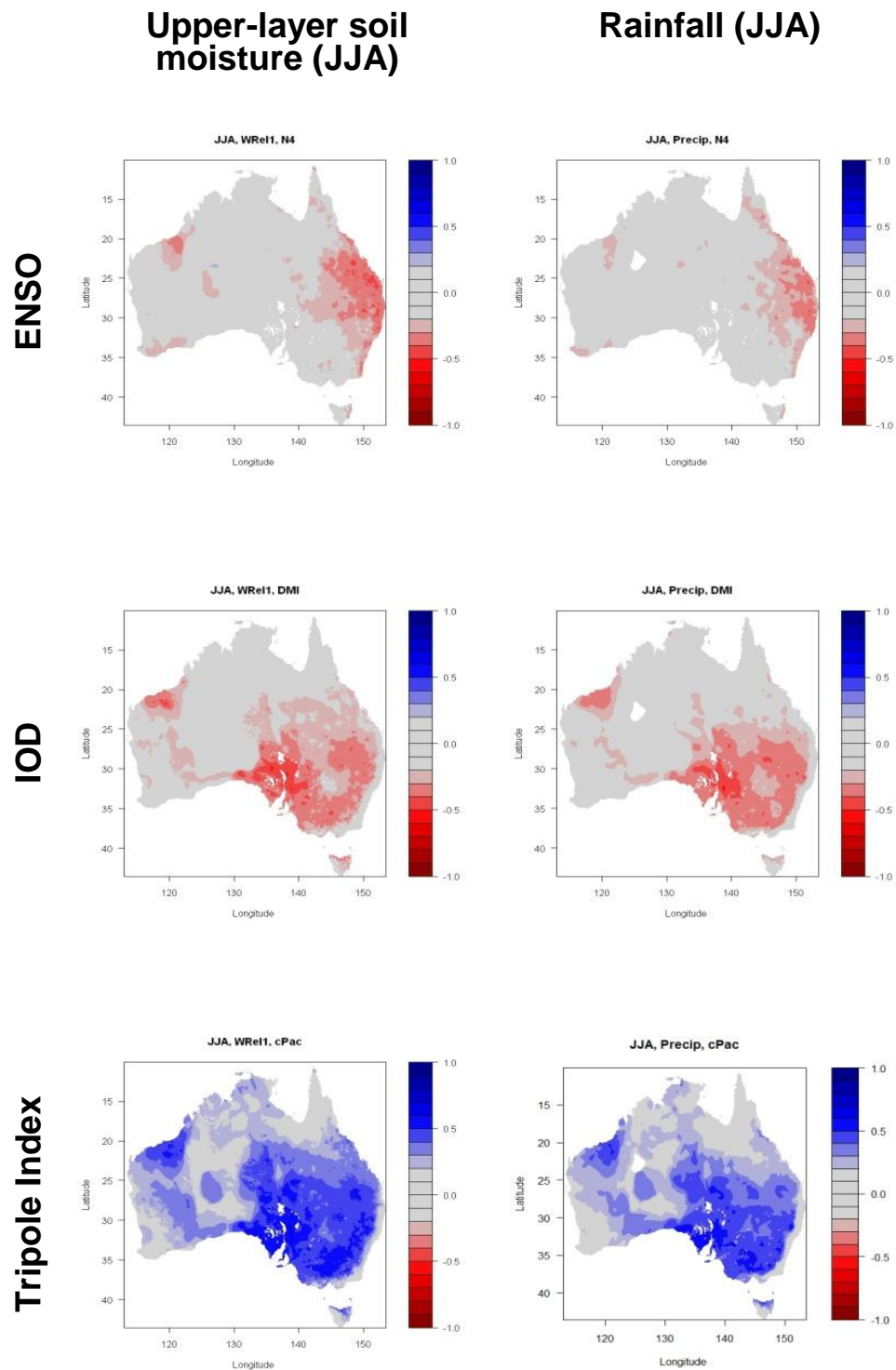


Figure 23. Zero-lag correlations between monthly winter (Jun-Jul-Aug) upper-layer soil moisture and rainfall with El Niño – Southern Oscillation (ENSO), the Indian Ocean Dipole (IOD) and the tripole index

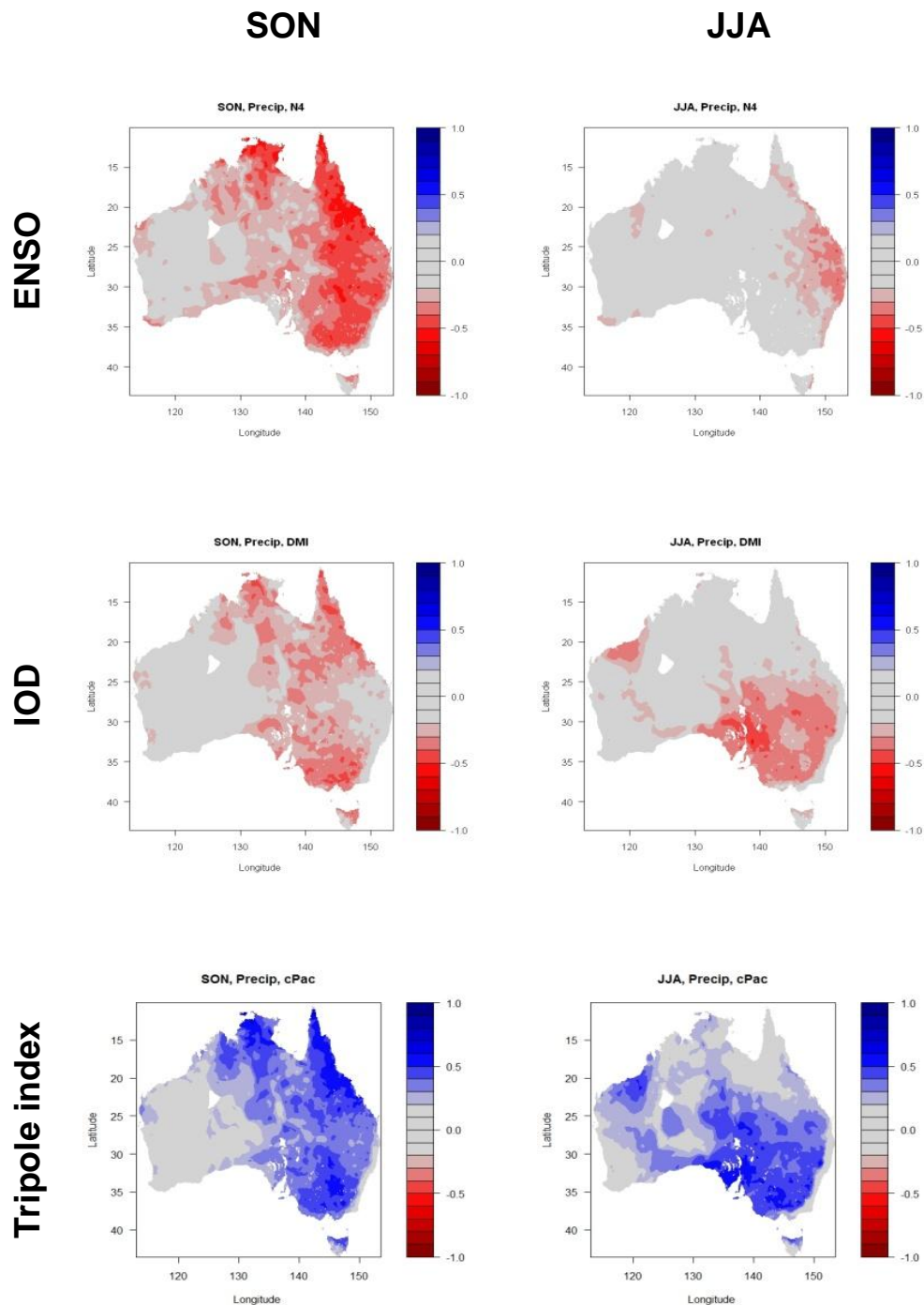


Figure 24. Simultaneous correlations between rainfall and indices for three modes of tropical sea-surface temperature variability: El Niño – Southern Oscillation (ENSO), the Indian Ocean Dipole (IOD) and the tripole index. Results are shown for winter (Jun-Jul-Aug) and spring (Sep-Oct-Nov), as these are the seasons when tropical variability is the most active. Due to the use of northern Australian sea-surface temperature in its definition, the tripole index has the largest association with rainfall

Multi-index statistical model for climate–water relationships

Here we describe the formulation of a statistical model that relates a set of water-balance responses to a set of climate indices.

The set of water-balance responses is drawn from both hydrological responses (soil moistures, runoff components, evaporation components) and proximate meteorological forcing variables (rainfall, solar

radiation, temperatures, etc.). The set of climate indices includes those for ENSO, IOD, SAM, STR, etc. Model parameters are determined by statistical fitting.

The general linear relationship between a single-point water-balance property $w(t)$ (e.g. rainfall, soil moisture, total runoff) and a set of N climate modes $a_n(t)$ (e.g. ENSO, IOD, STR) is:

$$w(t) = \sum_{n=1}^N x_n a_n t$$

where x_n is a set of N weights which constitute the model parameters. Considering this relationship across a set of M spatial points, this relationship can be written in the vector-matrix form:

$$\begin{pmatrix} w_1 \\ w_2 \\ \vdots \\ w_M \end{pmatrix} = \begin{pmatrix} a_{11} & a_{12} & a_{13} \\ a_{21} & a_{22} & a_{23} \\ \vdots & \vdots & \vdots \\ a_{M1} & a_{M2} & a_{M3} \end{pmatrix} \begin{pmatrix} x_1 \\ x_2 \\ x_3 \end{pmatrix}$$

or:

$$\mathbf{w} = \mathbf{A} \cdot \mathbf{x}$$

where the column vector \mathbf{w} is a time series of M values of a local water-balance property, the matrix \mathbf{A} is a set of time series of climate indices ($M \times N$), and the column vector \mathbf{x} is a set of N parameters. Typically we have $M \approx 1,000$ and $N \approx 3$.

The problem is to find the parameters \mathbf{x} , given climate indices \mathbf{A} and the water-balance property \mathbf{w} . This is done by minimising:

$$\text{Error}^2 = \mathbf{w} - \mathbf{A}\mathbf{x}^T \mathbf{w} - \mathbf{A}\mathbf{x}$$

This problem has an analytic solution which can be found by several methods and can be expressed in several equivalent ways:

1. Solution by variation yields:

$$\mathbf{x} = \mathbf{A}^T \mathbf{A}^{-1} \mathbf{A}^T \mathbf{w}$$

2. An alternative expression can be obtained using the singular value decomposition of \mathbf{A} :

$$\mathbf{A}_{M \times N} = \begin{pmatrix} \mathbf{U} \\ M \times M \\ \text{column-} \\ \text{orthonormal} \end{pmatrix} \begin{pmatrix} \mathbf{W} \\ M \times N \\ \text{diagonal} \end{pmatrix} \begin{pmatrix} \mathbf{V}^T \\ N \times N \\ \text{column-} \\ \text{orthonormal} \end{pmatrix}$$

This approach yields an equivalent expression for \mathbf{x} :

$$\mathbf{x} = \mathbf{V}\mathbf{W}^{-1}\mathbf{U}^T\mathbf{w}$$

3. We can form the correlation vector \mathbf{b} ($N \times 1$) between the climate indices and water-balance property \mathbf{w} , and also the correlation matrix \mathbf{C} ($N \times N$) between climate indices:

$$\mathbf{C} = \mathbf{M}^{-1}\mathbf{A}^T\mathbf{A}, \quad \mathbf{b} = \mathbf{M}^{-1}\mathbf{A}^T\mathbf{w}$$

Figure 23 shows spatial maps of components of \mathbf{b} for the set of climate indices (the tripole index and the indices for ENSO and IOD). In terms of these quantities, the solution for the parameters \mathbf{x} is:

$$\mathbf{x} = \mathbf{C}^{-1}\mathbf{b}$$

Any of the mathematically identical forms (1), (2) and (3) constitutes the analytic solution for the statistical model $\mathbf{w} = \mathbf{A}\mathbf{x}$. We note that:

- The model as described above is for a single point. Large-scale (e.g. Australian continent) application is simply a question of applying this model repeatedly for water-balance time series \mathbf{w} in different cells (there are about 278,000 0.05 degree cells in the continental AWAP dataset). The result is a set of N parameters \mathbf{x} in each cell ($N = 3$ for three climate indices) which give the weights describing the relationship between the water-balance property and multiple climate indices.
- Solution for model parameters \mathbf{x} can be done analytically in the linear version described here (that is, without searching numerically for a minimum in model-measurement squared differences). This makes the model very fast to apply.
- The model can be generalised to allow properties such as time lags and threshold effects to emerge from fitted parameters rather than being externally imposed *a priori*. In this case the matrix \mathbf{A} is a matrix of non-linear functions of climate indices, and the parameters of the non-linear functions have to be found by numerical minimisation of the squared error given above.

This model, developed in 2009/10, will be applied and tested in 2010/11.

Conclusions

- The AWAP hydrometeorological dataset has been recomputed with new (V3) meteorological data, revealing a significant (10 to 20 percent) decrease in MDB total runoff in the later part of the 20th century relative to the runoff from the earlier (V1) meteorological data.
- The AWAP dataset has been used to find a distinct asymmetry in the impacts of opposite phases of both ENSO and IOD on Australian hydrology, and significant differences between the dominant drivers of drought at inter-annual and decadal timescales (Ummenhofer et al., in press).
- Continental correlation maps between AWAP water-balance properties (rainfall and upper-layer soil moisture) and climate indices (the tripole index and the indices for ENSO and IOD) show that the tripole has the largest association with rainfall and soil moisture.

Links to other projects

In 2009/10, Project 1.2 supplied AWAP data to and collaborated with Project 1.1b on the association between global warming and declining soil moisture and runoff (Cai et al. 2009a), and on the link between positive IOD events and bushfires (Cai et al. 2009b). A collaboration with Caroline Ummenhofer and other CMAR and UNSW colleagues has applied AWAP data to increase understanding of the climate drivers of the water balance in south-eastern Australia, particularly with respect to long periods of drought. These results are reported here and in Ummenhofer et al. 2010. Including SEACI projects, the growing AWAP data user list consists of over 90 people representing 32 government, university, and industry bodies, involving over 60 active, completed, or proposed projects. Three quarters of these activities involve the use of CSIRO AWAP model products separately or in conjunction with Bureau of Meteorology (BoM) AWAP meteorology. With the support of SEACI, AWAP model results are made available to the Australian community on a weekly basis via the CSIRO AWAP website at <<http://www.csiro.au/awap>>.

CHAPTER 5: PROJECT 2.1

Climate change projections

Francis Chiew, Dewi Kirono, Jin Teng, David Kent and Bertrand Timbal

Abstract

The research in Project 2.1 builds on results from Phase 1 of SEACI to improve the assessment and selection of global climate models (GCMs) for hydrological applications. It also investigates and accounts for the relative uncertainties in the different components for modelling climate change impact on runoff.

There were two activities in 2009/10. The first activity assessed the representation of the Australian sub-tropical ridge (STR) in the GCMs from the Intergovernmental Panel on Climate Change Fourth Assessment Report (IPCC AR4), and the implications for future rainfall projections for south-eastern Australia (SEA). The study showed that:

- the multi-model mean replicates the observed annual cycle of STR-intensity and STR-position well, but only a few of the GCMs can capture this annual cycle
- most GCMs show the relationship between weak STR and high rainfall, but the modelled relationship is much weaker than the observed STR–rainfall relationship
- the STR is likely to become more intense and move further south, suggesting a likely reduction in future rainfall in SEA.

The inability of most of the GCMs to closely reproduce the observed behaviour of the STR and the observed STR–rainfall relationship is of some concern because the STR is an important feature of the Southern Hemisphere’s general circulation of the climate system and it is one of the key drivers of rainfall in SEA.

The second activity carried out two modelling studies in SEA to investigate the relative uncertainties in the three main modelling components in the majority of studies on climate change impact on runoff: (i) interpretation of GCM projections; (ii) downscaling GCM simulations to obtain catchment-scale rainfall; (iii) and hydrological modelling to predict climate change impact on runoff. The modelling studies showed that:

- the largest uncertainties come from the GCM projections
- the difference in simulations using different downscaling methods is about half the range of future projections from different GCMs
- the difference in runoff simulations using different lumped conceptual rainfall-runoff models is small compared to the differences amongst GCM projections and downscaling methods.

Background

The main goal of the research in Theme 2 is to improve hydroclimate projections for SEA. The research in Theme 2 is at the climate–water interface, and its link to climate science and hydrological modelling science is shown schematically in Figure 25.

Hydrological models are generally tailored for specific applications, and are developed and calibrated using local data. There are two main steps involved in estimating climate impact on future runoff characteristics and water availability. The first step uses GCM projections and downscaling models to obtain future catchment-scale climate series to drive hydrological models. Project 2.1 carries out research in this area. The second step involves driving hydrological models with future climate series to estimate future runoff. This may require adapting models to account for changes in the rainfall–temperature–runoff relationship and changes in the dominant hydrological processes in a drier, warmer environment with higher levels of carbon dioxide (CO₂). Project 2.2 carries out research in this area. Both projects in Theme 2 are closely related to – and use information from – the projects in Theme 1.

The research in Project 2.1 builds on results from Phase 1 of SEACI to improve the assessment and selection of GCMs for hydrological applications and to investigate and account for the relative uncertainties in the different components for modelling climate change impact on runoff. This will lead to more accurate and updated future catchment-scale climate series to drive hydrological models in climate change impact studies.

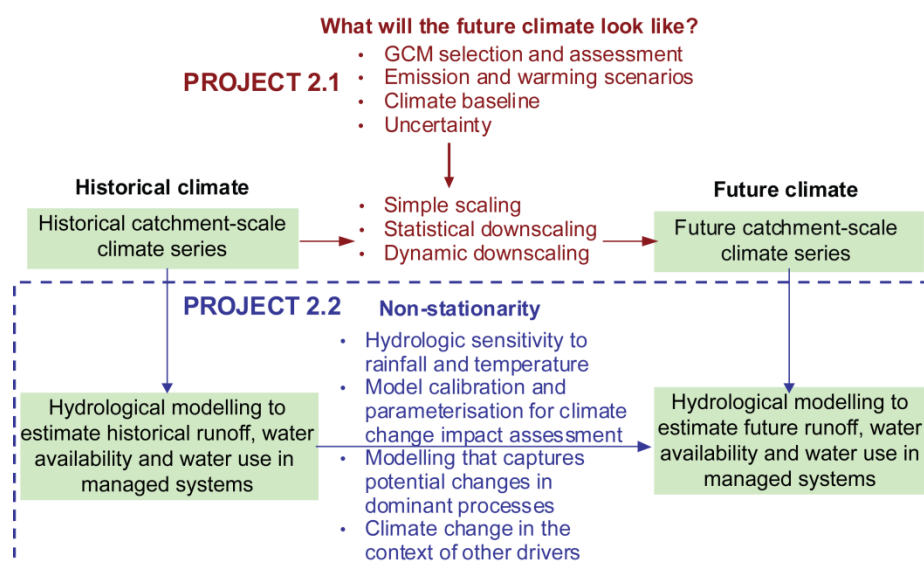


Figure 25. Modelling climate change impact on runoff

Objectives

Assessment of global climate model simulation of the sub-tropical ridge

- Assess the representation of the Australian sub-tropical ridge (STR) in the IPCC AR4 GCMs and the implications for future rainfall projections for SEA.

Uncertainty in climate–water prediction

- Investigate the relative uncertainty in GCM projections, downscaling methods and hydrological models that model climate change impact on runoff.

Methods and results

Assessment of global climate model simulation of the sub-tropical ridge

This study is described in detail in a paper submitted to the *International Journal of Climatology* (Kent et al., submitted).

Rainfall is the key driver of runoff, and in Australia, the range of projected changes in rainfall (allowing for model-to-model differences) is relatively large (CSIRO and BoM, 2007). On the other hand, the end-users (policy makers and water managers) require reduced uncertainty in projections of future climate. This leads to the model selection issue which poses questions such as: How does one select a model? Should one use all the available models to obtain a better representation of uncertainty? Should one assess and select models and on what criteria should the selection be based? There have been several studies with different views and approaches attempting to address this GCM evaluation and selection issue. Some researchers assessed GCMs based on their ability to simulate climate variables such as rainfall and temperature, while others explored the performance of GCMs in simulating climate drivers such as El Niño – Southern Oscillation and the Indian Ocean Dipole.

In terms of the climate drivers, the results from Theme 1 in Phase 1 of SEACI suggested that the STR is an important feature of the Southern Hemisphere general circulation of the climate system, and that its intensity has a strong negative relationship with rainfall in SEA (Timbal, 2009). For this reason, this study examines the representation of the STR in the IPCC AR4 GCMs. In particular, the mean state and variability of the STR's intensity and position, and the teleconnection between STR-intensity and rainfall in SEA, are diagnosed and compared to observations for the 20th century. The results are subsequently used to examine the influence of choice of GCMs on projected changes in rainfall.

In this study, monthly mean sea-level pressure (MSLP) data from the 23 IPCC AR4 GCMs were used to calculate monthly and annual time series representing the characteristics of the STR. Each of these modelled time series was compared to time series derived from the NCEP reanalysis (Kalnay et al., 1996) from 1948 to 2002 and those derived by Drosowsky (2005) (updated to 2008) who used an operational Australian Bureau of Meteorology (BoM) MSLP dataset from 1890 to 2008 (referred to here as the BoM dataset). The two parameters representing the STR were calculated following the method of Drosowsky (2005) which were refined by Timbal and Smith (2009). The two metrics used were the latitude (referred to as 'STR-position') and value (referred to as 'STR-intensity') of the maximum MSLP between 9 to 45°S and a selected longitude band (140 to 150°E for the observations, different for different GCMs). The model performance scores were calculated following the approach of Pierce et al. (2009) and were represented as the Euclidian distance from each model's score to a perfect score of one (Δ_{ss}).

The results are discussed in detail in Kent et al. (submitted), and the key findings are summarised below:

- The multi-model mean replicates the observed annual cycle of STR-intensity and STR-position well, but only a few of the GCMs can capture this annual cycle (Figure 26). Models that represent the annual cycle relatively well include CCSM3, CSIRO-Mk3.0, GFDL-CM2.1 and INMCM3.0.
- While the mean annual cycle of the STR-intensity and STR-position are moderately well represented, the inter-annual cycle of variability is not as well captured.
- Most models show the relationship between weak STR and high rainfall, but the modelled relationship is much weaker than the observed relationship. The fact that most models are able to show the teleconnection is satisfying, but the fact that the relationship is much weaker than that in the observed data is a concern.
- The STR (as seen in the ensemble mean) is likely to become more intense and move further south (Figure 27). This suggests a likely reduction in future rainfall in SEA.

- The modelled relationship between STR-intensity and rainfall in the 21st century is broadly similar to that in the 20th century.

To some extent, the use of the better GCMs (those which can reproduce the observed STR) compared to the use of all the 23 GCMs indicates a more intense STR and slightly larger decline (and smaller range) in future rainfall (Figure 28).

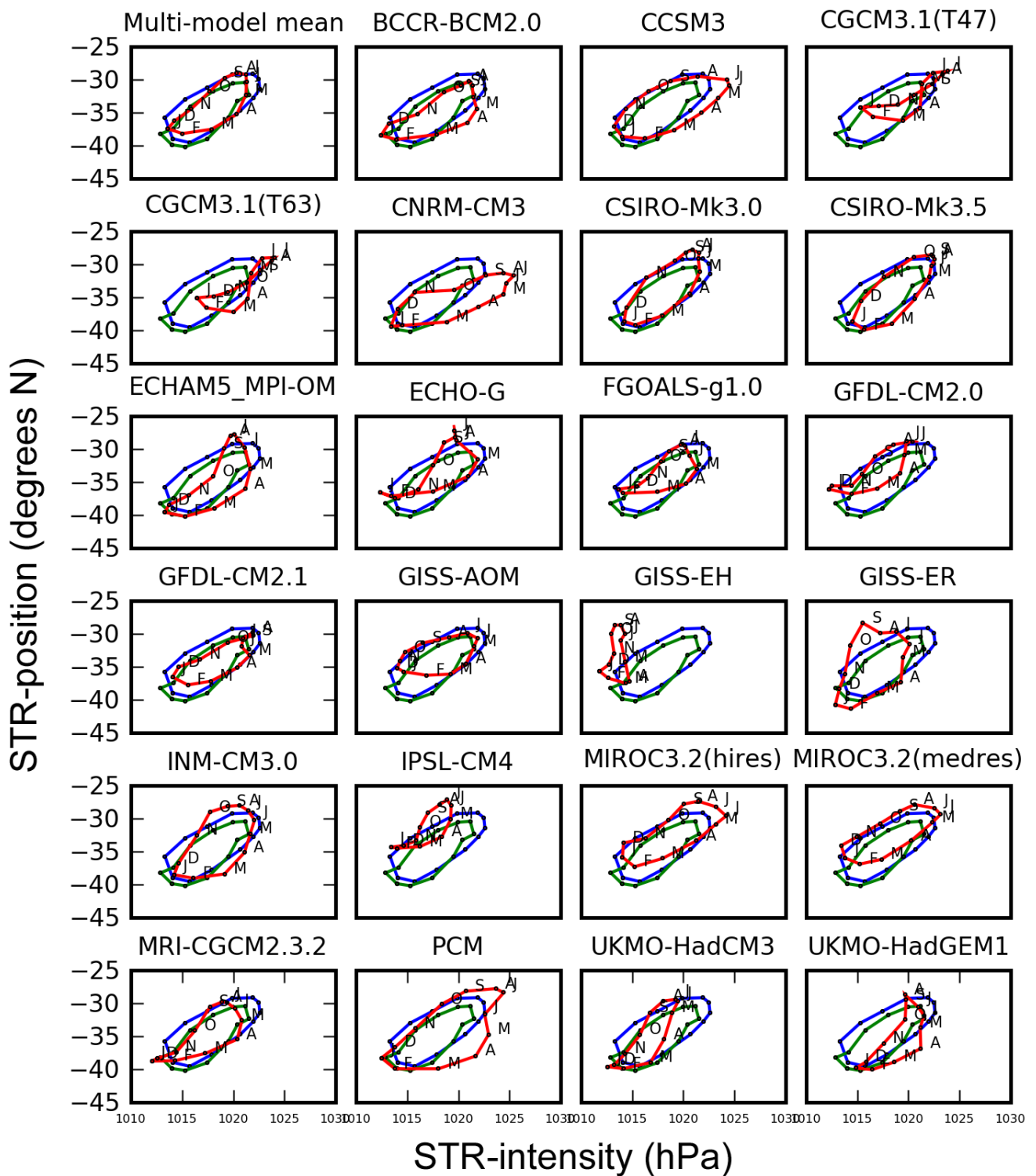
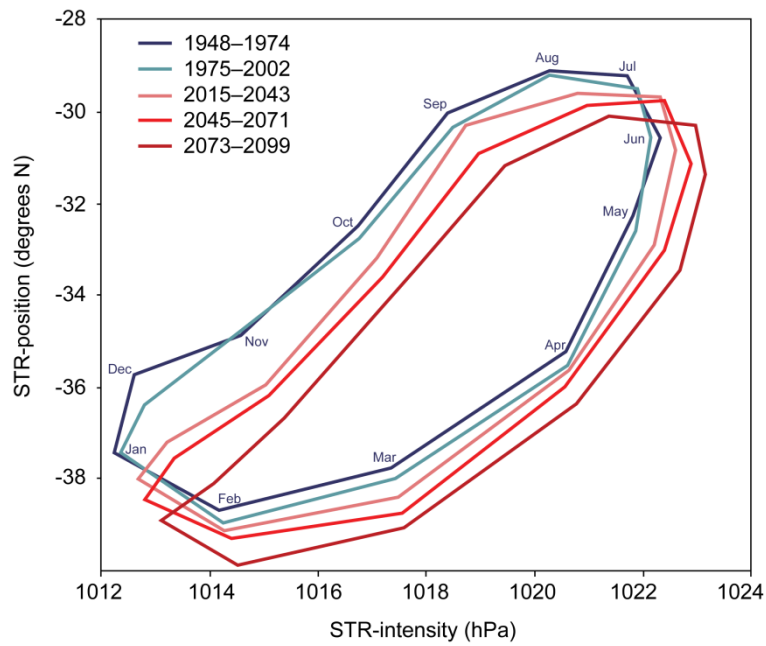


Figure 26. The annual cycle of sub-tropical ridge intensity (STR-intensity) and sub-tropical ridge position (STR-position). Observations from NCEP reanalysis are shown in green; observations from the Bureau of Meteorology are shown in blue; and modelled results using 23 global climate models (and a multi-model mean) are shown in red

(a)



(b)

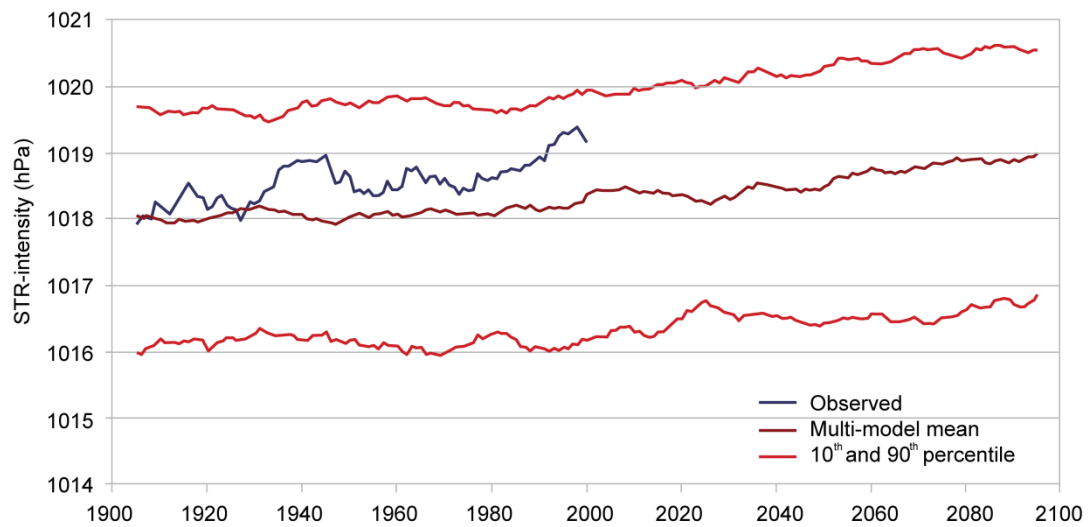


Figure 27. (a) Projected annual cycle of sub-tropical ridge intensity (STR-intensity) and sub-tropical ridge position (STR-position) for five time periods, based on a multi-model mean (using 23 models). (b) Observed and modelled STR-intensity (smoothed) for 1900–2100

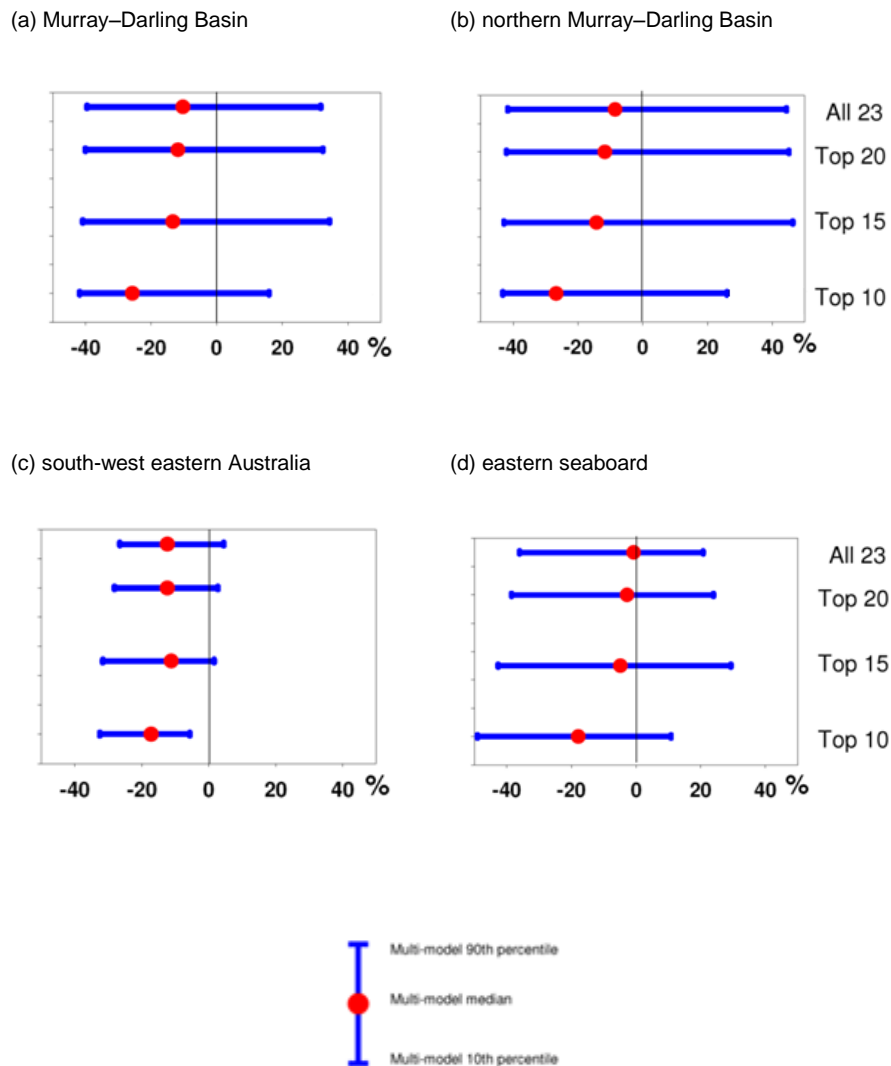


Figure 28. Projected percentage changes in rainfall per degree global warming for selected regions from south-eastern Australia: (a) Murray–Darling Basin; (b) northern Murray–Darling Basin; (c) south-west eastern Australia; and (d) the eastern seaboard. Different numbers of global climate models are used, based on their ability to reproduce the observed sub-tropical ridge

Uncertainty in climate–water prediction

This activity carried out two modelling studies. The second study has been published in the *Journal of Hydrology* (Chiew et al., 2010).

The main components in modelling climate change impact on future runoff are:

- interpreting GCM projections of future climate and/or large-scale atmospheric–oceanic drivers of regional/local climate (in particular rainfall)
- downscaling GCM simulations to obtain catchment-scale daily climate series – in particular rainfall – to drive hydrological models
- hydrological modelling to predict climate change impact on runoff.

This activity carried out two modelling studies to investigate the relative uncertainties in these three main modelling components adopted in the majority of studies of climate change impact on runoff.

The first modelling study used five lumped conceptual daily rainfall-runoff models to estimate the impact of climate change on runoff. The runoff was modelled for about 50,000 0.05° grid cells across SEA. The climate change projections were informed by 15 of the 23 IPCC AR4 GCMs. A daily scaling (or perturbation) method was used to scale the historical daily rainfall (and potential evaporation) series to reflect a future climate (for a 1 °C global warming). The method is described in detail in Chiew et al. (2007) and was used to model the future (range) of runoff in Phase 1 of SEACI (Post et al., 2008) and in the CSIRO Sustainable Yields Projects <<http://www.csiro.au/partnerships/SYP.html>>.

The spatial plots in Figure 29 show the percentage change in future mean annual runoff (for a 1 °C global warming) modelled by the five rainfall-runoff models, informed by projections from the 15 GCMs. The plots in Figure 30 summarise the range of results from the five rainfall-runoff models and 15 GCMs for mean annual runoff, mean summer runoff and mean winter runoff averaged across the entire study area in SEA.

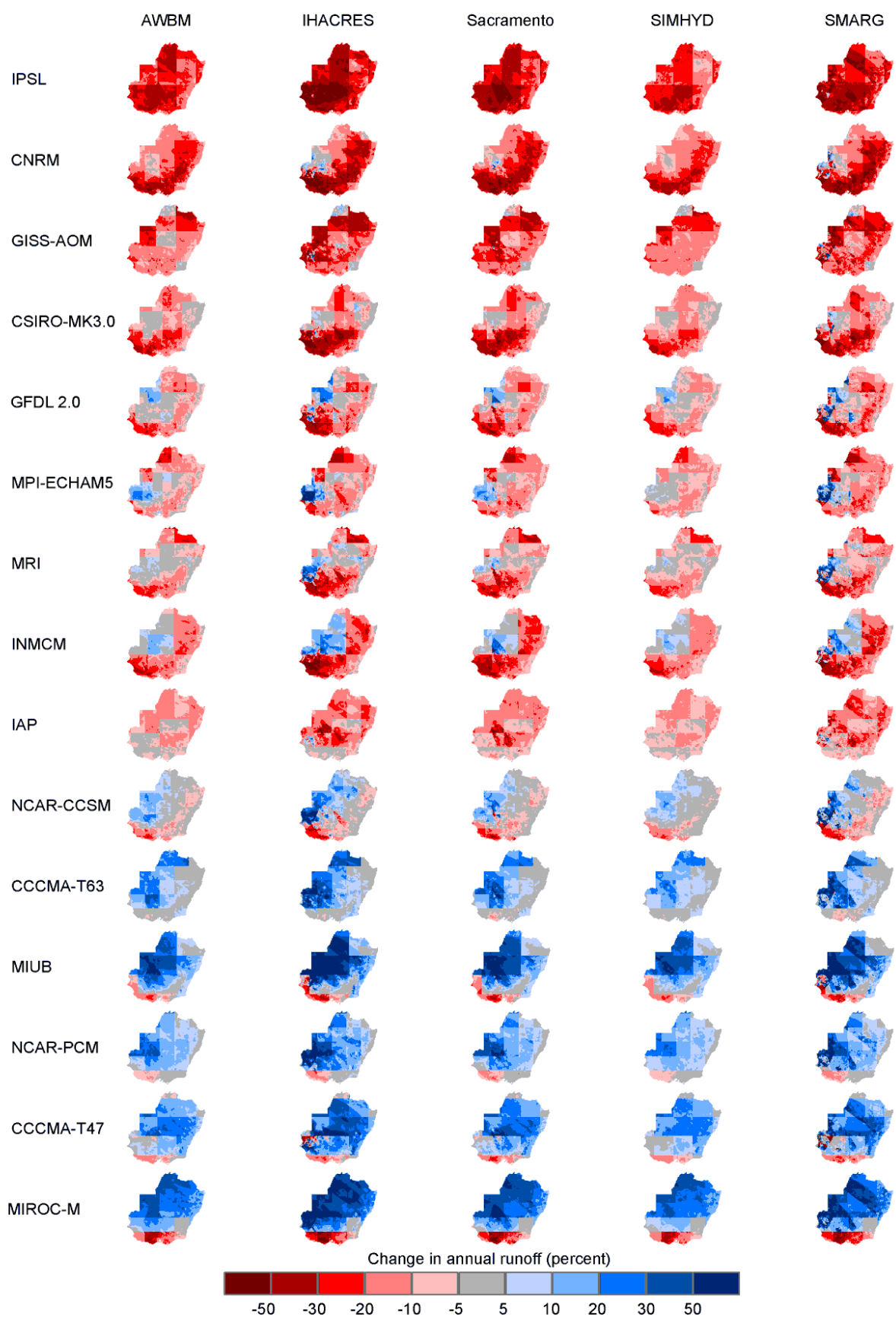


Figure 29. Percentage change in future mean annual runoff (for a 1 °C global warming) modelled by five rainfall-runoff models informed by rainfall projections from 15 global climate models

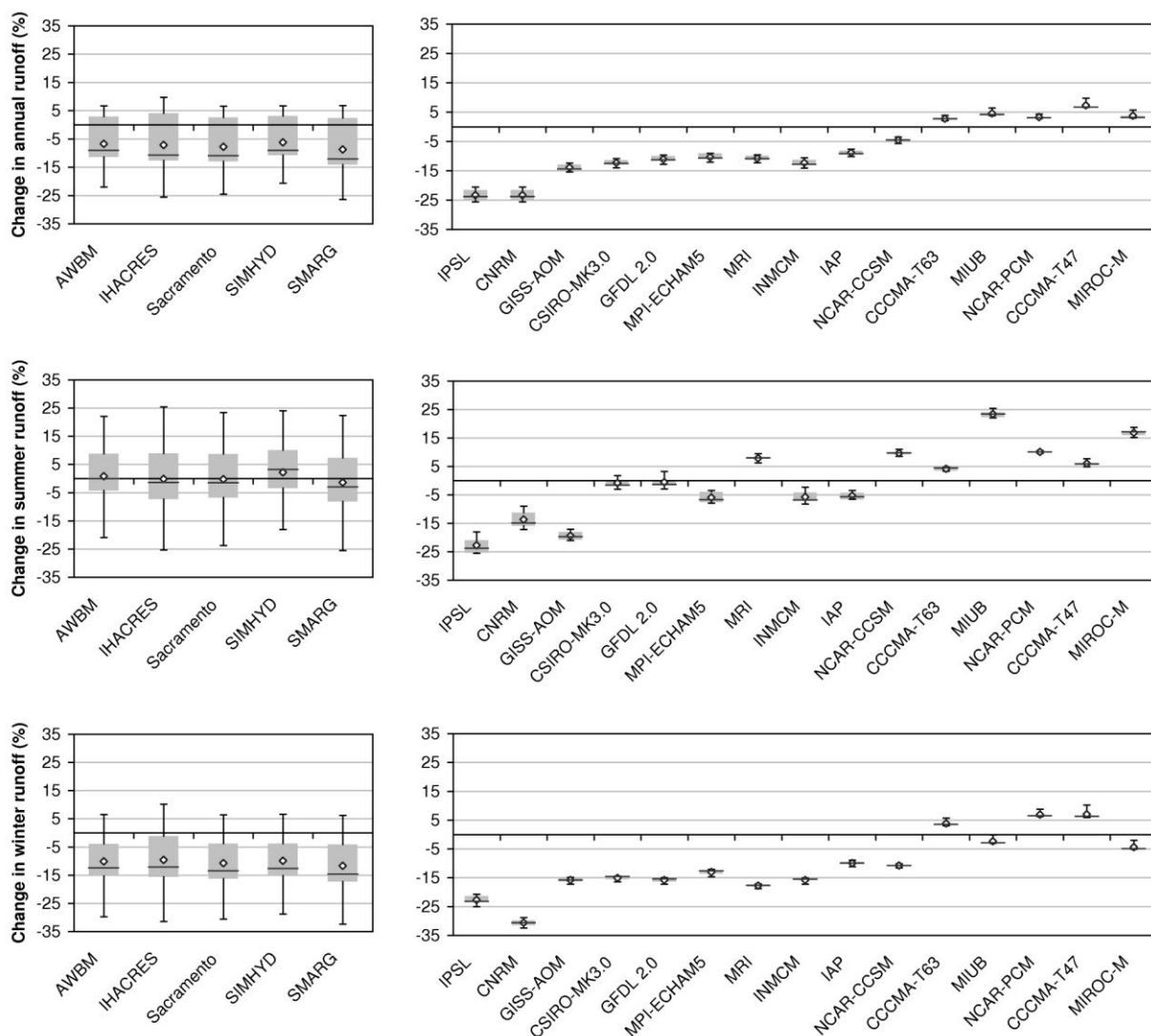


Figure 30. Range of percentage change in future mean annual, summer and winter runoff (for a 1 °C global warming) from five rainfall-runoff models and 15 global climate models averaged across south-eastern Australia

The range in results from the rainfall-runoff models is small (up to 5 percent for mean annual runoff, higher for other runoff characteristics) compared to the range of future runoff modelled using rainfall projections from the range of GCMs (about 30 percent for mean annual runoff) (Figure 29). Note that the implementation of the rainfall-runoff models is similar to that in most climate change impact studies: the models are calibrated against observed historical data, and potential non-stationarity in rainfall–temperature–runoff and in dominant hydrological processes is not explicitly accounted for. Practically all the GCMs agree on a reduction in winter rainfall leading to a reduction in modelled winter and also annual runoff, since runoff from the high-runoff generation areas in the region is mainly winter-dominated (Figure 30). The variability in summer is large, with about half the GCMs indicating a decline in future summer rainfall, and about half the GCMs indicating an increase in future summer rainfall. Although relatively small compared to the range in the GCM future projections, the difference between the rainfall-runoff models is larger for the very dry future rainfall projections (Figure 31).

The second modelling study:

- assessed the rainfall downscaled from three GCMs using five downscaling models

- assessed the runoff modelled by the SIMHYD rainfall-runoff model using the downscaled daily rainfall
- compared the modelled changes in future rainfall and runoff characteristics.

This study was carried out with support from Phase 1 of SEACI, the Australian Climate Change Science Program and the eWater CRC. A paper on the study has been published in the *Journal of Hydrology* (Chiew et al., 2010).

The modelling study was carried out using rainfall and streamflow data from eight unimpaired catchments near the headwaters of the Murray–Darling Basin in SEA. The downscaling models used, in increasing order of complexity, were a daily scaling model; an analogue statistical downscaling model; two parametric statistical downscaling models, GLIMCLIM and the non-homogenous hidden Markov Model (NHMM); and the cubic conformal atmospheric model (CCAM) dynamic downscaling model. The downscaling models and rainfall-runoff models were developed and calibrated using 1981–2000 data. All the downscaling models can generally reproduce the observed historical rainfall characteristics. The rainfall-runoff modelling using downscaled rainfall also generally reproduces the observed historical runoff characteristics. The future projections (for 2046–2065 relative to 1981–2000) are most similar between the daily scaling, analogue and NHMM models, all of them projecting a drier future. The GLIMCLIM and CCAM models simulate a smaller decline in future rainfall. The differences between the modelled future runoff using the different downscaled rainfall are about half the range of GCM projections discussed earlier. The simpler-to-apply daily scaling and analogue models (which also directly provide gridded rainfall inputs) can be relatively easily used for impact assessments over very large regions. The parametric downscaling models offer potential improvements as they capture a fuller range of daily rainfall characteristics.

Percentage change (2046-2065 relative to 1981-2000) in various runoff characteristics (weighted by the values of the variables in the eight catchments)

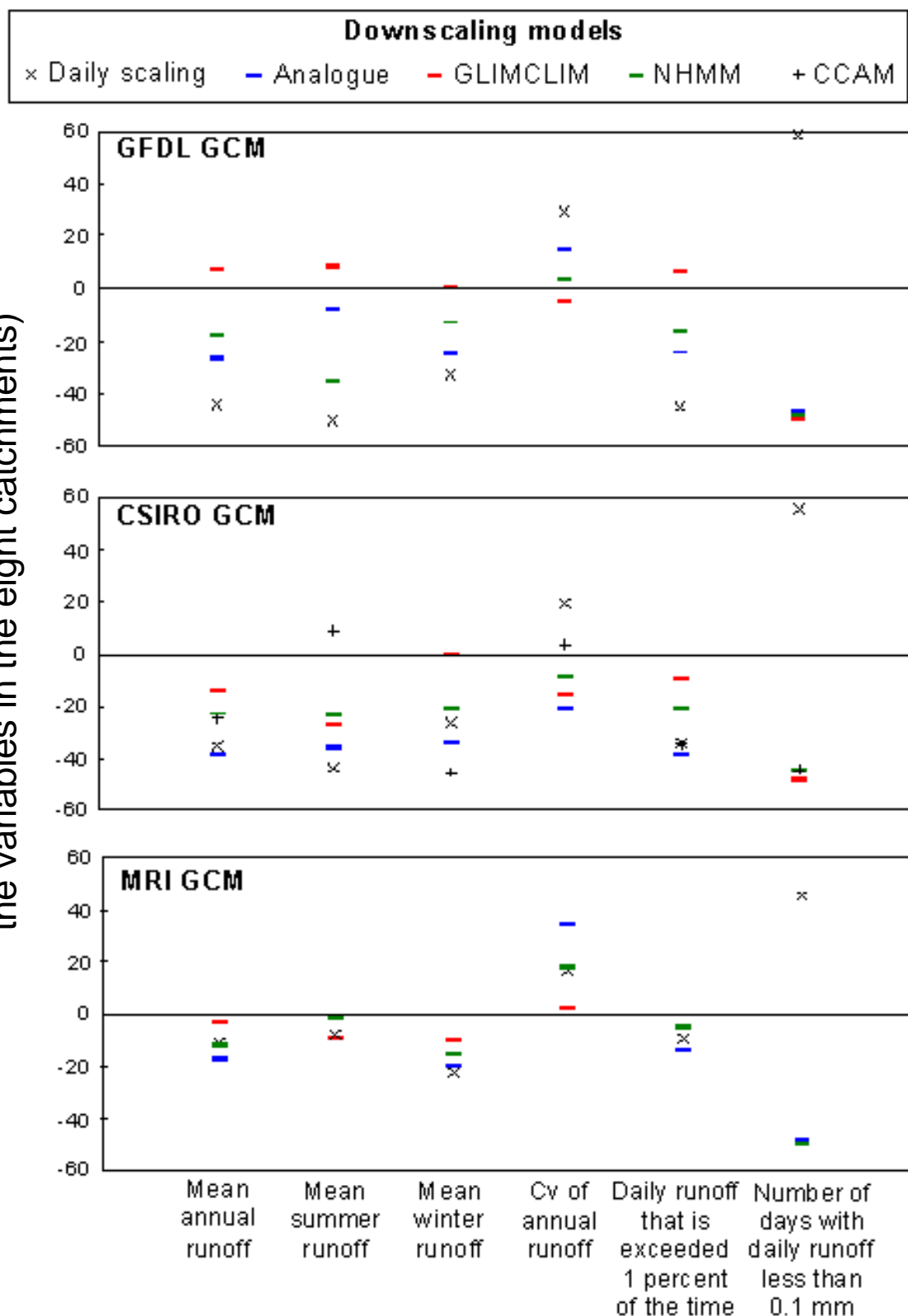


Figure 31. Percentage change in runoff characteristics for the future period (2046–2065) relative to the historical period (1981–2000) modelled by the SIMHYD rainfall-runoff model with daily rainfall downscaled using five downscaling models informed by three global climate models. The data points show the weighted values for the eight catchments, weighted by the values of the variables on the x-axis

Conclusions

The research activities in Project 2.1 build on results from Phase 1 of SEACI to improve GCM assessment and selection for hydrological applications and to investigate and account for the relative uncertainties in the different components for modelling climate change impact on runoff. This will lead to more accurate and updated future catchment-scale climate series to drive hydrological models in climate change impact studies, and will result in a reduction of associated uncertainties.

There were two activities in 2009/10. The first activity assessed the representation of the Australian STR in the IPCC AR4 GCMs and the implications for future rainfall projections for SEA. The study showed that (i) the multi-model mean replicates the observed STR very well, but only a few of the GCMs can capture the annual cycle; (ii) most GCMs show the relationship between weak STR and high rainfall, but the modelled relationship is much weaker than the observed STR–rainfall relationship; and (iii) the STR is likely to become more intense and move further south, suggesting that future rainfall in SEA is likely to be less than historical rainfall. The GCMs are unable to exactly reproduce the observed STR and the observed STR–rainfall relationship, although most of the GCMs can reproduce the broad features. This is of some concern because the STR is an important feature of the Southern Hemisphere’s general circulation of the climate system and it is one of the key drivers of rainfall in SEA.

The second activity carried out two modelling studies in SEA to investigate the relative uncertainties in the three main modelling components in the majority of studies of climate change impact on runoff:

(i) interpretation of GCM projections; (ii) downscaling GCM simulations to obtain catchment-scale rainfall; (iii) and hydrological modelling to predict climate change impact on runoff. The modelling studies showed that (i) the largest uncertainty comes from the GCM projections; (ii) the difference in simulations using different downscaling methods is about half the range of future projections from different GCMs; and (iii) the difference in runoff simulations using different lumped conceptual rainfall-runoff models is small compared to the differences amongst GCM projections and downscaling methods.

Links to other projects

Project 2.1 is strongly linked to Theme 1 and Project 2.2. The GCM assessment and selection is carried out in the context of the major drivers for rainfall in SEA identified in Theme 1 and the hydrological modelling in Project 2.2. The more accurate and updated future catchment-scale climate series (and associated uncertainties) from Project 2.1 will be used to drive the hydrological models in Project 2.2 and elsewhere to improve prediction of climate change impact on future runoff.

CHAPTER 6: PROJECT 2.2

Hydroclimate impacts for south-eastern Australia

Francis Chiew, Nick Potter, Jai Vaze, David Post, Tim McVicar, Randall Donohue and Lu Zhang

Abstract

The research in Project 2.2 builds on results from Phase 1 of SEACI to enhance knowledge of climate–water processes in a changing climate, and to use this to improve models for predicting the impact of climate change on water.

There were three studies in 2009/10. The first study attributes the runoff decline in the Campaspe River basin (representative of the runoff declines in the southern Murray–Darling Basin and Victoria) to hydroclimatic features of the recent drought using a rainfall-runoff model and several scenarios of rainfall and potential evaporation. The results indicate that the mean annual reduction in rainfall accounts for 58 percent of the reduction in mean annual runoff. The remainder is not explained by any single hydroclimatic feature, but can be attributed mainly to the combination of changes in rainfall variability outside monthly and annual timescales (lack of high rainfall years or events), changed seasonality of rainfall, the interaction between rainfall variability and the mean annual rainfall decline, and increased potential evaporation.

In the second study, researchers carried out modelling experiments using four rainfall-runoff models and climate and streamflow data from 61 catchments in south-eastern Australia (SEA) to investigate the reliability of hydrological models for use in the assessment of the impact of climate change on runoff. For use in climate change impact studies the models, when calibrated using more than 20 years of data, can generally be used to assess the impact of climate change on runoff when the projected change in mean annual rainfall is less than 15 percent (relative to the historical calibration period). It is generally more difficult for a model calibrated over a wet period to predict runoff over a dry period than it is for a model calibrated over a dry period to predict runoff over a wet period. Therefore, for SEA, there is good reason to use the recent records to calibrate rainfall-runoff models to represent the recent drought over the region and for climate change impact studies where the large majority of climate models predict a drier future across the region.

The third study was a preliminary review of biophysical responses to a changing climate and their impacts on catchment water yield. The review and preliminary analysis of observed data confirm results from global studies of increased water availability in energy-limited catchments. However, the analysis suggests that water availability in water-limited catchments may reduce due to biophysical responses in a warmer, drier environment with higher levels of carbon dioxide (CO₂). This needs to be investigated further with a larger dataset to tease out a process-driven explanation.

Background

The main goal of the research in Theme 2 is to improve hydroclimate projections for SEA. The research in Theme 2 is at the climate–water interface, and its link to climate science and hydrological modelling science is shown schematically in Figure 32.

Hydrological models are generally tailored for specific applications, and are developed and calibrated using local data. There are two main steps involved in estimating climate impact on future runoff characteristics

and water availability. The first step uses GCM projections and downscaling models to obtain future catchment-scale climate series to drive hydrological models. Project 2.1 carries out research in this area. The second step involves driving hydrological models with future climate series to estimate future runoff. This may require adapting models to account for changes in the rainfall-temperature-runoff relationship and changes in the dominant hydrological processes in a drier, warmer environment with higher levels of carbon dioxide (CO₂). Project 2.2 carries out research in this area. Both projects in Theme 2 are closely related to – and use information from – the projects in Theme 1.

Researchers in Project 2.2 are building on results from Phase 1 of SEACI to enhance knowledge of climate–water processes and modelling. This research leads to more accurate and updated estimates of the impact of climate change on catchment water yield and streamflow, and also reduces associated uncertainties. This report summarises results from the three activities in the first year of this 3-year project.

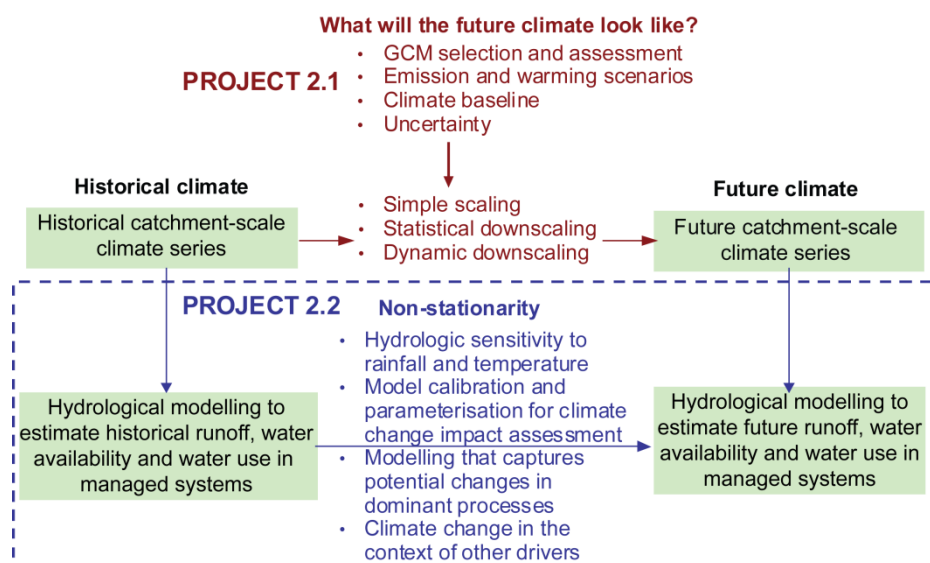


Figure 32. Modelling climate change impact on runoff

Objectives

Attribution of runoff decline

- Attribute the decline in runoff in SEA to hydroclimate features of the recent drought using a rainfall-runoff model.

Reliability of assessments of impact of climate change on runoff

- Investigate the reliability of the assessment of the impact of climate change on runoff using hydrological models calibrated against observed historical data.

Biophysical responses to a changing climate

- Carry out a preliminary review of biophysical responses to a changing climate and their impacts on catchment water yield.

Methods and results

Attribution of runoff decline

This study is described in detail in a paper recently submitted to *Water Resources Research* (Potter and Chiew, submitted).

SEA has experienced a severe and prolonged drought, characterised by unprecedented declines in rainfall and runoff. Rainfall and runoff in the past 12 years (1997–2008) averaged across the southern Murray–Darling Basin and Victoria are more than 10 percent and 35 percent lower, respectively, than the long-term means.

The recent drought has occurred at the end of a 50- to 60-year trend of increasing temperatures and declining rainfall. However, the magnitude of the effect of changing temperatures on runoff is difficult to quantify, since runoff is much more sensitive to changes in rainfall than other climate variables. The reduction in annual runoff is much greater compared to historical droughts with similar low mean annual rainfall. Several reasons have been suggested for this, including: greater proportional reduction in autumn and winter rainfall; lack of high rainfall years; increasing temperature; and changes in daily distribution of rainfall amounts and sequencing.

The long-term relationship between runoff and climate has traditionally been quantified using elasticity-based methods, which consider the proportional change in runoff divided by the proportional change in a relevant climate variable. However, the attribution of particular periods of low runoff cannot be assessed using elasticity-based methods as they are based on long-term average conditions. Cai and Cowan (2008b) used a partial regression analysis to calculate relationships between residual (i.e. unrelated to rainfall) temperature and inflows for the Murray–Darling Basin and showed that the increase in maximum temperature observed since 1950 contributes to 27 percent of the total reduction in inflows. However, Kiem and Verdon-Kidd (2010) have pointed out that the hydrological processes responsible for such a large reduction in runoff cannot be accounted for solely by increased temperatures.

This study attributes the runoff decline in the Campaspe River basin to hydroclimatic features of the recent drought using a rainfall-runoff model and several scenarios of rainfall and potential evaporation. The Campaspe River basin is representative of the southern Murray–Darling Basin and Victoria where the runoff decline is typical of the largest reductions over 1997–2008. Note that all the key studies for this region use modelled runoff data, and therefore the modelled runoff response should be able to be attributed to the input climate data.

In this study, we take the 1997–2008 time period as a baseline for modelling, and by modifying the climate input time series to look more like the long-term climatology, we estimate the effect of the hydroclimatic features of the recent drought on runoff. This is achieved by constructing the following scenarios:

- To estimate the effect of a decline in mean annual rainfall, we scale the 1997–2008 daily rainfall series by a constant factor so that the annual mean of the scaled rainfall series is equal to the long-term mean.
- To estimate the effect of changed rainfall seasonality, we scale the 1997–2008 daily rainfall series by a different factor for each month, so that the reduction in mean annual rainfall from the long-term mean is preserved, but mean monthly rainfall is proportional to the long-term monthly means.
- To estimate the direct effect of increased temperatures (through an increase in potential evaporation only), the 1997–2008 daily potential evaporation series is scaled down so that the annual mean of the scaled series is equal to the long-term mean.
- To estimate the effect of changed variability of rainfall at timescales other than monthly or annually, we take each 12-year block of historical data, and scale the rainfall data so that the mean monthly rainfall is equal to the 1997–2008 monthly means. Mean annual runoff over 1997–2008 is then averaged over all 12-year blocks to give an estimate of the effect of rainfall variability.

- We also combine these scenarios to assess the interactions between the effects.

Figure 33 shows the proportion of the observed runoff decline over 1997–2008 in the Campaspe River basin that is attributable to the scenarios described above and their interactions. The mean annual reduction in rainfall accounts for 58 percent of the reduction in mean annual runoff. The remainder is not explained by any single hydroclimatic feature, but can be attributed mainly to the combination of changes in rainfall variability outside monthly and annual timescales (lack of high rainfall years or events), changed seasonality of rainfall, the interaction between rainfall variability and the mean annual rainfall reduction, and increased potential evaporation.

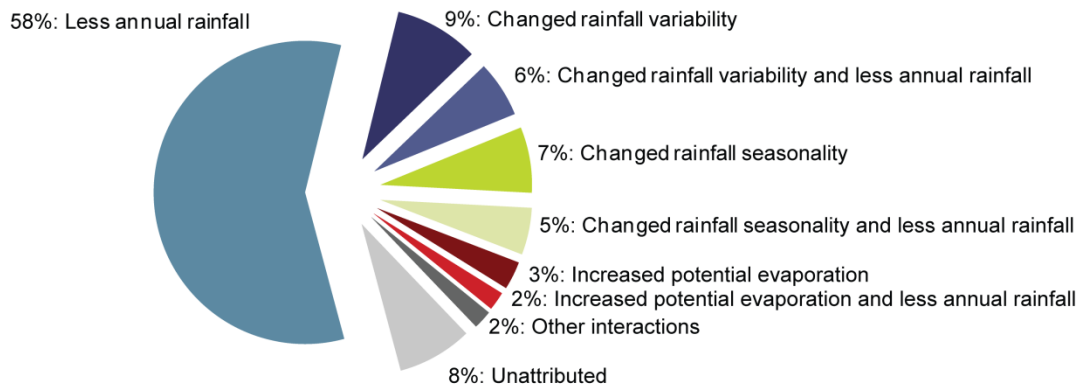


Figure 33. Attribution of reduction in mean annual runoff over 1997–2008 compared to the long term in the Campaspe River basin

Reliability of hydrological models for assessment of impact of climate change on runoff

This study is described in detail in a paper that has been accepted for publication in the *Journal of Hydrology* (Vaze et al., submitted).

This activity is partly supported in CSIRO Water for a Healthy Country Flagship and the eWater CRC through the National Water Commission's 'Catchment Water Yield Estimation Tool' project.

There is likely to be changes in the rainfall–temperature–runoff relationship and changes in dominant hydrological processes in a drier, warmer environment with higher levels of CO₂. If these changes (known as 'hydroclimate non-stationarity') are large, they need to be captured in hydrological models to predict the impact of climate change on runoff. Project 2.2 will be investigating this over the next two years. This year we investigated whether hydrological models calibrated with observed historical data can be used to reliably predict runoff response to changes in future climate inputs (note that this type of calibration is standard practice in most modelling studies).

The modelling experiments are carried out for four rainfall-runoff models using long historical daily climate and streamflow records from 61 catchments in SEA. Eight modelling periods were considered: the driest 10-, 20-, 30- and 40-year periods and the wettest 10-, 20-, 30- and 40-year periods. The models were calibrated against the daily streamflow data in each of the eight periods and the optimised parameter values were used to model runoff in the other seven periods. The simulation results using parameter values from calibration against another period were then compared to the calibration results.

The results are discussed in detail in Vaze et al. (submitted) and are summarised in Figure 34. The plots show the reduction in the daily modelled runoff (measured by the Nash-Sutcliffe efficiency) when parameter values from calibration against another period are used (compared to the calibration results). The values are plotted against the percentage difference in the mean annual rainfall in the two modelling periods. The broad results for the four rainfall-runoff models are generally similar. The models, when calibrated using more than 20 years of data, can generally be used for climate impact studies when the projected change in

mean annual rainfall is less than 15 percent (relative to the historical calibration period). It is generally more difficult for a model calibrated over a wet period to predict runoff over a dry period than it is for a model calibrated over a dry period to predict runoff over a wet period. Therefore, for SEA, there is good reason to use the recent records to calibrate rainfall-runoff models to represent the recent prolonged drought over the region and for climate change impact studies where the large majority of climate models predict a drier future across the region.

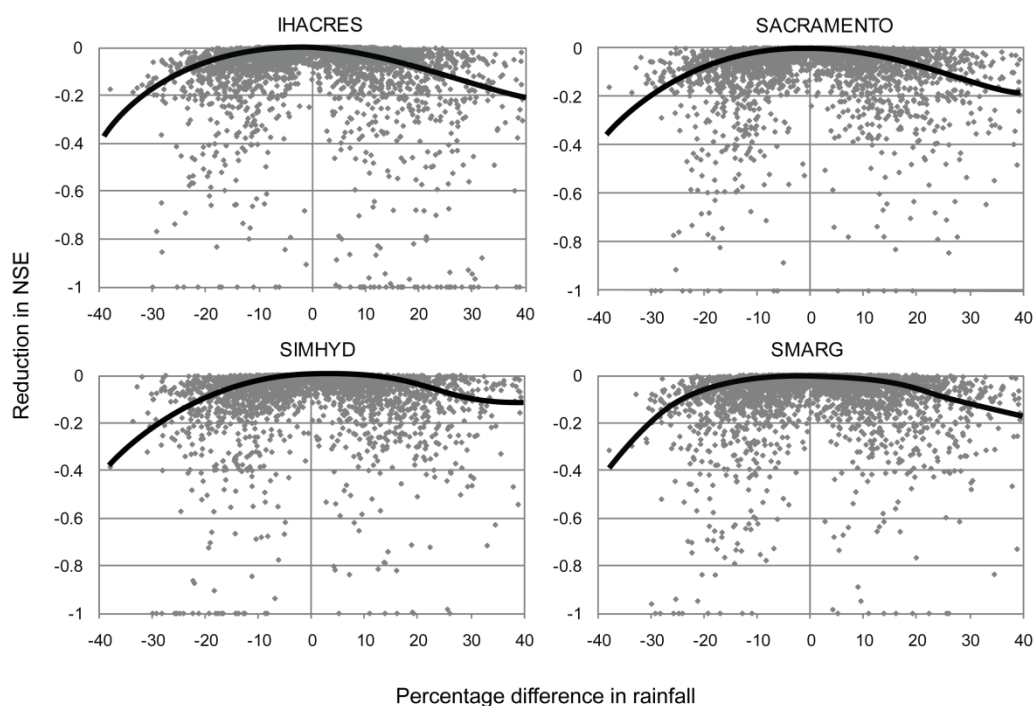


Figure 34. Reduction in daily modelled runoffs (measured by the Nash-Sutcliffe efficiency (NSE)) in the four rainfall-runoff models when parameter values from calibration against another period are used compared to the calibration results. Reduction in NSE is plotted against the percentage difference in the mean annual rainfall in the two modelling periods

Biophysical responses to a changing climate

Increased atmospheric CO₂ concentration is believed to have increased leaf-level water use efficiency. However, a key challenge is how to upscale this physiological response to a hydrological response at the catchment scale. This is difficult as catchments are located in a range of thermodynamic environments and all climate variables governing the catchment water balance are changing; the increase in atmospheric CO₂ concentrations is not occurring in isolation. In this part of Project 2.2, initial research to upscale the leaf-level physiological response to a catchment-scale hydrological response has been conducted using an ecohydrological framework, based on the Budyko framework, to understand catchment responses to changes in the climatological supply of water and the atmospheric demand for water. A key concept of the Budyko framework is to understand the limits of actual evaporation: in wet places actual evaporation is limited by available energy (and is referred to as 'energy-limited') and in dry places actual evaporation is limited by available water (and is referred to as 'water-limited').

Several previous studies have indicated that streamflow has increased globally which has been attributed to increased atmospheric CO₂ concentrations (Gedney et al., 2006, Huntington, 2008). However, since these studies were primarily conducted in energy-limited environments and since important Australian catchments are predominantly water-limited (Figure 35), it is unclear if these previous findings are relevant to all Australian catchments.

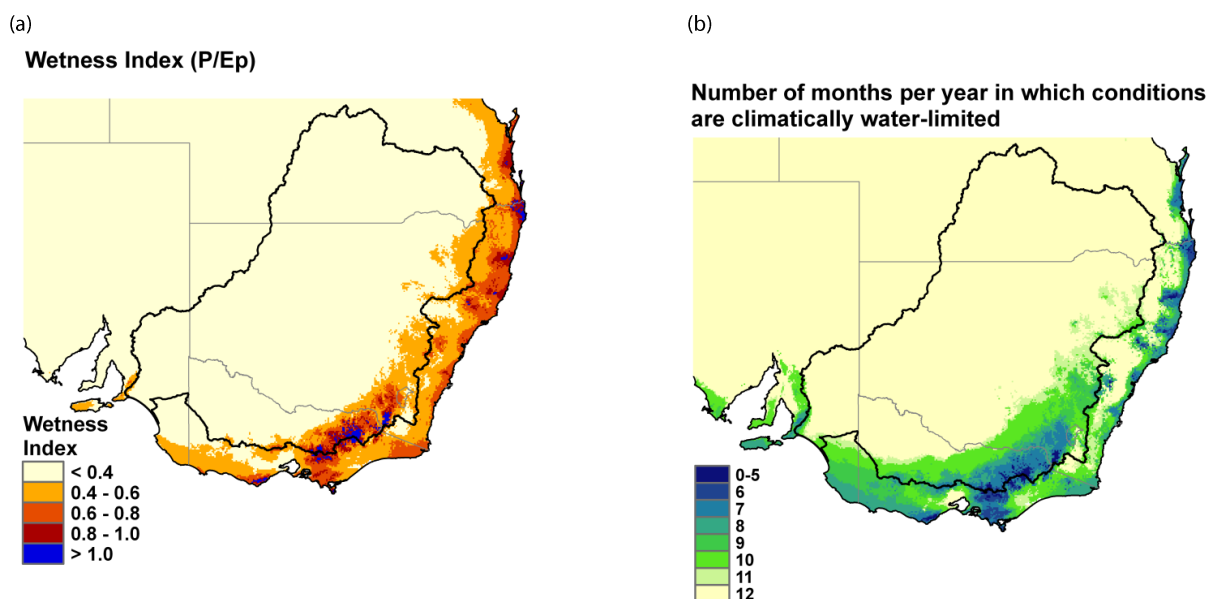


Figure 35. Climatic water limitation across south-eastern Australia. (a) The annual wetness index (precipitation (P) divided by Penman potential evaporation (Ep)), with energy-limited areas in blue. (b) The average number of months within the year for which the evaporative demand exceeds precipitation

For energy-limited Australian catchments responding to increased atmospheric CO_2 concentrations, it is expected (and early results show) that streamflow increases in line with global studies. In water-limited catchments, increased CO_2 concentration means that water availability effectively increases. However, based on the resource constraint framework, we expect (and early results show) that vegetation will adapt to the resources available to it. This means that vegetation will use most of the additional available water to increase its capture of carbon, resulting in a thickening of vegetation and minimal change in overall water use and catchment streamflow. Long-term (1981–2006) satellite remote sensing of vegetation cover reveals an 8 percent increase in total vegetation cover across the Australian continent. This increase is primarily comprised of increases of perennial vegetation (Donohue et al., 2009).

While this provides observational evidence of a vegetation-functioning non-stationarity, in this current research we extend this to assess a hydrological response. We analysed long-term (1981–2006), monthly, catchment-average precipitation, Penman potential evaporation (Ep), satellite-derived vegetation cover and streamflow data. These data were examined using Budyko's hydrological model to determine whether the observed changes in streamflow are in line with the expected changes in streamflow given the known changes in precipitation and Ep (Donohue et al., 2010). We restricted analyses to catchments without major shifts in climate conditions or vegetation cover throughout the study period and without major hydrological storages or diversions.

Initial results for 132 catchments suggest there is a pattern in the differences between observed and predicted streamflow trends and that these differences vary depending on the thermodynamic limitation (i.e. energy-limited or water-limited). On average, the increase in observed streamflow has been greater than that predicted for energy-limited catchments and, in stark contrast, streamflow in water-limited catchments has decreased more than predicted (Figure 36). This decrease of streamflow in water-limited catchments was an unexpected finding; it may be caused by changes in vegetation rooting depth and/or increases in rainfall interception (due to increasing amounts of vegetation cover). Current research aims to provide a

process-driven explanation. So far, these results confirm the possibility of the expected differential increased CO₂-streamflow response.

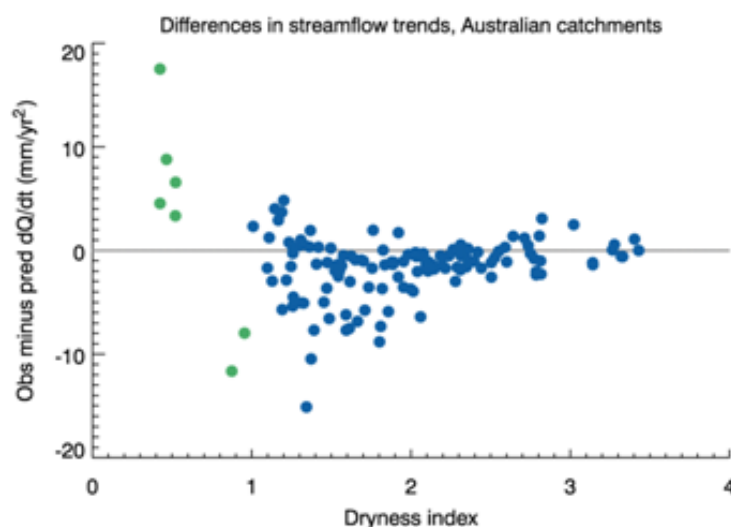


Figure 36. Differences between observed and predicted catchment streamflow trends (dQ/dt). Green indicates energy-limited catchments and blue indicates water-limited catchments (based on the annual average climatology from 1981–2006)

Future research aims to study more energy-limited catchments which have gauged streamflow data. Members of this project are currently involved in a scoping project with the Murray–Darling Basin Authority to provide insight into the vegetation-functioning non-stationarity associated with climate change and increased atmospheric CO₂ concentrations for longer term water resource planning (i.e. over 20 to 70 years). A potential longer term research project is being developed with the aim to couple the assessments of hydroclimatic non-stationarity and vegetation-functioning non-stationarity to provide water resource managers with a more complete assessment of risk to the water supply generated from the high water yielding catchments of SEA.

Conclusions

The research activities in Project 2.2 build on results from Phase 1 of SEACI to enhance knowledge of climate–water processes and modelling. This leads to more accurate and updated estimates of the impact of climate change on catchment water yield and streamflow, and reduces associated uncertainties.

There were three studies in 2009/10. The first study attributed the runoff decline in the Campaspe River basin (representative of the runoff declines in the southern Murray–Darling Basin and Victoria) to hydroclimatic features of the recent drought using a rainfall-runoff model and several scenarios of rainfall and potential evaporation. The mean annual reduction in rainfall accounts for 58 percent of the reduction in mean annual runoff. The remainder is not explained by any single hydroclimatic feature, but can be attributed mainly to the combination of changes in rainfall variability outside monthly and annual timescales (lack of high rainfall years or events), changed seasonality of rainfall, the interaction between rainfall variability and the mean annual rainfall reduction, and increased potential evaporation.

Researchers used four rainfall-runoff models and climate and streamflow data from 61 catchments in SEA to investigate the reliability of hydrological models calibrated with observed historical data. The models, when calibrated using more than 20 years of data, can generally be used to assess the impact of climate change on

runoff when the projected change in mean annual rainfall is less than 15 percent (relative to the historical calibration period). It is generally more difficult for a model calibrated over a wet period to predict runoff over a dry period than it is for a model calibrated over a dry period to predict runoff over a wet period. Therefore, for SEA, there is good reason to use the recent records to calibrate rainfall-runoff models to represent the recent prolonged drought over the region and for climate change impact studies where the large majority of climate models predict a drier future across the region.

The third study was a preliminary review of biophysical responses to a changing climate and their impacts on catchment water yield. The review and preliminary analysis of observed data confirm results from global studies of increased water availability in energy-limited catchments. However, the analysis suggests that water availability in water-limited catchments may reduce due to biophysical responses in a warmer, drier environment with higher levels of CO₂, and this needs to be investigated further with a larger dataset to tease out a process-driven explanation.

Links to other projects

Project 2.2 is strongly linked to Project 2.1 and, by extension, to Theme 1. The future climate series required to drive the hydrological models come from Project 2.1. The improvement in future climate projections will come from climate characterisation and attribution studies in Theme 1 and global climate model selection and assessment and testing of downscaling models in Theme 1 and Project 2.1 in the context of the hydrological modelling in Project 2.2.

CHAPTER 7: PROJECT 3.1

Advancing seasonal predictions for south-eastern Australia

Eun-Pa Lim, Harry Hendon, Oscar Alves, Yonghong Yin, Guomin Wang, Debbie Hudson and Maggie Zhao

Abstract

We have assessed the impact of improved ocean initial conditions and reduced sea-surface temperature (SST) mean bias on the skill of the Predictive Ocean Atmosphere Model for Australia (POAMA) in predicting tropical Indo-Pacific SST and south-eastern Australian climate. Two sets of 10-member ensemble hindcasts for 1980–2007 were produced from two different versions of POAMA2 that were initialised with the ocean initial conditions produced from the new ocean data assimilation system, POAMA Ensemble Ocean Data Assimilation System (PEODAS). One version of POAMA2 was flux-corrected to reduce mean state drift (model version p24b) and another version was not flux-corrected (p24a). Hindcasts were also produced from POAMA1.5b (p15b, the version that was used in Phase 1 of SEACI).

Analysis of these hindcasts suggests that predictive skill for El Niño is improved at lead times longer than 2 months using p24a compared to p15b. Flux correction (p24b) improves the predictive skill of SST in the central Pacific, which is a region to which Australian climate is particularly sensitive. However, neither versions of POAMA2 are as skilful as p15b for forecasts of the Indian Ocean Dipole (IOD).

In south-eastern Australia (SEA), rainfall and maximum temperature (Tmax) are better predicted by both versions of POAMA2 and by a multi-model ensemble consisting of p15b and POAMA2 than by p15b alone, at least for short lead times (zero to 2 months). At lead times longer than 3 months, skill in predicting rainfall and Tmax decreases rapidly in all versions of POAMA, despite skilful prediction of El Niño–related SST variability (the main driver of predictable Australian climate variability) for lead times of at least 9 months. For forecasts with such long lead times, available statistical post-processing techniques will be tested using POAMA2 hindcasts.

These results are summarised in Lim et al. (2009) and Lim et al. (submitted) which have been submitted as a Centre for Australian Weather and Climate Research (CAWCR) Technical Report.

Background

The aim of this project is to evaluate the predictive skill, quality and reliability of forecasts from the POAMA2 seasonal forecast system. The POAMA2 system uses a new state-of-the-art ensemble-based ocean data assimilation system (PEODAS) that provides improved ocean initial conditions (Yin et al., in press). This assessment will guide the use of new POAMA2 products for input to hydrological prediction models for SEA, whether by using climate predictions directly or by first downscaling the predictions of large-scale circulations to regional climate. Also, the evaluation of predictive skill will guide the final configuration of POAMA2, which will be adopted for operational seasonal forecasting for the next 2 to 4 years prior to the uptake of the Australian Community Climate and Earth-System Simulator (ACCESS)-based POAMA system.

Objectives

- Configure final version of POAMA2 and complete comprehensive hindcasts.
- Assess predictive skill from direct output of POAMA2 hindcasts for SEA, including assessment of predictions of large-scale meteorological fields that can be directly used or downscaled for hydrological application in Project 3.2.

Methods

Two final versions of POAMA2 were configured: the non-flux-corrected and the flux-corrected versions (p24a and p24b, respectively; Lim et al. (2009)). Two sets of 10-member ensembles were initialised on the first day of each month for 1980–2007 using the two different versions of POAMA2.

Forecasts from p15b (the current operational version) and from the two versions of POAMA2 were verified against the HadISST dataset and the National Climate Centre’s monthly gridded rainfall and Tmax analysis.

To assess the skill in predicting tropical Indo-Pacific SST, we examined three SST indices: (i) the NINO3 Index (NINO3), which depicts SST variations in the equatorial eastern Pacific associated with traditional El Niño development; (ii) the El Niño Modoki Index (EMI), which captures SST variations in the equatorial central Pacific associated with central-Pacific-warming El Niño development; and (iii) the Indian Ocean Dipole Mode Index (DMI) that captures the variation of the Indian Ocean Dipole (IOD) Mode (Figure 37; see Lim et al. (submitted) for the specification of the indices). The predictive skill was measured with correlation, normalised root-mean-square error, and normalised standard deviation (formulas are defined at the end of this chapter).

Probabilistic climate forecasts of rainfall and Tmax exceeding their medians were assessed by calculating the percentage correct (the percentage of forecasts which were correct, also referred to as hit rates; Lim et al. (in press)). Calibration of forecasts was attempted by combining the currently available version of POAMA (p15b) and the non-flux-corrected and flux-corrected versions of POAMA2 (p24a and p24b, respectively). The predictive skill of the combined forecasts was assessed by calculating the percentage correct.

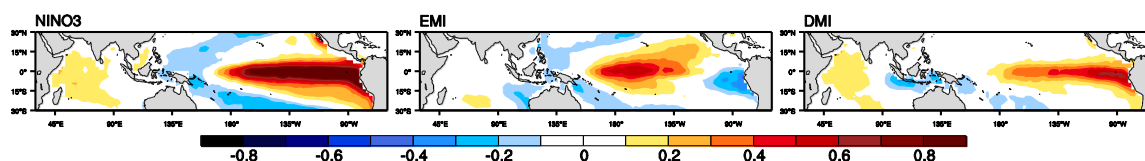


Figure 37. Regression of monthly sea-surface temperature anomaly on the NINO3 Index (NINO3), El Niño Modoki Index (EMI), and Indian Ocean Dipole Mode Index (DMI)

Results

Tropical Indo-Pacific SST variation explains significant proportions of climate variability in SEA. For instance, as shown in Figure 38, rainfall in SEA is highly correlated with NINO3 in spring, with EMI in autumn, and with DMI in winter and spring (correlation coefficients greater than 0.38 are statistically significant at the 5 percent level by the Student’s *t*-test with 27 degrees of freedom).

In comparison, Tmax in SEA is strongly associated with NINO3 and DMI in spring and with EMI in autumn to early winter (Figure 38). Therefore, it is important to ensure that POAMA has sufficient skill to predict the leading modes of variability of tropical SST associated with El Niño, Modoki El Niño and the IOD.

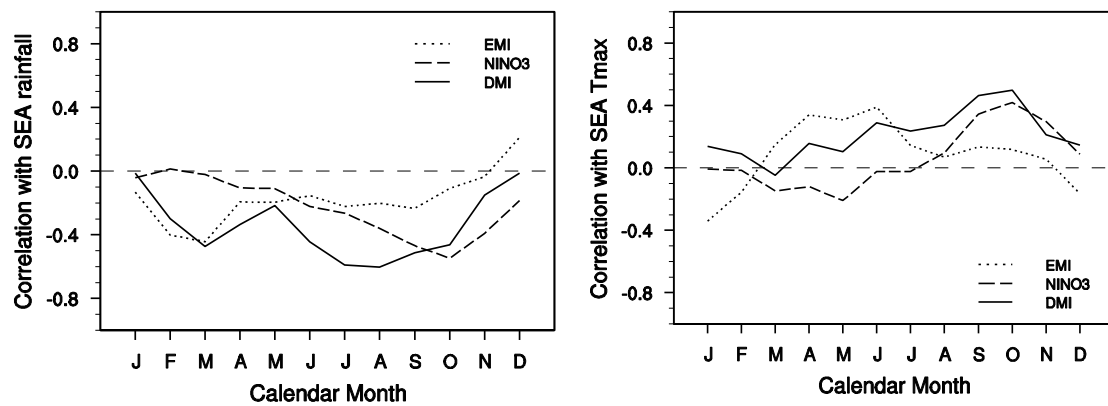


Figure 38. Correlation of seasonally averaged south-eastern Australian mean rainfall (left) and maximum temperature (Tmax) (right) with the NINO3 Index (NINO3), El Niño Modoki Index (EMI), and Indian Ocean Dipole Mode Index (DMI) as a function of calendar month

As seen in Figure 39, Figure 40 and Figure 41, p24a demonstrates improvement in forecasting NINO3 at lead times longer than 2 months compared to p15b. This is a major accomplishment, considering the dominance of El Niño for climate variability in SEA. p24b shows greater skill in predicting the EMI at lead times of 1 to 5 months, which reflects the benefit of maintaining a correct mean state for which El Niño and its flavours can then evolve. However, both versions of POAMA2 tend to significantly underestimate the amplitudes of NINO3 and EMI. Also, the DMI is less skilfully predicted with POAMA2 than with p15b, which requires further investigation.

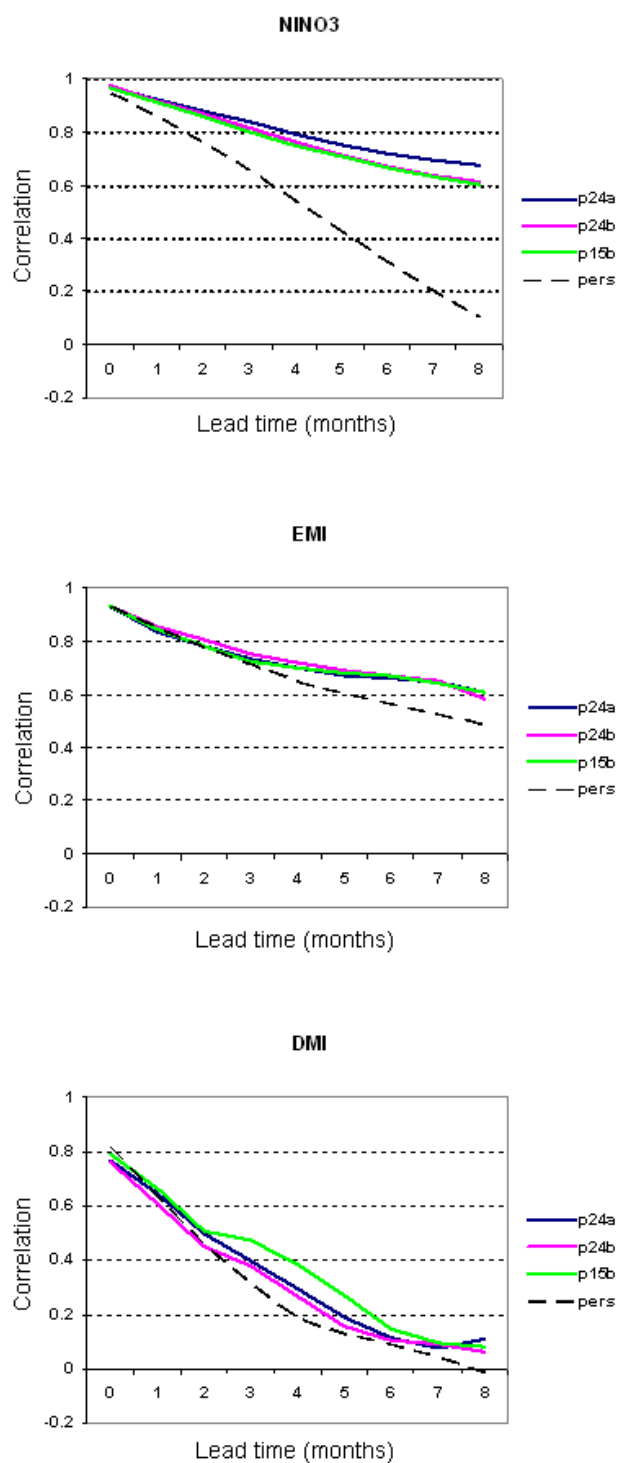


Figure 39. Correlation of predicted NINO3 Index (NINO3), El Niño Modoki Index (EMI), and Indian Ocean Dipole Mode Index (DMI) from POAMA1.5b (p15b), non-flux-corrected POAMA2 (p24a), and flux-corrected POAMA2 (p24b) verified against respective observed indices using the HadISST dataset

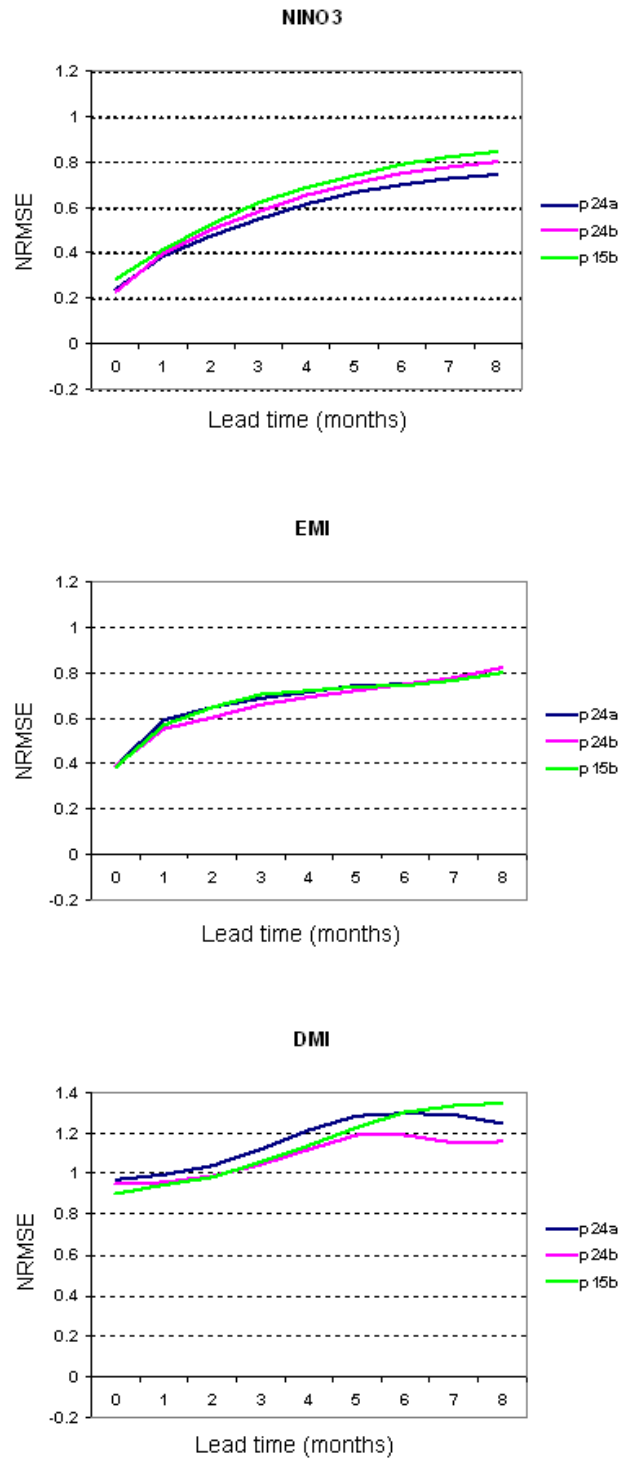


Figure 40. Normalised root-mean-square error (NRMSE) of predicted NINO3 Index (NINO3), El Niño Modoki Index (EMI), and Indian Ocean Dipole Mode Index (DMI) from POAMA1.5b (p15b), non-flux-corrected POAMA2 (p24a), and flux-corrected POAMA2 (p24b) verified against respective observed indices using the HadISST dataset

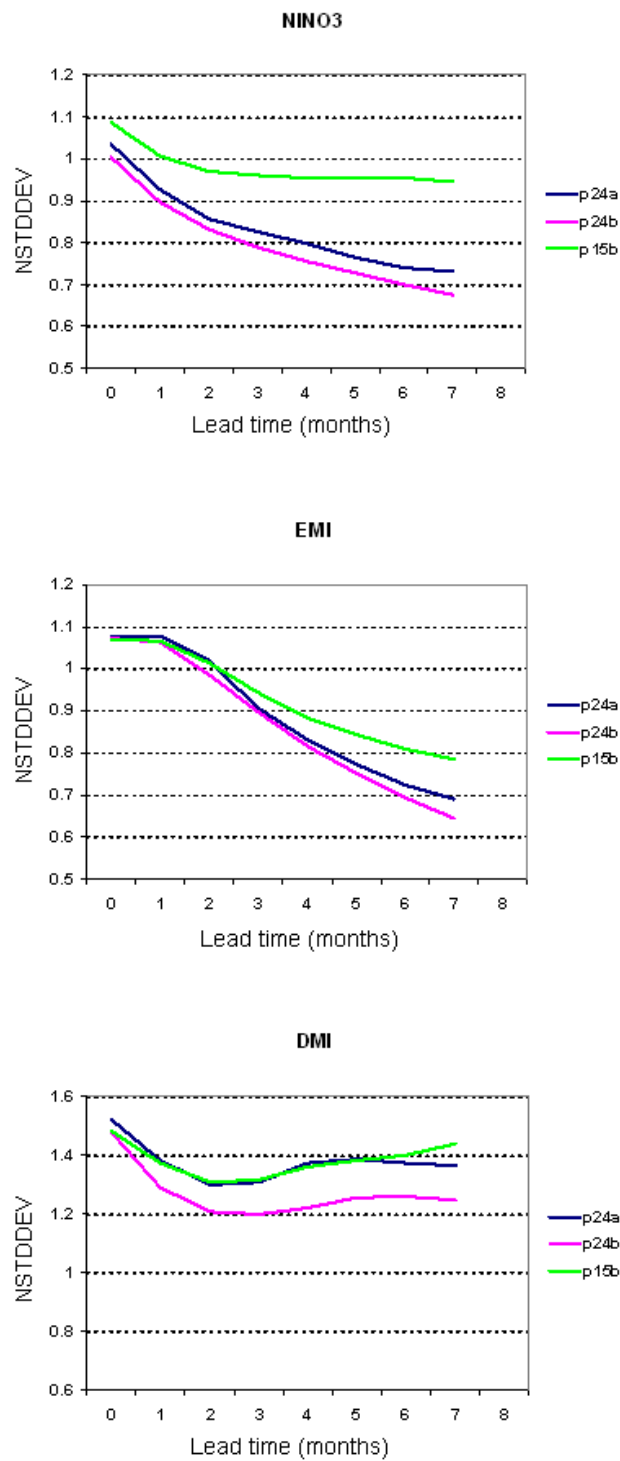


Figure 41. Normalised standard deviation (NSTDDEV) of predicted NINO3 Index (NINO3), El Niño Modoki Index (EMI), and Indian Ocean Dipole Mode Index (DMI) from POAMA1.5b (p15b), non-flux-corrected POAMA2 (p24a), and flux-corrected POAMA2 (p24b) verified against respective observed indices using the HadISST dataset

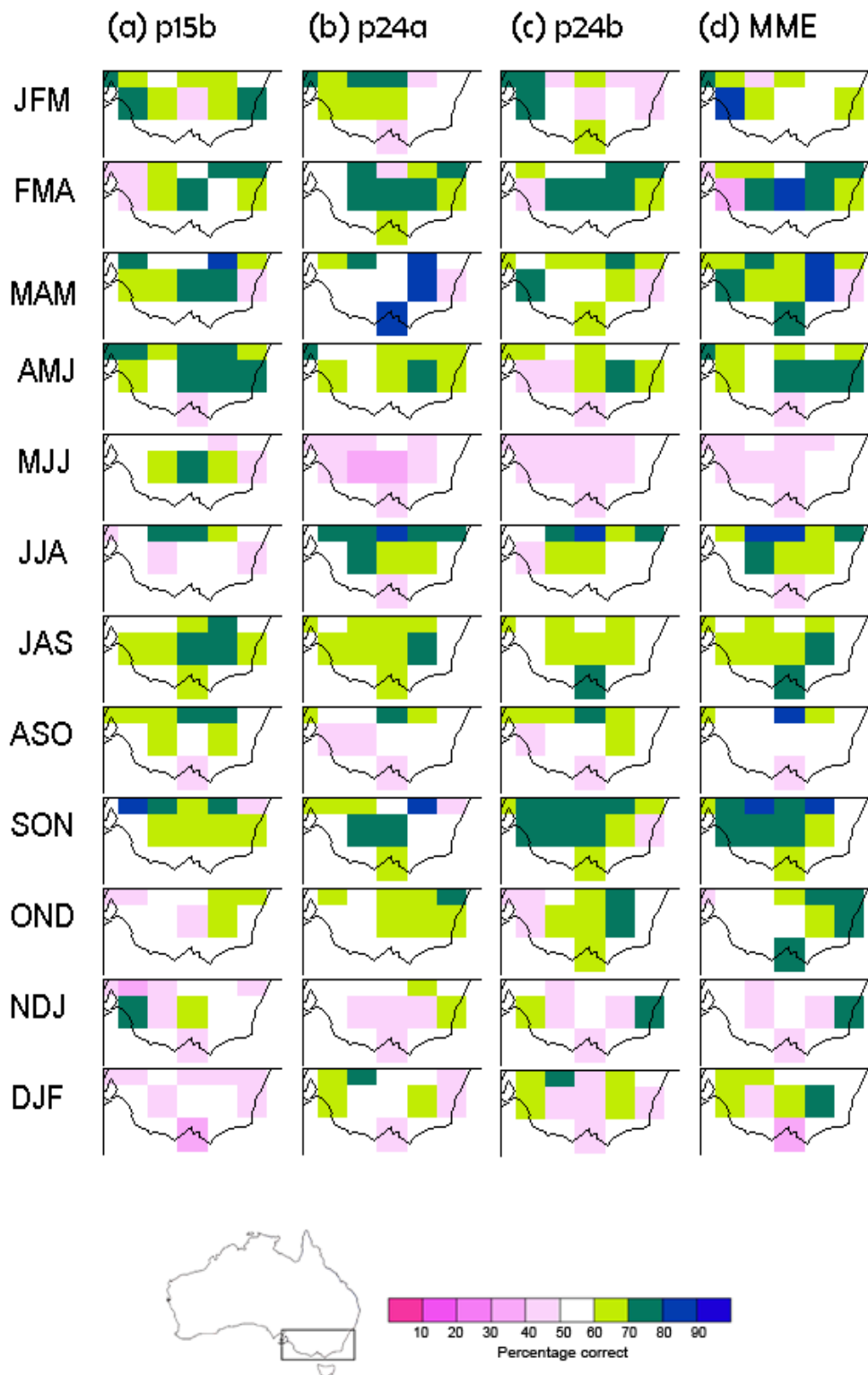
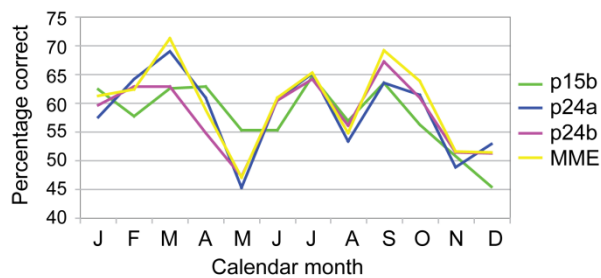


Figure 42. Percentage of forecasts which correctly predict rainfall being above the median at a lead time of zero months using (a) POAMA1.5b (p15b); (b) non-flux-corrected POAMA2 (p24a); (c) flux-corrected POAMA2 (p24b); and (d) the multi-model ensemble (MME). Each row shows results for 3-month moving windows

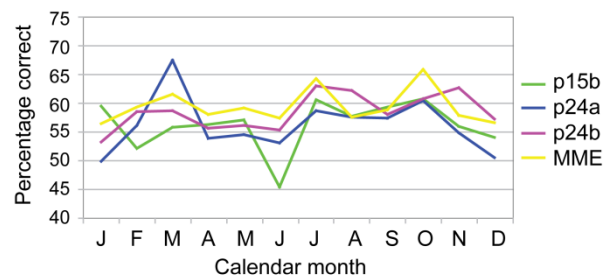
POAMA's predictive skill for climate in SEA is assessed by calculating the percentage of probabilistic forecasts which correctly predict above-median rainfall and Tmax. Figure 42 displays this value for three versions of POAMA with a lead time of zero months. In general, POAMA2 rainfall forecasts show a higher percentage correct than p15b in late summer (Feb-Mar-Apr), winter (Jun-Jul-Aug), and spring to early summer (Sep-Oct-Nov to Dec-Jan-Feb). Since all three versions demonstrate a moderate to good percentage correct (greater than 60 percent) in most of the seasons, and each of the versions shows some independent

skill, we combined all three versions to form a multi-model ensemble. Figure 42(d) suggests that, at this shortest lead time, this ensemble offers more skilful forecasts than the individual versions of POAMA in most of the seasons except for late autumn (Apr-May-Jun) and late winter (Aug-Sep-Oct). Maximum hit rate reaches above 80 percent over some locations in SEA. The improvement in skill for predictions of rainfall made by POAMA2 or the multi-model ensemble over p15b alone seems achievable with up to a 2-month lead time as shown in Figure 43, which shows the average percentage correct of above-median forecasts over SEA. However, with a 3-month lead time, all three versions of POAMA provide forecasts whose overall skill is only comparable to that of a climatological forecast (Figure 44(a), (b) and (c)). As the individual component versions do not have good skill in predicting rainfall at this lead time of 3 months, the effect of combining three component models is not obvious (Figure 43(d) and Figure 44(d)).

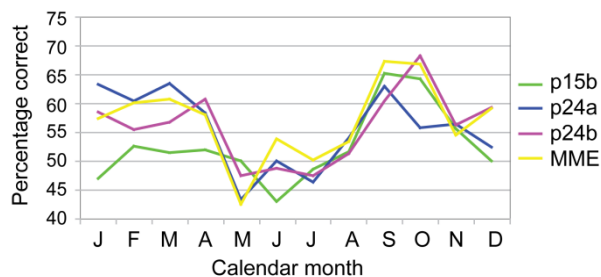
(a) zero lead time



(b) 1-month lead time



(c) 2-month lead time



(d) 3-month lead time

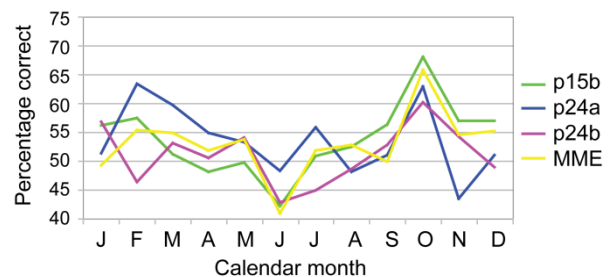


Figure 43. Mean percentage of forecasts (averaged over south-eastern Australia) which correctly predict rainfall being above the median using POAMA1.5b (p15b); non-flux-corrected POAMA2 (p24a); flux-corrected POAMA2 (p24b); and the multi-model ensemble (MME) at lead times of zero to 3 months

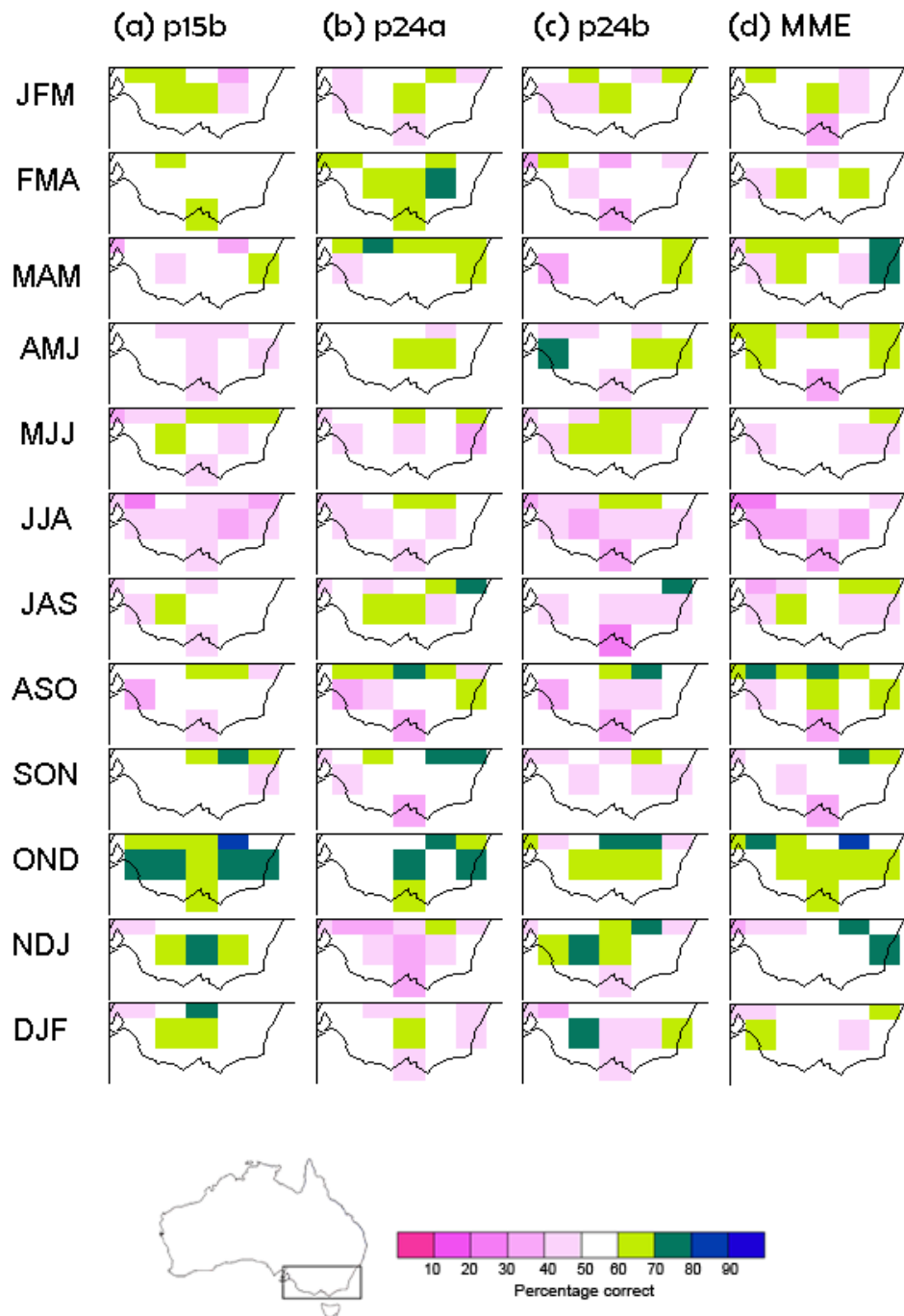


Figure 44. Percentage of forecasts which correctly predict rainfall being above the median at a lead time of 3 months using (a) POAMA1.5b (p15b); (b) non-flux-corrected POAMA2 (p24a); (c) flux-corrected POAMA2 (p24b); and (d) the multi-model ensemble (MME). Each row shows results for 3-month moving windows

With regard to Tmax forecasts over SEA, the non-flux-corrected p24a demonstrates higher skill than p15b throughout the year except for late summer to autumn (Feb-Mar-Apr to Mar-Apr-May) at the shortest lead time, and the flux-corrected forecasts seem as skilful as the non-flux-corrected ones (Figure 45).

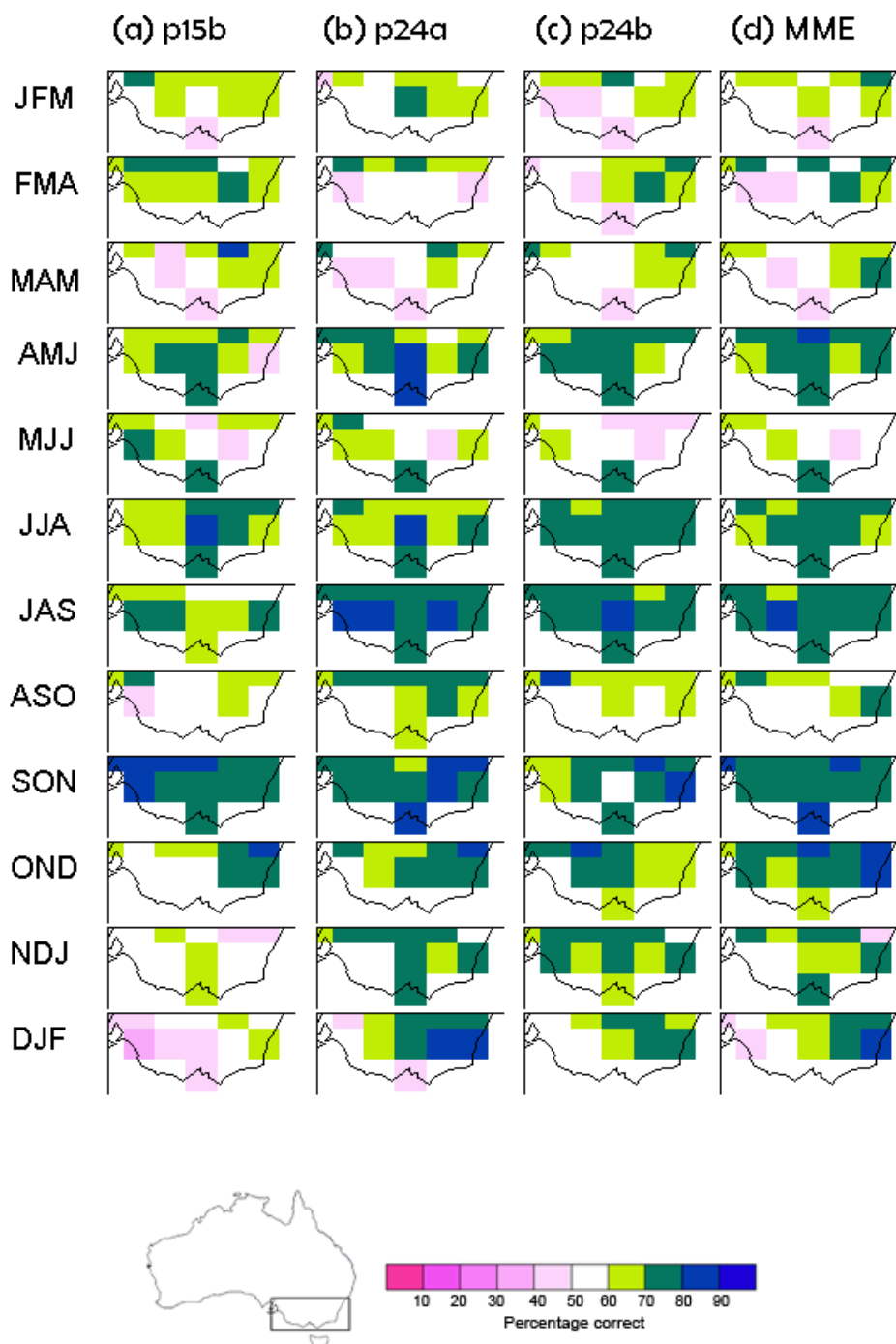


Figure 45. Percentage of forecasts which correctly predict maximum temperature (T_{max}) being above the median at a lead time of zero months using (a) POAMA1.5b (p15b); (b) non-flux-corrected POAMA2 (p24a); (c) flux-corrected POAMA2 (p24b); and (d) the multi-model ensemble (MME). Each row shows results for 3-month moving windows

In particular, substantial improvements are found in late spring to summer in POAMA2 compared to p15b. The multi-model ensemble forecasts of T_{max} are as skilful as those of POAMA2 but seem not to outperform the non-flux-corrected p24a which is the best single model for T_{max} prediction over SEA at this short lead time. By a 3-month lead time, T_{max} predictive skill from all three versions of POAMA reduces significantly but is still better than a climatological forecast in most seasons, especially in spring to early summer (Figure 46). The non-flux-corrected p24a still provides the best forecasts out of the three versions, and the multi-model ensemble demonstrates additional skill in spring to summer at lead times of 1 to 3 months (not shown).

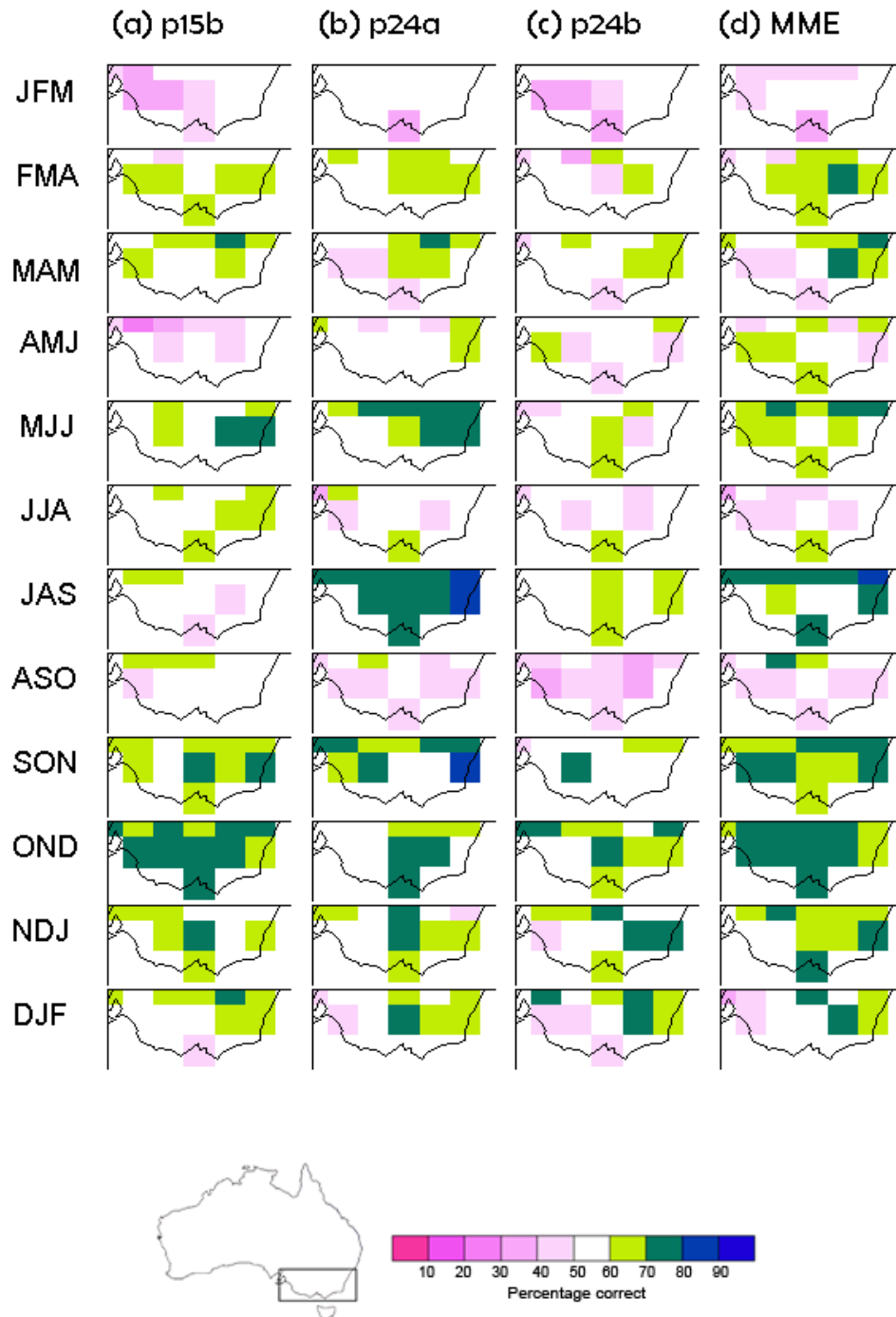


Figure 46. Percentage of forecasts which correctly predict maximum temperature (T_{max}) being above the median at a lead time of 3 months using (a) POAMA1.5b (p15b); (b) non-flux-corrected POAMA2 (p24a); (c) flux-corrected POAMA2 (p24b); and (d) the multi-model ensemble (MME). Each row shows results for 3-month moving windows

Conclusions

As part of a continuous effort to improve the predictive skill for leading modes of tropical Indo-Pacific SST variability and Australian climate, a major upgrade has been made to POAMA by improving the ocean initial conditions. The new ocean initial conditions are produced by PEODAS, which assimilates temperature and salinity and produces an ensemble of ocean states at any point in time. This ensemble of ocean states is then directly used as perturbed initial conditions for forecasts with POAMA2. Additionally, we attempted to remove POAMA's mean state drift by applying an explicit flux-correction scheme to POAMA2. Therefore, the aim of this study is to assess the impact of these improved ocean initial conditions and the removal of mean SST bias on the skill of POAMA in predicting tropical Indo-Pacific SSTs and Australian climate, with a focus on SEA.

Our findings suggest that non-flux-corrected POAMA 2 (p24a) has improved skill in predicting traditional eastern-Pacific-warming El Niño whereas the flux-corrected POAMA2 (p24b) has improved skill in predicting central-Pacific-warming El Niño. However, predicting DMI is less skilful with POAMA2 than the current operational version of POAMA (p15b).

For probabilistic predictions of rainfall in SEA being above the median, predictive skill of the two versions of POAMA2 and of p15b are comparable at zero- to 3-month lead time. As the three versions of POAMA appear to have independent skill in forecasting rainfall, we combined them to form a multi-model ensemble. The resultant multi-model ensemble forecasts demonstrate higher skill than any individual versions of POAMA for rainfall in SEA at short lead times of zero to 1 month, but at lead times longer than 3 months, both the multi-model ensemble and the individual POAMA models produce forecasts that are similar to or marginally better than a climatological forecast. Hence, at shorter lead times, the multi-model ensemble is a viable alternative to the individual versions of POAMA for providing improved forecast accuracy and reliability.

For Tmax, the predictive skill of POAMA2, especially the non-flux-corrected p24a, is better than that of p15b at short lead times of zero to 3 months. The multi-model ensemble prediction is as skilful as the non-flux-corrected p24a prediction at a lead time of zero months and slightly more skilful than the best single version of POAMA at lead times of zero to 3 months.

Links to other projects

This project is linked to Project 3.2, which plans to use downscaled POAMA outputs to drive a hydrological model for streamflow predictions.

Formulas

Sea-surface temperature (SST) indices

The NINO3 Index (NINO3):

$$\text{NINO3} = \overline{SST}_{(90^{\circ}\text{W}-150^{\circ}\text{W}, 5^{\circ}\text{S}-5^{\circ}\text{N})}$$

The El Niño Modoki Index (EMI):

$$\text{EMI} = \overline{SST}_{(165^{\circ}\text{E}-140^{\circ}\text{W}, 10^{\circ}\text{S}-10^{\circ}\text{N})} - 0.5 * \overline{SST}_{(70^{\circ}\text{W}-110^{\circ}\text{W}, 15^{\circ}\text{S}-5^{\circ}\text{N})} - 0.5 * \overline{SST}_{(125^{\circ}\text{E}-145^{\circ}\text{E}, 10^{\circ}\text{S}-20^{\circ}\text{N})}$$

The Indian Ocean Dipole Mode Index (DMI):

$$\text{DMI} = \overline{SST}_{(50^{\circ}\text{E}-70^{\circ}\text{E}, 10^{\circ}\text{S}-10^{\circ}\text{N})} - \overline{SST}_{(90^{\circ}\text{E}-110^{\circ}\text{E}, 10^{\circ}\text{S}-0^{\circ})}$$

Skill measures

F' forecast anomaly (model climatology is removed)

O' observed anomaly

$\sigma_{F'}$ standard deviation of forecasts

$\sigma_{O'}$ standard deviation of observation

I number of samples

Correlation (r):

$$r = \frac{\sum_{i=1}^I F'_i * O'_i}{\sigma_{F'} * \sigma_{O'} * (I - 1)}$$

Normalised root-mean-square error (NRMSE):

$$\text{NRMSE} = \frac{\sqrt{\frac{\sum_{i=1}^I (F'_i - O'_i)^2}{I}}}{\sigma_{O'}}$$

Normalised standard deviation (NSTDDEV):

$$\text{NSTDDEV} = \frac{\sigma_{F'}}{\sigma_{O'}}$$

CHAPTER 8: PROJECT 3.2

Hydrological application of seasonal predictions

QJ Wang and David Robertson

Abstract

This project made excellent progress in the first year of Phase 2 of SEACI. The Bayesian joint probability (BJP) modelling approach for forecasting seasonal streamflows at multiple sites was further developed, including extending the modelling approach to handle zero flows, improving the suite of methods for verification of probabilistic forecasts, and formulating and implementing a predictor selection method. The further-developed BJP modelling approach was successfully tested on a number of catchments and was shown to provide forecasts that are reliable (with quantifiable uncertainty) and robust (over time and event size).

The BJP modelling approach was applied and evaluated on a collection of catchments, mostly in south-eastern Australia (SEA). Predictive skill varies with catchment and season. Forecasts are more skilful for catchments that have deep soil profiles and large groundwater storage and therefore long memory. Forecasts tend to be the most skilful for seasons that contain the receding limb of the annual hydrograph (ie when streamflow is declining). Most of the predictive skill is derived from predictors representing initial catchment conditions. In contrast, predictors of future climate make only a small contribution to the predictive skill and only for late-winter and spring seasons, demonstrating the challenge in skilfully forecasting seasonal rainfall.

A highlight of the project is the adoption of the BJP modelling approach by the Australian Bureau of Meteorology (BoM). An experimental seasonal streamflow forecasting service, including a website, was developed in a collaboration between BoM, CSIRO and water managers. BoM officially commenced issuing experimental seasonal streamflow forecasts to registered users during December 2009 with the release of a public operational forecast service scheduled for December 2010 or January 2011.

Background

Forecasts of future seasonal streamflows are potentially valuable to a range of water managers and users, including irrigators, urban and rural water-supply authorities, environmental managers and hydroelectricity generators. Such forecasts can inform planning and management decisions to maximise returns on investments and available water resources and to ensure security of supply (Plummer et al., 2009).

Research in Phase 1 of SEACI has led to the development of a statistical method, the Bayesian joint probability (BJP) modelling approach, for forecasting seasonal streamflows at multiple sites (Wang et al., 2009). The BJP approach uses a Yeo-Johnson transformed multivariate normal distribution to model the joint distribution of future streamflows and their predictors such as antecedent streamflows, El Niño – Southern Oscillation indices, and other climate indices. The model parameters and their uncertainties are inferred from historical data using a Bayesian method. The parameters are then used to produce joint probabilistic forecasts of streamflows at multiple sites for future events.

The BJP modelling approach needed to be further developed to make it a practical tool for streamflow forecasting in SEA. In the first year of Phase 2 of SEACI, the development work focused on:

- extending the BJP modelling approach to handle zero flows, which occur in dry seasons occasionally on perennial streams, frequently on intermittent streams and regularly on ephemeral streams
- completing a suite of methods and tools for verification of probabilistic forecasts
- formulating a method for selecting predictors that represent initial catchment condition and future climate influences on seasonal streamflows.

In addition, a major effort was devoted to the application and evaluation of the BJP modelling approach and on technology transfer to the BoM in establishing a national service of seasonal streamflow forecasting.

Objectives

The overall project objectives are to:

- further develop and evaluate the BJP modelling approach for seasonal streamflow forecasting
- incorporate dynamic climate and hydrological modelling into the BJP modelling approach
- transfer the technology for practical applications.

Specific objectives of the project in 2009/10 were to:

- further develop the BJP modelling approach (for handling zero flows, verifying probabilistic forecasts, and selecting predictors)
- apply, evaluate and transfer the technology of the BJP modelling approach for applications in SEA.

Methods

In the BJP modelling setting, zero streamflows may occur in any combination of predictors and predictands. Mathematically this leads to a mixed discrete-continuous multivariate probability distribution, which is extremely difficult to formulate and manipulate. We turn this difficult mathematical problem into one of modelling a continuous multivariate probability distribution. In model parameter inference, the zero observed streamflows are treated as censored data, having unknown precise values but equal to or below zero. In forecasting, censored predictor values are augmented to 'known' values, and negative values of streamflow forecasts are converted to zero. Detailed mathematical formulation and numerical implementation can be found in Wang and Robertson (submitted).

The quality of forecasts is assessed using a leave-one-out cross-validation procedure. The cross-validation procedure is implemented by sampling the posterior distribution of the parameters using a likelihood function based on all available data except one event. The streamflows for the left-out event are then forecast and compared with the observed data. A number of statistical and graphical methods are developed to assess the skill, reliability and robustness of the forecasts. Details of the methods can be found in Wang and Robertson (submitted).

Statistical methods commonly used for forecasting climate and streamflows require the selection of appropriate predictors. Poorly designed predictor selection procedures can result in poor forecasts for

independent events. A rigorous predictor selection method has been developed for the BJP modelling approach. The method compares forecasting models in terms of the pseudo Bayes factor (PsBF) calculated from cross-validation predictive densities. A stepwise expansion of a base model is carried out by including the candidate predictor with the highest PsBF that exceeds a selection threshold. Predictors representing the initial catchment conditions are selected on their ability to forecast streamflows, and predictors representing future climate influences are selected on their ability to forecast rainfall. The final forecasting model combines selected predictors representing both initial catchment conditions and future climate influences to jointly forecast seasonal streamflows at multiple sites. Details of the method can be found in Robertson and Wang (in prep.).

The further-developed BJP modelling approach has been applied and evaluated on a number of catchments, most of which are in SEA. The research team worked closely with the BoM in adopting the BJP modelling approach for the establishment of a national service on seasonal streamflow forecasting.

Results

A method was developed for handling zero flows and was implemented in the BJP modelling approach. A suite of verification methods for probabilistic forecasts was also further developed. The extended BJP modelling approach and verification methods were tested on the Burdekin River catchment and shown to be successful. June to August streamflows and catchment average rainfall were jointly forecast from the NINO4 Index for the previous month and total streamflows for the previous two months. Cross-validation results show that the BJP probabilistic forecasts of streamflows have some predictive skill and are free from obvious bias and other errors, and have an appropriate spread in uncertainty. The skill of rainfall forecasts is lower than streamflow forecasts, demonstrating the importance of using initial catchment condition for streamflow forecasts. Details of the results can be found in Wang and Robertson (submitted).

A rigorous predictor selection method was developed for the BJP modelling approach to seasonal streamflow forecasting at multiple sites. Applications of the predictor selection method to two catchments in eastern Australia show that the best predictors representing initial catchment conditions and future climate influences vary with location and forecast date. Antecedent streamflows are the best indicator of the initial catchment conditions. Predictors representing future climate influences are only selected for forecasts made between July and January. Indicators of El Niño dominate the selected predictors representing future climate influences. The skill of subsequent streamflow forecasts varies considerably between locations and throughout the year, with the highest skill scores obtained for forecast seasons that contain the receding limb of the annual hydrograph. Skill scores for the perennial streams of the Goulburn River catchment exceed 40 percent for several seasons, while for the intermittent streams in the Burdekin River catchment the skill scores are much lower. Artificial skill due to predictor selection is generally very low, but occasionally can exceed 10 percent. Details of the results can be found in Robertson and Wang (in prep.).

The BJP modelling approach has also been applied and evaluated on the following sites (including a few outside SEA):

- Total inflows to Lake Dartmouth, unregulated inflows to Lake Hume, total flow of Ovens River to Murray River, and total flow of Kiewa River to Murray River
- Streamflows at four gauging stations in the Goulburn River catchment: Acheron River at Taggerty (405209), Goulburn River at Dohertys (405219), Delatite River at Tonga Bridge (405214), and Acheron River at Taggerty (405205)
- Streamflows at two gauging stations in the Upper Murray River catchment: Mitta Mitta River at Hinnomunjie (401203) and Murray River at Biggara (401012)

- Streamflows at four gauging stations in the Murrumbidgee River catchment: Goodradigbee River at Wee Jasper (410024), Adjungbilly Creek at Darbalara (410038), Goobarragandra River at Lacmalac (410057), and Adelong Creek at Batlow Rd (410061)
- Major inflows to Melbourne Water storages: Thomson Reservoir, Upper Yarra Reservoir, O'Shannassy Reservoir and Maroondah Reservoir
- Representative inflows to the Hydro Tasmania storages: Mersey-Forth Power Development inflows and King River Power Development inflows
- Streamflows at three sites in the Burdekin River catchment: Burdekin River at Sellheim (120002), Suttor River at St Anns (120303), and Cape River at Taemas (120302)
- Streamflows at one site in the Nogoa River Catchment: Nogoa River at Craigmore (130209)
- Major inflows to Goulburn-Murray Water storages: Lake Eildon, Waranga Basin, Lake Eppalock, Tullaroop Reservoir, Cairn Curran Reservoir and Lake Nillacootie. This work is currently in progress.

Evaluation of results from cross-validation hindcasts shows that predictive skill varies with catchment and season. Forecasts are more skilful for catchments that have deep soil profiles and large groundwater storage and therefore long memory. Forecasts tend to be the most skilful for seasons that contain the receding limb of the annual hydrograph. Most of the predictive skill is derived from the predictors representing initial catchment conditions. In contrast, predictors of future climate make only a small contribution to the predictive skill and only for late-winter and spring seasons, demonstrating the challenge in skilfully forecasting seasonal rainfall.

One of the highlights of this project (and the complementary seasonal streamflow forecasting project under the Water Information Research and Development Alliance (WIRADA) between CSIRO and the BoM) is the adoption of the BJP modelling system by the BoM. An experimental seasonal streamflow forecasting service, including a website, was developed in a collaboration between the BoM, CSIRO and water managers. The BoM's Extended Hydrological Prediction team officially commenced issuing experimental seasonal streamflow forecasts to registered users during December 2009 with the release of a public operational forecast service scheduled for December 2010 or January 2011. These forecasts have been produced using the BJP modelling system. The website provides a suite of forecast products. Figure 47 shows one of the products.

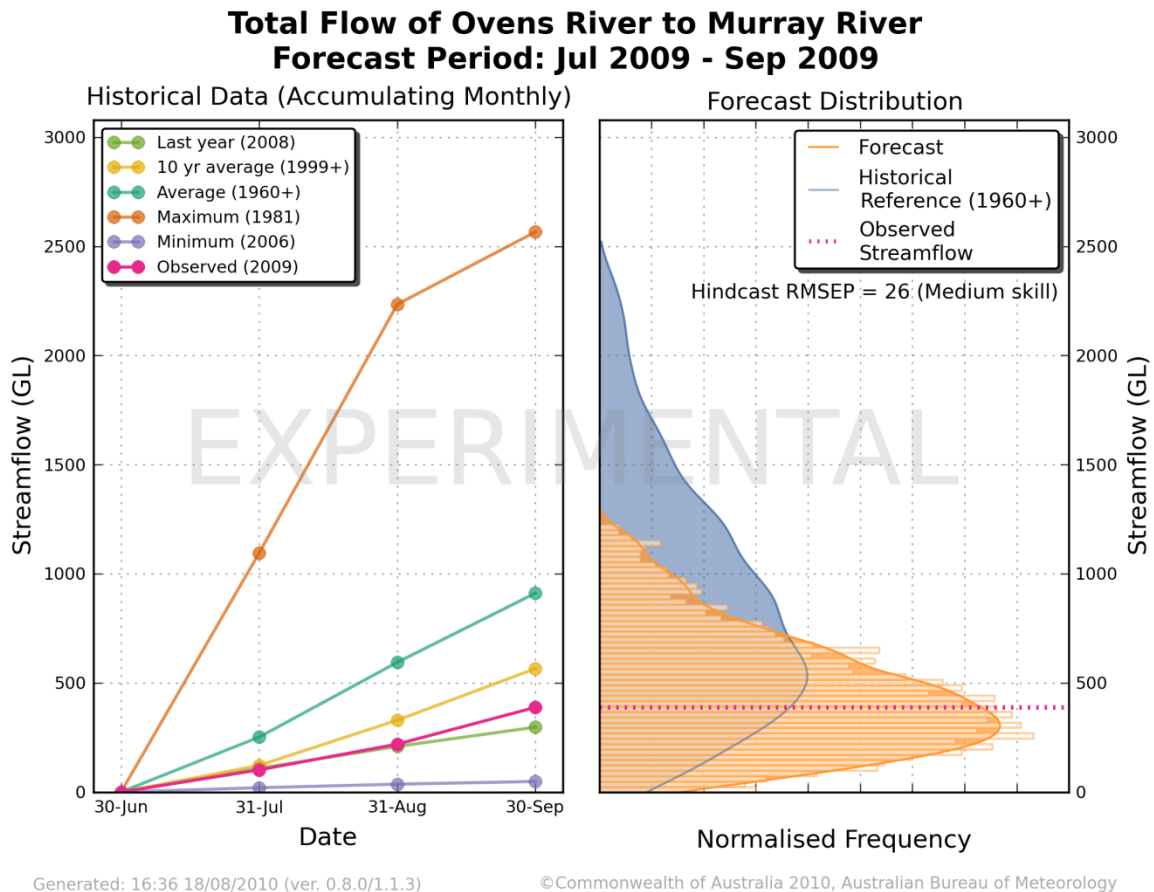


Figure 47. Seasonal streamflow forecast issued by the Bureau of Meteorology for total flows of the Ovens River to the Murray River for July to September 2009. The probabilistic forecast was produced by using the Bayesian joint probability modelling approach

Conclusions

In the first year of Phase 2 of SEACI, the BJP modelling approach for forecasting seasonal streamflows at multiple sites was further developed, including extending the modelling approach to handle zero flows, improving the suite of methods for verification of probabilistic forecasts, and formulating and implementing a predictor selection method. The further-developed BJP modelling approach was successfully tested on a number of catchments and shown to provide forecasts that are reliable (with quantifiable uncertainty) and robust (over time and event size).

The BJP modelling approach was applied and evaluated on a collection of catchments, mostly in SEA. Predictive skill varies with catchment and season. Forecasts are more skilful for catchments that have deep soil profiles and large groundwater storage and therefore long memory. Forecasts tend to be the most skilful for seasons that contain the receding limb of the annual hydrograph. Most of the predictive skill is derived from predictors representing initial catchment conditions. In contrast, predictors of future climate make only a small contribution to the predictive skill and only for late-winter and spring seasons, demonstrating the challenge in skilfully forecasting seasonal rainfall.

A highlight of the project is the adoption of the BJP modelling approach by the BoM. An experimental seasonal streamflow forecasting service, including a website, was developed in a collaboration between the BoM, CSIRO and water managers. The BoM officially commenced issuing experimental seasonal streamflow forecasts to registered users during December 2009 with the release of a public operational forecast service scheduled for December 2010 or January 2011.

Links to other projects

This project and WIRADA Project 4.2 ('Seasonal to long-term water forecasting and prediction') represent a joint effort in developing seasonal streamflow forecasting methods and tools for adoption by the Australian Bureau of Meteorology and key water management agencies in Australia.

The project has a strong linkage with Project 3.1 in Phase 2 of SEACI in two ways. The first is the use of dynamic climate model predictions for streamflow forecasting. The second is the use of the BJP method for calibration of climate model predictions to overcome bias and reliability problems and for combining dynamic modelling with empirical modelling to improve rainfall predictions.

The project also draws on results from Project 1.1a and Project 1.1b in Phase 2 of SEACI, especially results on climate drivers.

CHAPTER 9: NEXT STEPS

In the first year of Phase 2 of SEACI, research has progressed well. All projects are on track, already producing some very useful research findings, and all should continue producing innovative research and useful outputs for the remainder of Phase 2 of SEACI and beyond.

This Chapter summarises research directions for 2010/11. Progress against these research directions will be reported in the SEACI Program Annual Report for 2010/11, due to be released in September 2011.

Theme 1: Understanding past hydroclimate variability and change in south-eastern Australia

Research in Project 1.1 has been instrumental in characterising the nature of the recent drought, including comparing its severity to previous droughts, and in attributing the causes of the drought in light of climate change.

Further research in Project 1.1 will continue to refine the understanding of the nature and causes of the observed rainfall decline. A key focus will be to examine the changes in the characteristics of daily climatic variables and their relationships, and changes in the nature of synoptic systems delivering rainfall.

More sophisticated analyses will also be undertaken of the role of the sub-tropical ridge, and its interplay with the retreat of the summer monsoon, in the autumn rainfall decline. Researchers will also use surface and upper-air information to examine the nature of changes in the meridional circulation over the past two decades, with a view to better understanding the behaviour of the sub-tropical ridge and other key phenomena that are relevant to Australia. Additionally, outputs from a global climate model will be used to attempt to link observed changes in the mean meridional circulation to external forcings.

Research in Project 1.2 will use the AWAP data set to derive time series of hydrological responses (soil moisture, runoff and evaporation components) and meteorological forcing variables (rainfall, solar radiation, temperatures etc) over the whole of Australia (including SEA) and apply the general statistical model (previously developed in Project 1.2) to relate water balance responses over Australia to a set of climate indices. This will provide a better understanding of what drives variations in the rainfall-runoff response over time.

Theme 2: Long-term hydroclimate projections in south-eastern Australia

Research in Project 2.1 has shown that most of the uncertainty in future predictions of water availability comes from uncertainty in the global climate models. Further research will therefore focus on evaluating the ability of global climate models to reproduce observed seasonal climate variables and the major atmospheric-oceanic drivers of rainfall in SEA identified in Theme 1. A range of approaches for evaluating model performance will be considered, and the implications of different model selection methods for rainfall and runoff projections in SEA will also be evaluated.

In addition, this project will build on earlier research to conduct a more detailed assessment of the relative uncertainties associated with the various stages of the process of determining climate change impacts on runoff (i.e. GCM projections, downscaling methods, and rainfall-runoff models). In the light of these evaluations, the best methods for determining the expected impacts of climate change on runoff will be determined, and used to produce updated projections of future rainfall and runoff.

Research in Project 2.2 will apply a variety of analytical techniques with a view to better understanding the nature of the observed changes in rainfall-runoff relationships and associated hydrological processes under drier and warmer conditions. Researchers will also investigate how best to adapt hydrological models to account for these changes.

Theme 3: Seasonal hydroclimate prediction in south-eastern Australia

Research in Project 3.1 has improved rainfall forecasts with a 3-month lead time using the POAMA model. Future research in Project 3.1 is aimed at providing the necessary assessment of forecast skill, quality and reliability from the improved POAMA2 seasonal forecast system for subsequent uptake into hydrological seasonal forecasts for SEA.

A comprehensive assessment will be made of the forecast skill from the direct outputs of POAMA2, including an assessment of predictions of large-scale meteorological fields that can be directly used or downscaled for hydrological applications.

In addition, an assessment will also be made of the ability of POAMA2 to simulate and predict the major climate drivers that are important for SEA (e.g. El Nino/Modoki, IOD). The most appropriate forecast products for use in Project 3.2 will be determined based on these assessments.

Research in Project 3.2 will aim to further improve the forecasting skill of the Bayesian Joint Probability modelling approach (that was developed through previous SEACI and WIRADA research programs) for forecasting streamflow at multiple sites across south-eastern Australia. Specifically, research in 2010/11 will be aimed at better representation of initial catchment conditions and future climate influences.

REFERENCES

- Akaike H (1974) New look at statistical-model identification. *IEEE Transactions on Automatic Control* Ac19, 716–723.
- Cai W and Cowan T (2008a) Dynamics of late autumn rainfall reduction over south-eastern Australia. *Geophysical Research Letters* 35, L09708, doi:10.1029/2008GL033727.
- Cai W and Cowan T (2008b) Evidence of impacts from rising temperature on inflows to the Murray-Darling Basin. *Geophysical Research Letters* 35, L07701, doi:10.1029/2008GL033390.
- Cai W, Cowan T, Hendon H and van Rensch P (in prep.) Impact pathways of the ENSO and the IOD: tropical and extra-tropical responses. (To be submitted to *Journal of Climate*.)
- Cai W, Cowan T and Raupach M (2009b) Positive Indian Ocean Dipole events precondition southeast Australia bushfires. *Geophysical Research Letters* 36, L19710, doi:10.1029/2009GL039902.
- Cai W, Sullivan A and Cowan T (2009a) Recent unprecedented skewness towards positive Indian Ocean Dipole occurrences and its impact on Australian rainfall. *Geophysical Research Letters* 36, L11705, doi:10.1029/2009GL037604.
- Cai W, Sullivan A and Cowan T (2009c) Climate change contributes to more frequent consecutive positive Indian Ocean Dipole events, *Geophysical Research Letters*, 36, L23704, doi:10.1029/2009GL040163.
- Chiew FHS, Kirono DGC, Kent DM, Frost AJ, Charles SP, Timbal B, Nguyen KC and Fu G (2010) Comparison of runoff modelled using rainfall from different downscaling methods for historical and future climates. *Journal of Hydrology* 387, 10–23, doi:10.1016/j.jhydrol.2010.03.025.
- Chiew FHS, Teng J, Vaze J, Post DA, Perraud JM, Kirono DGC and Viney NR (2007) Estimating climate change impact on runoff across south-east Australia: method, results and implications of modelling method. *Water Resources Research* 45, W10414, doi:10.1029/2008WR007338.
- CSIRO and BoM (2007) Climate change in Australia. Technical Report. Available online at <<http://www.climatechangeinaustralia.com.au/resources.php>>.
- CSIRO (2010) Climate variability and change in south-eastern Australia: a synthesis of findings from Phase 1 of the South Eastern Australian Climate Initiative (SEACI). SEACI report, 36 pp. Available online at <<http://www.seaci.org>>.
- Donohue RJ, McVicar TR and Roderick ML (2009) Climate-related trends in Australian vegetation cover as inferred from satellite observations, 1981–2006. *Global Change Biology* 15, 1025–1039.
- Donohue RJ, McVicar TR and Roderick ML (2010) Assessing the ability of potential evaporation formulations to capture the dynamics in evaporative demand within a changing climate. *Journal of Hydrology* 386, 186–197.
- Drosowsky W (2005) The latitude of the subtropical ridge over eastern Australia: the L index revisited. *International Journal of Climatology* 25, 1291–1299, doi:10.1002/joc.1196.
- Feldstein, SB (2002) The recent trend and variance increase of the annular mode. *Journal of Climate* 15, 88–94.
- Gedney N, Cox PM, Betts RA, Boucher O, Huntingford C and Stott PA (2006), Detection of a direct carbon dioxide effect in continental river runoff records, *Nature*, 439, 835–838.
- Hendon HH, Lim EP, Wang G, Alves O and Hudson D (2009) Prospects for predicting two flavours of El Niño. *Geophysical Research Letters* 36, L19713, doi:10.1029/2009GL040100.
- Huntington TG (2008), CO₂-induced suppression of transpiration cannot explain increasing runoff, *Hydrol. Process.*, 22, 311–314.

- Johanson CM and Fu Q (2009) Hadley cell widening: model simulations versus observations. *Journal of Climatology* 22, 2713–2725.
- Jones DA, Wang W and Fawcett R (2009) High-quality spatial climate data-sets for Australia. *Australian Meteorological and Oceanographic Journal* 58, 233–248.
- Jones DA, Wang W and Fawcett R (2007) Climate data for the Australian Water Availability Project: final milestone report. National Climate Centre, Bureau of Meteorology, Melbourne.
- Jones DA and Simmonds I (1993) A climatology of Southern Hemisphere extratropical cyclones. *Climate Dynamics* 9, 131–145.
- Kalnay E, Kanamitsu M, Kistler R, Collins W, Deaven D, Gandin L, Iredell M, White G, Woollen J, Zhu Y, Chelliah M, Ebisuzaki W, Higgins W, Janowiak J, Mo CK, Ropelewski C, Wang J, Leetmaa A, Reynolds R, Jenne R and Joseph D (1979) The NCEP/NCAR 40-year reanalysis project. *Bulletin of the American Meteorological Society* 77, 437–471.
- Kent DM, Kirono DGC, Timbal B and Chiew FHS (submitted) Representation of the Australian sub-tropical ridge in the CMIP3 models. (Submitted to *International Journal of Climatology*.)
- Kiem AS and Verdon-Kidd DC (2009) Climatic drivers of Victorian streamflow: is ENSO the dominant influence? *Australian Journal of Water Resources* 13(1), 17–30.
- Kiem AS and Verdon-Kidd DC (2010) Towards understanding hydroclimatic change in Victoria, Australia: preliminary insights into the 'Big Dry'. *Hydrology and Earth Systems Science* 14, 433–445, doi:10.5194/hess-14-433-2010.
- King EA, Paget MJ, Briggs PR, Trudinger CM and Raupach MR (2009) Operational delivery of hydro-meteorological monitoring and modeling over the Australian continent. *IEEE Journal of Selected Topics in Applied Earth Observations and Remote Sensing (JSTARS)* 2, doi:10.1109/JSTARS.2009.2031331.
- Kushner PJ, Held IM and Delworth TL (2001) Southern Hemisphere atmospheric circulation response to global warming. *Journal of Climatology* 14, 2238–2249.
- Lim EP, Hendon HH, Alves O, Yin Y, Wang G, Hudson D, Zhao M and Shi L (submitted) Dynamical seasonal prediction of tropical Indo-Pacific SST and Australian rainfall with improved ocean initial conditions. (Submitted to Centre for Australian Weather and Climate Research as a Technical Report.)
- Lim EP, Hendon HH, Alves O, Yin Y, Zhao M, Wang G, Hudson D and Liu G (2009) Impact of SST bias correction on prediction of ENSO and Australian winter rainfall. *The Centre for Australian Weather and Climate Research, Research Letters*. vol.3, iv. Available online at <<http://www.cawcr.gov.au/publications/researchletters.php>>
- Lim EP, Hendon HH, Anderson DTL, Charles A and Alves O (in press) Dynamical, statistical-dynamical and multi-model ensemble forecasts of Australian spring season rainfall. *Monthly Weather Review*.
- Love, G (1985) Cross-equatorial influence of winter hemisphere subtropical cold surges. *Monthly Weather Review* 113, 1487–1498.
- Marshall GJ (2003) Trends in the Southern Annular Mode from observations and reanalyses. *Journal of Climatology* 16, 4134–4143.
- Meneghini B, Simmonds I and Smith IN (2007) Association between Australian rainfall and the Southern Annular Mode. *International Journal of Climatology* 27, 109–121.
- Mitas CM and Clement A (2005) Has the Hadley cell been strengthening in recent decades? *Geophysical Research Letters* 32, doi:10.1029/2004GL021765.
- Mitas CM and Clement A (2006) Recent behaviour of Hadley cell and tropical thermodynamics in climate models and re-analyses. *Geophysical Research Letters* 33, doi: 10.1029/2005GL024406.
- Murphy BF and Timbal B (2008) A review of recent climate variability and climate change in south-eastern Australia. *International Journal of Climatology* 28(7), 859–879.

- Nicholls N (2010) Local and remote causes of the southern Australian autumn-winter rainfall decline 1958–2007. *Climate Dynamics* 34, 835–845, doi:10.1007/s00382-009-0527-6.
- Plummer N, Tuteja NK, Wang QJ, Wang E, Robertson DE, Zhou S, Schepen A, Alves O, Timbal B and Puri K (2009) A seasonal water availability prediction service: opportunities and challenges. In: *18th World IMACS/MODSIM Congress* (edited), Modelling and Simulation Society of Australia and New Zealand Inc., Cairns.
- Post DA, Chiew FHS, Vaze J, Teng J and Perraud JM (2008) Future runoff projections (~2030) for southeast Australia. South Eastern Australian Climate Initiative Report, 32 pp. Available online at <http://www.seaci.org/publications/documents/SEACI-1%20Reports/S1_FR222.pdf>.
- Potter NJ and Chiew FHS (submitted) Attribution of low runoff in south-east Australia using rainfall-runoff models. (Submitted to *Geophysical Research Letters*.)
- Raupach MR, Briggs PR, Haverd V, King EA, Paget M and Trudinger CM (2009) Australian Water Availability Project (AWAP), CSIRO Marine and Atmospheric Research component: final report for Phase 3. CAWCR Technical Report No. 013, Centre for Australian Weather and Climate Research (Bureau of Meteorology and CSIRO), Melbourne, Australia, 67 pp.
- Robertson DE and Wang QJ (in prep.) Selection of predictors for the Bayesian joint probability approach to seasonal streamflow forecasting. (To be submitted to *Journal of Hydrometeorology*.)
- Robertson, DE, Wang, QJ, Schepen, A, Peaty, T, Zhou, S, Perkins, J, Shin, D, Plummer, N, Allie, S. (submitted). Evaluation of the Bayesian joint probability modelling approach to seasonal streamflow forecasting for inflows into Melbourne Water and Hydro Tasmania storages, CSIRO: Water for a Healthy Country National Research Flagship Technical Report.
- Schneider T (2006) The general circulation of the atmosphere. *Annual Review of Earth and Planetary Sciences* 34, 655–688.
- Seidel DJ, Fu Q, Randel WJ and Reichler TJ (2007) Widening of the tropical belt in a changing climate. *Nature Geoscience*, doi:10.1038/ngeo.2007.38.
- Solomon S, Qin D, Manning M, Chen Z, Marquis M, Averyt K, Tignor M and Miller HM (eds) (2007) Climate change 2007: the physical science basis, contribution of Working Group I to the Fourth Assessment Report of the Intergovernmental Panel on Climate Change. Cambridge University Press, Cambridge, United Kingdom and New York, NY, USA, 996 pp.
- Thompson DWJ and Wallace JM (2000) Annular modes in the extratropical circulation. Part I. Month-to-month variability. *Journal of Climatology* 13, 1000–1016.
- Timbal B (2009) Theme 1: highlights from SEACI-1 final years. Presentation at the SEACI annual review meeting.
- Timbal B (2010) A discussion on aspects of the seasonality of the rainfall decline in south-eastern Australia. *The Centre for Australian Weather and Climate Research, Research Letters*. Available online at <<http://www.cawcr.gov.au/publications/researchletters.php>>.
- Timbal B, Arblaster J, Braganza K, Fernandez E, Hendon H, Murphy B, Raupach M, Rakich C, Smith I, Whan K and Wheeler M (2010) Understanding the anthropogenic nature of the observed rainfall decline across south-eastern Australia. *The Centre for Australian Weather and Climate Research, Technical Report no.026*. Available online at <<http://www.cawcr.gov.au/publications/technicalreports.php>>.
- Timbal B and Smith I (2009) Assessing the relationship between the Hadley circulation and the position and intensity of the sub-tropical ridge in the Australian region. SEACI Final Report for Project 1.1.1P.
- Trewin B and Fawcett R (2010) Reconstructing historical rainfall averages for the Murray-Darling Basin. *Bulletin of the Australian Meteorological and Oceanographic Society* 22, 158–164.
- Ummenhofer CC, Sen Gupta A, Briggs PR, England MH, McIntosh PC, Meyers GA, Pook MJ, Raupach MR and Risbey JS (in press) Indian and Pacific Ocean influences on southeast Australian drought and soil moisture. *Journal of Climate*.

Vaze J, Post DA, Chiew FHS, Perraud JM, Viney NR and Teng J (submitted) Climate non-stationarity: validity of calibrated rainfall-runoff models for use in climate change studies. (Submitted to *Journal of Hydrology*.)

Wang QJ, Robertson DE and Chiew FHS (2009) A Bayesian joint probability modelling approach for seasonal forecasting of streamflows at multiple sites. *Water Resources Research* 45.

Wang QJ and Robertson DE (submitted) Multisite probabilistic forecasting of seasonal flows for streams with zero value occurrences. (Submitted to *Water Resources Research*.)

Yin Y, Alves O and Oke P (in press) An ensemble ocean data assimilation system for seasonal prediction. *Monthly Weather Review*.

LIST OF PUBLICATIONS ARISING FROM SEACI RESEARCH IN 2009/10

Project 1.1a

- Timbal, B. (2010) The climate of the eastern seaboard of Australia: a challenging entity now and for future projections. *Proceedings of the 2010 IOP Conference Series: Earth and Environmental Sciences* 11, 012013, doi: 10.1088/1755-1315/11/1/012013.
- Timbal B (2010) A discussion on aspects of the seasonality of the rainfall decline in south-eastern Australia. *The Centre for Australian Weather and Climate Research, Research Letters*. Available online at <<http://www.cawcr.gov.au/publications/researchletters.php>>.
- Timbal B, Arblaster J, Braganza K, Fernandez E, Hendon H, Murphy B, Raupach M, Rakich C, Smith I, Whan K and Wheeler M (2010) Understanding the anthropogenic nature of the observed rainfall decline across south-eastern Australia. *The Centre for Australian Weather and Climate Research, Technical Report no.026*. Available online at <<http://www.cawcr.gov.au/publications/technicalreports.php>>.

Project 1.1b

- Cai W, Cowan T, Hendon H and van Rensch P (in prep.) Impact pathways of the ENSO and the IOD: tropical and extra-tropical responses. (To be submitted to *Journal of Climate*.)
- Li Y and Cai W (submitted) The influence of climate drivers on the inflow to the Murray–Darling Basin. (To be submitted to *Journal of Hydrometeorology*.)
- Cai W, Cowan T, Briggs P and Raupach M (2009) Rising temperature depletes soil moisture and exacerbates severe drought conditions across southeast Australia. *Geophysical Research Letters* 36, L21709, doi:10.1029/2009GL040334.
- Cai W, Sullivan A and Cowan T (2009) Climate change contributes to more frequent consecutive positive Indian Ocean Dipole events. *Geophysical Research Letters* 36, L23704, doi:10.1029/2009GL040163.
- Cai W, Cowan T and Sullivan A (2009) Recent unprecedented skewness towards positive Indian Ocean Dipole occurrences and its impact on Australian rainfall. *Geophysical Research Letters* 36, L11705, doi:10.1029/2009GL037604.

Project 1.2

- Cai W, Cowan T and Raupach M (2009) Positive Indian Ocean Dipole events precondition southeast Australia bushfires. *Geophysical Research Letters* 36, L19710, doi:10.1029/2009GL039902.
- King EA, Paget MJ, Briggs PR, Trudinger CM and Raupach MR (2009) Operational delivery of hydro-meteorological monitoring and modeling over the Australian continent. *IEEE Journal of Selected Topics in Applied Earth Observations and Remote Sensing (JSTARS)* 2, doi:10.1109/JSTARS.2009.2031331.
- Raupach MR, Briggs PR, Haverd V, King EA, Paget M and Trudinger CM (2009) Australian Water Availability Project (AWAP), CSIRO Marine and Atmospheric Research component: final report for Phase 3. CAWCR Technical Report No. 013, Centre for Australian Weather and Climate Research (Bureau of Meteorology and CSIRO), Melbourne, Australia, 67 pp.
- Ummenhofer CC, Sen Gupta A, Briggs PR, England MH, McIntosh PC, Meyers GA, Pook MJ, Raupach MR and Risbey JS (in press) Indian and Pacific Ocean influences on southeast Australian drought and soil moisture. *Journal of Climate*.

Project 2.1

Chiew FHS, Kirono DGC, Kent DM, Frost AJ, Charles SP, Timbal B, Nguyen KC and Fu G (2010) Comparison of runoff modelled using rainfall from different downscaling methods for historical and future climates. *Journal of Hydrology* 387, 10–23, doi:10.1016/j.jhydrol.2010.03.025.

Kent DM, Kirono DGC, Timbal B and Chiew FHS (submitted.) Representation of the Australian sub-tropical ridge in the CMIP3 models. (Submitted to *International Journal of Climatology*).

Kirono, DGC and Kent DM. (2010) Assessment of rainfall and potential evaporation from global climate models and its implications for Australian regional drought projection. *International Journal of Climatology*. doi:10.1002/joc.2165.

Teng J, Vaze J, Chiew FHS, Wang B, Perraud JM (in prep.) Relative uncertainty in global climate model projections and rainfall-runoff modelling of climate change impact on runoff.

Project 2.2

Donohue RJ, McVicar TR and Roderick ML (2009) Climate-related trends in Australian vegetation cover as inferred from satellite observations, 1981–2006. *Global Change Biology* 15, 1025–1039.

Donohue RJ, McVicar TR and Roderick ML (2010) Assessing the ability of potential evaporation formulations to capture the dynamics in evaporative demand within a changing climate. *Journal of Hydrology* 386, 186–197.

Potter NJ and Chiew FHS (submitted) Attribution of low runoff in south-east Australia using rainfall-runoff models. (Submitted to *Water Resources Research*.)

Potter NJ, Chiew FHS and Frost AJ (2010) An assessment of the severity of recent reductions of rainfall and runoff in the Murray-Darling Basin. *Journal of Hydrology* 381, 52–64, doi:10.1016/j.jhydrol.2009.11.025.

Vaze J, Post DA, Chiew FHS, Perraud JM, Viney NR and Teng J (2010) Climate non-stationarity: validity of calibrated rainfall-runoff models for use in climate change studies. *J. Hydrology* 394:447–457.

Project 3.1

Lim EP, Hendon HH, Alves O, Yin Y, Wang G, Hudson D, Zhao M and Shi L (submitted) Dynamical seasonal prediction of tropical Indo-Pacific SST and Australian rainfall with improved ocean initial conditions. (Submitted to Centre for Australian Weather and Climate Research as a Technical Report.)

Lim EP, Hendon HH, Alves O, Yin Y, Zhao M, Wang G, Hudson D and Liu G (2009) Impact of SST bias correction on prediction of ENSO and Australian winter rainfall. *The Centre for Australian Weather and Climate Research, Research Letters*. vol.3, iv. Available online at <<http://www.cawcr.gov.au/publications/researchletters.php>>

Lim EP, Hendon HH, Anderson DTL, Charles A and Alves O (in press) Dynamical, statistical-dynamical and multi-model ensemble forecasts of Australian spring season rainfall. *Monthly Weather Review*.

Yin Y, Alves O and Oke P (in press) An ensemble ocean data assimilation system for seasonal prediction. (*Monthly Weather Review*.)

Project 3.2

Robertson DE and Wang QJ (in prep.) A Bayesian approach to predictor selection for seasonal streamflow forecasting. (To be submitted to *Journal of Hydrometeorology*.)

Robertson, DE, Wang, QJ, Schepen, A, Peaty, T, Zhou, S, Perkins, J, Shin, D, Plummer, N, Allie, S. (submitted) Evaluation of the Bayesian joint probability modelling approach to seasonal streamflow forecasting for inflows into Melbourne Water and Hydro Tasmania storages, CSIRO: Water for a Healthy Country National Research Flagship Technical Report.

Wang QJ and Robertson DE (submitted) Multisite probabilistic forecasting of seasonal flows for streams with zero value occurrences. (Submitted to *Water Resources Research*.)

For more information:

Email seaci@csiro.au

Visit www.seaci.org



Australian Government

**Department of Climate Change
and Energy Efficiency**

Bureau of Meteorology

